

Status of versatile GRASP retrieval algorithm

Towards “the universal” retrieval approach



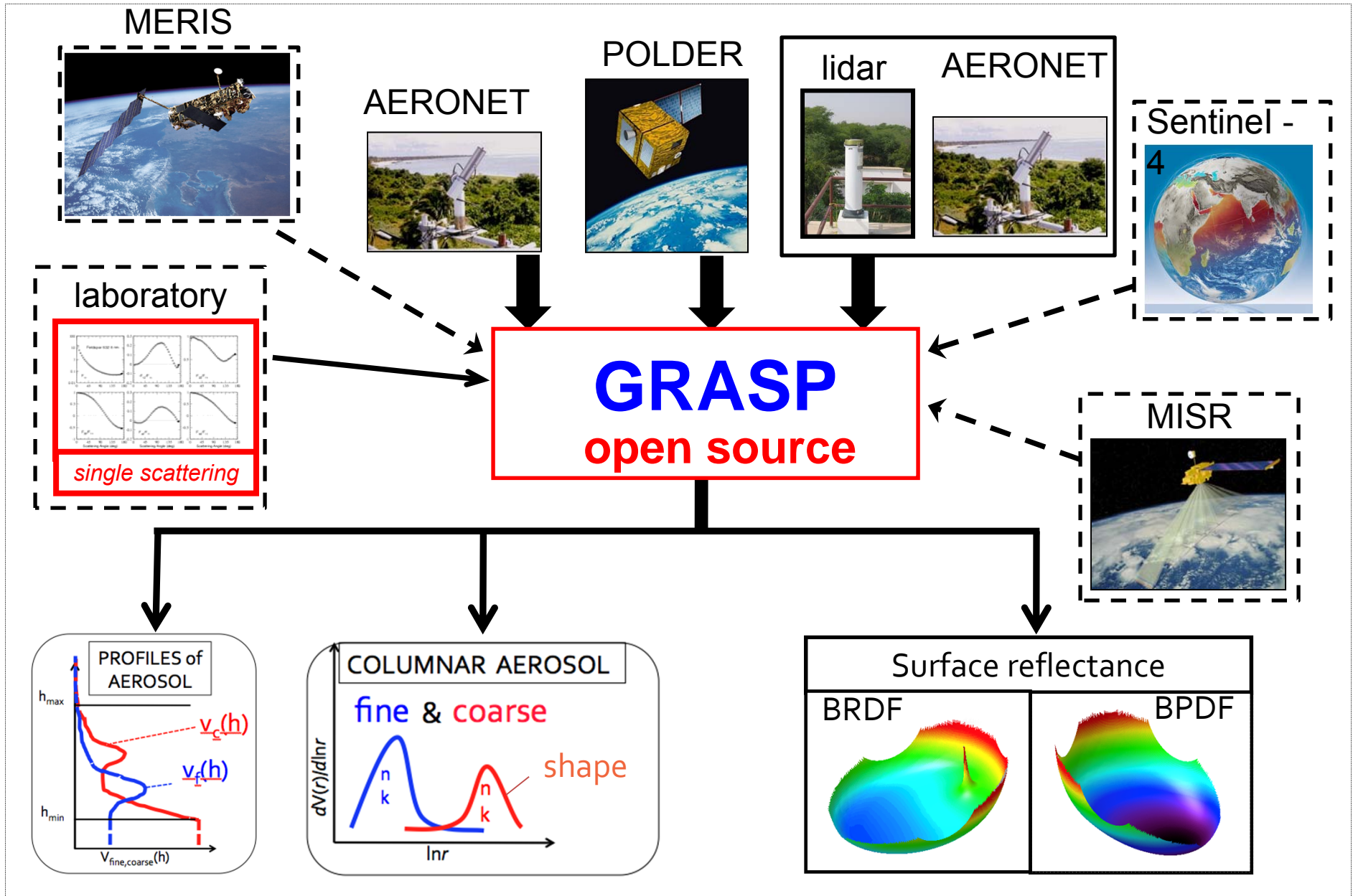
Oleg Dubovik¹, Pavel Litvinov², Tatyana Lapyonok¹, Anton Lopatin¹,
David Fuertes², Fabrice Ducos¹, Xin Huang¹, Benjamin Torres²,
Qiaoyun Hu, Yevgeny Derimian¹, Cheng Chen¹, Lei Li¹, Michael
Aspetsberger³ and Christian Federspiel³

1 - Laboratoire d'Optique Atmosphérique, CNRS – Université Lille 1, France;

2 - GRASP-SAS, LOA, Université Lille 1, Villeneuve d'Ascq, France

3 - Catalysts GmbH, High Performance Computing, Linz, Austria

GRASP: Generalized Retrieval of Aerosol and Surface Properties





Diverse applications of GRASP

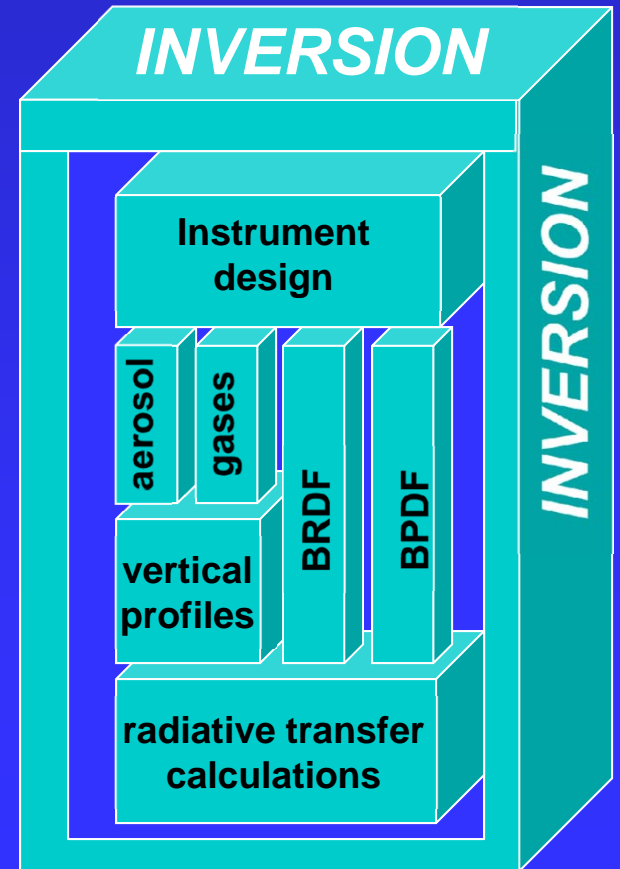
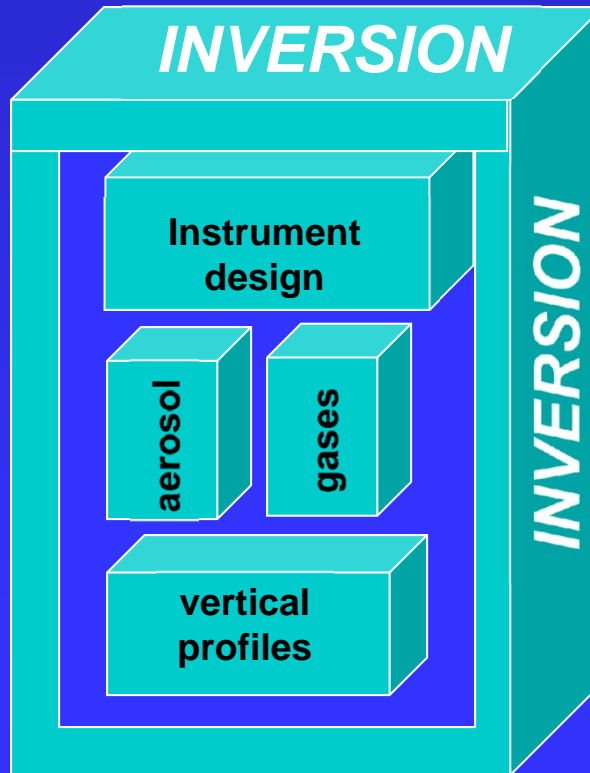
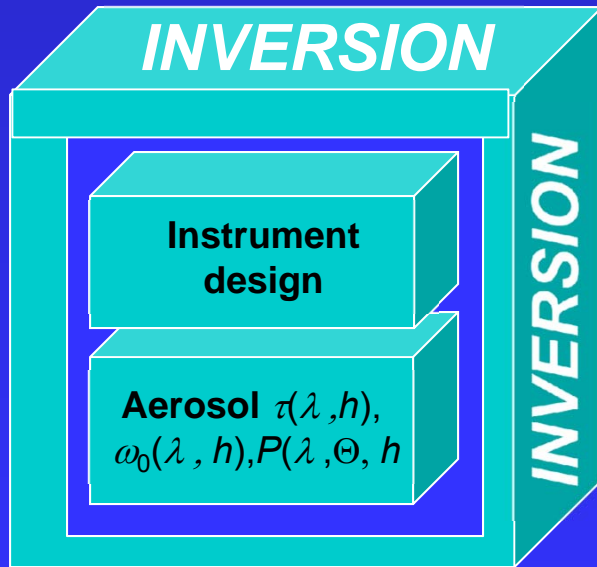
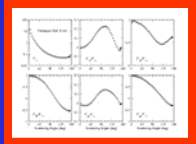
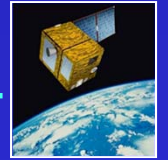
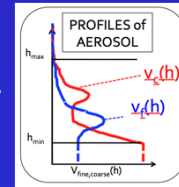


Nephelometer

Sun-photometer

Lidar

AERONET
PARASOL



All modules are fully consistent !!!

Multi-Source LSM approach:

$$P_{1,2,3} = P_1 P_2 P_{3\dots} \sim \exp\left(-\frac{1}{2\sigma_1^2} \sum_i \frac{\sigma_1^2}{\sigma_i^2} (\Delta \mathbf{f}_i^T \Delta \mathbf{f}_i)\right) = \max \longrightarrow \sum_i \frac{\sigma_1^2}{\sigma_i^2} (\Delta \mathbf{f}_i^T \Delta \mathbf{f}_i) = \min$$

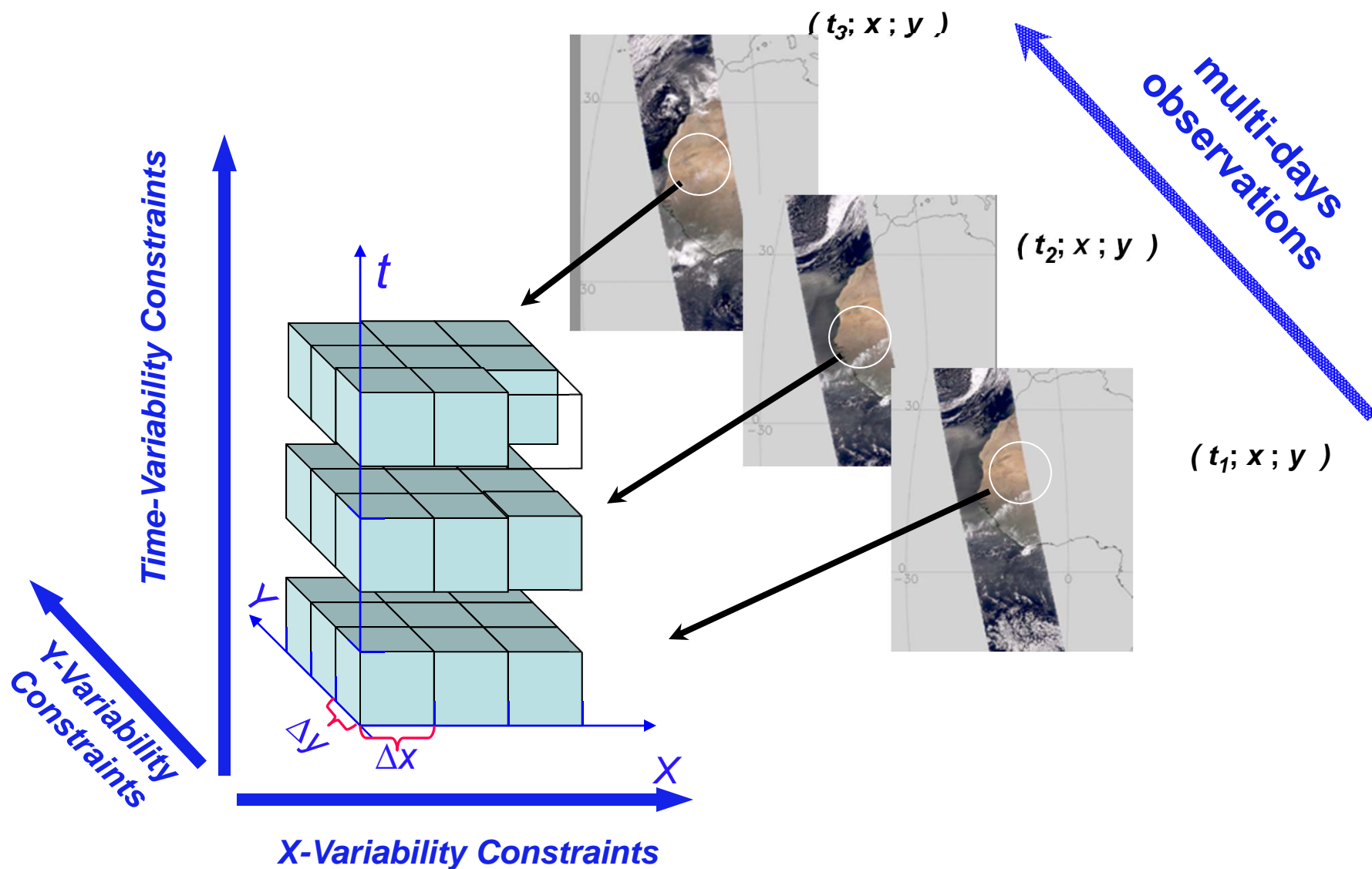
where $\Delta_i = \mathbf{f}_i^* - \mathbf{f}_i(\mathbf{a})$ and \mathbf{f}_i^* - measurements or *a priori data*

$P(\dots)$ - Probability Density Function (**Likelihood**)

- *Optimum data combination*
- *Optimum use of a priori information*
- *Continuous solution space*
- *Rigorous error estimations*
- *Large number of retrieved parameters with less assumption*

- *More “sophisticated”*
- *Generally more time consuming*

The concept of multi-pixel retrieval



Multi-term LSM Multi-Pixel Solution:

$$\begin{pmatrix} \mathbf{a}_1 \\ \mathbf{a}_2 \\ \mathbf{a}_3 \end{pmatrix} = \begin{pmatrix} \mathbf{F}_1^T \mathbf{W}_1^{-1} \mathbf{F}_1 & 0 & 0 \\ 0 & \mathbf{F}_2^T \mathbf{W}_2^{-1} \mathbf{F}_2 & 0 \\ 0 & 0 & \mathbf{F}_3^T \mathbf{W}_3^{-1} \mathbf{F}_3 \end{pmatrix} + \begin{pmatrix} \gamma_1 \Omega_1 & 0 & 0 \\ 0 & \gamma_2 \Omega_2 & 0 \\ 0 & 0 & \gamma_3 \Omega_3 \end{pmatrix} + \gamma_x \Omega_x + \gamma_y \Omega_y + \gamma_t \Omega_t \begin{pmatrix} \mathbf{F}_1^T \mathbf{W}_1^{-1} \Delta \mathbf{f}_1^p \\ \mathbf{F}_2^T \mathbf{W}_2^{-1} \Delta \mathbf{f}_2^p \\ \mathbf{F}_3^T \mathbf{W}_3^{-1} \Delta \mathbf{f}_3^p \end{pmatrix}^{-1}$$

$$\Omega_x = \mathbf{s}_x^T \mathbf{s}_x; \quad \Omega_y = \mathbf{s}_y^T \mathbf{s}_y; \quad \Omega_t = \mathbf{s}_t^T \mathbf{s}_t;$$

- \mathbf{a}_v
- \mathbf{a}_n
- \mathbf{a}_n
- \mathbf{a}_h
- \mathbf{a}_{sph}
- \mathbf{a}_{vc}
- $\mathbf{a}_{brdf,1}$
- $\mathbf{a}_{brdf,2}$
- $\mathbf{a}_{brdf,3}$
- \mathbf{a}_{bpdf}

$$\gamma_{\Delta} \Omega = \begin{pmatrix} \gamma_{\Delta,1} \Omega_1 & 0 & 0 & 0 & 0 & 0 & 0 & 0 & 0 \\ 0 & \gamma_{\Delta,2} \Omega_2 & 0 & 0 & 0 & 0 & 0 & 0 & 0 \\ 0 & 0 & \gamma_{\Delta,3} \Omega_3 & 0 & 0 & 0 & 0 & 0 & 0 \\ 0 & 0 & 0 & 0 & 0 & 0 & 0 & 0 & 0 \\ 0 & 0 & 0 & 0 & 0 & 0 & 0 & 0 & 0 \\ 0 & 0 & 0 & 0 & 0 & 0 & \gamma_{\Delta,4} \Omega_4 & 0 & 0 \\ 0 & 0 & 0 & 0 & 0 & 0 & 0 & \gamma_{\Delta,5} \Omega_5 & 0 \\ 0 & 0 & 0 & 0 & 0 & 0 & 0 & 0 & \gamma_{\Delta,6} \Omega_6 \\ 0 & 0 & 0 & 0 & 0 & 0 & 0 & 0 & 0 \end{pmatrix}$$

$$\mathbf{s}_y^T \mathbf{s}_y = \begin{pmatrix} \begin{pmatrix} I_{d_{11}} & I_{d_{12}} & I_{d_{13}} \\ I_{d_{21}} & I_{d_{22}} & I_{d_{23}} \\ I_{d_{31}} & I_{d_{32}} & I_{d_{33}} \end{pmatrix} & \begin{pmatrix} 0 & 0 & 0 \\ 0 & 0 & 0 \\ 0 & 0 & 0 \end{pmatrix} & \begin{pmatrix} 0 & 0 & 0 \\ 0 & 0 & 0 \\ 0 & 0 & 0 \end{pmatrix} \\ \begin{pmatrix} 0 & 0 & 0 \\ 0 & 0 & 0 \\ 0 & 0 & 0 \end{pmatrix} & \begin{pmatrix} I_{d_{11}} & I_{d_{12}} & I_{d_{13}} \\ I_{d_{21}} & I_{d_{22}} & I_{d_{23}} \\ I_{d_{31}} & I_{d_{32}} & I_{d_{33}} \end{pmatrix} & \begin{pmatrix} 0 & 0 & 0 \\ 0 & 0 & 0 \\ 0 & 0 & 0 \end{pmatrix} \\ \begin{pmatrix} 0 & 0 & 0 \\ 0 & 0 & 0 \\ 0 & 0 & 0 \end{pmatrix} & \begin{pmatrix} 0 & 0 & 0 \\ 0 & 0 & 0 \\ 0 & 0 & 0 \end{pmatrix} & \begin{pmatrix} I_{d_{11}} & I_{d_{12}} & I_{d_{13}} \\ I_{d_{21}} & I_{d_{22}} & I_{d_{23}} \\ I_{d_{31}} & I_{d_{32}} & I_{d_{33}} \end{pmatrix} \end{pmatrix};$$

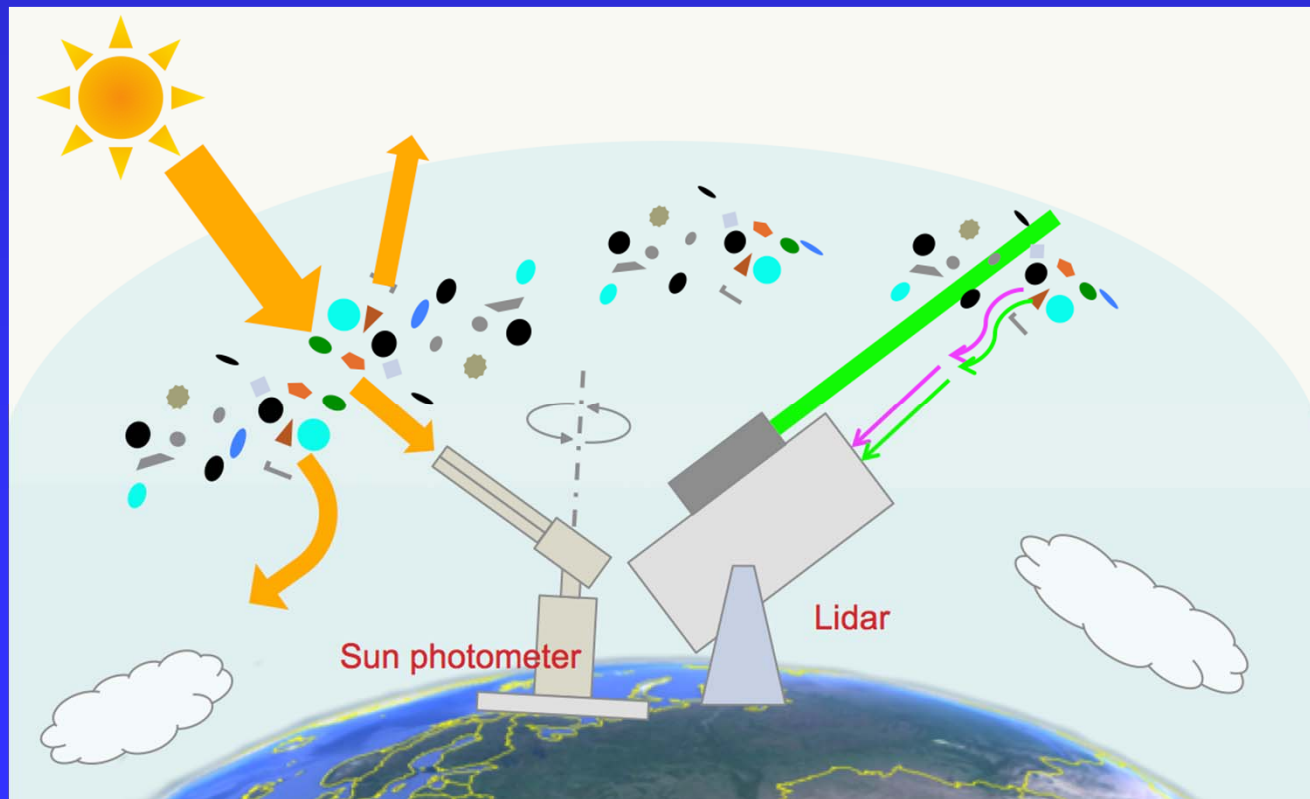
$$\mathbf{s}_y^T \mathbf{s}_y = \begin{pmatrix} \begin{pmatrix} I_{d_{11}} & I_{d_{12}} & I_{d_{13}} \\ I_{d_{21}} & I_{d_{22}} & I_{d_{23}} \\ I_{d_{31}} & I_{d_{32}} & I_{d_{33}} \end{pmatrix} & \begin{pmatrix} 0 & 0 & 0 \\ 0 & 0 & 0 \\ 0 & 0 & 0 \end{pmatrix} & \begin{pmatrix} 0 & 0 & 0 \\ 0 & 0 & 0 \\ 0 & 0 & 0 \end{pmatrix} \\ \begin{pmatrix} 0 & 0 & 0 \\ 0 & 0 & 0 \\ 0 & 0 & 0 \end{pmatrix} & \begin{pmatrix} I_{d_{11}} & I_{d_{12}} & I_{d_{13}} \\ I_{d_{21}} & I_{d_{22}} & I_{d_{23}} \\ I_{d_{31}} & I_{d_{32}} & I_{d_{33}} \end{pmatrix} & \begin{pmatrix} 0 & 0 & 0 \\ 0 & 0 & 0 \\ 0 & 0 & 0 \end{pmatrix} \\ \begin{pmatrix} 0 & 0 & 0 \\ 0 & 0 & 0 \\ 0 & 0 & 0 \end{pmatrix} & \begin{pmatrix} 0 & 0 & 0 \\ 0 & 0 & 0 \\ 0 & 0 & 0 \end{pmatrix} & \begin{pmatrix} I_{d_{11}} & I_{d_{12}} & I_{d_{13}} \\ I_{d_{21}} & I_{d_{22}} & I_{d_{23}} \\ I_{d_{31}} & I_{d_{32}} & I_{d_{33}} \end{pmatrix} \end{pmatrix};$$

$$\mathbf{s}_t^T \mathbf{s}_t = \begin{pmatrix} \begin{pmatrix} I_{d_{11}} & 0 & 0 \\ 0 & I_{d_{11}} & 0 \\ 0 & 0 & I_{d_{11}} \end{pmatrix} & \begin{pmatrix} I_{d_{12}} & 0 & 0 \\ 0 & I_{d_{12}} & 0 \\ 0 & 0 & I_{d_{12}} \end{pmatrix} & \begin{pmatrix} I_{d_{13}} & 0 & 0 \\ 0 & I_{d_{13}} & 0 \\ 0 & 0 & I_{d_{13}} \end{pmatrix} \\ \begin{pmatrix} I_{d_{21}} & 0 & 0 \\ 0 & I_{d_{21}} & 0 \\ 0 & 0 & I_{d_{21}} \end{pmatrix} & \begin{pmatrix} I_{d_{22}} & 0 & 0 \\ 0 & I_{d_{22}} & 0 \\ 0 & 0 & I_{d_{22}} \end{pmatrix} & \begin{pmatrix} I_{d_{23}} & 0 & 0 \\ 0 & I_{d_{23}} & 0 \\ 0 & 0 & I_{d_{23}} \end{pmatrix} \\ \begin{pmatrix} I_{d_{31}} & 0 & 0 \\ 0 & I_{d_{31}} & 0 \\ 0 & 0 & I_{d_{31}} \end{pmatrix} & \begin{pmatrix} I_{d_{32}} & 0 & 0 \\ 0 & I_{d_{32}} & 0 \\ 0 & 0 & I_{d_{32}} \end{pmatrix} & \begin{pmatrix} I_{d_{33}} & 0 & 0 \\ 0 & I_{d_{33}} & 0 \\ 0 & 0 & I_{d_{33}} \end{pmatrix} \end{pmatrix}$$

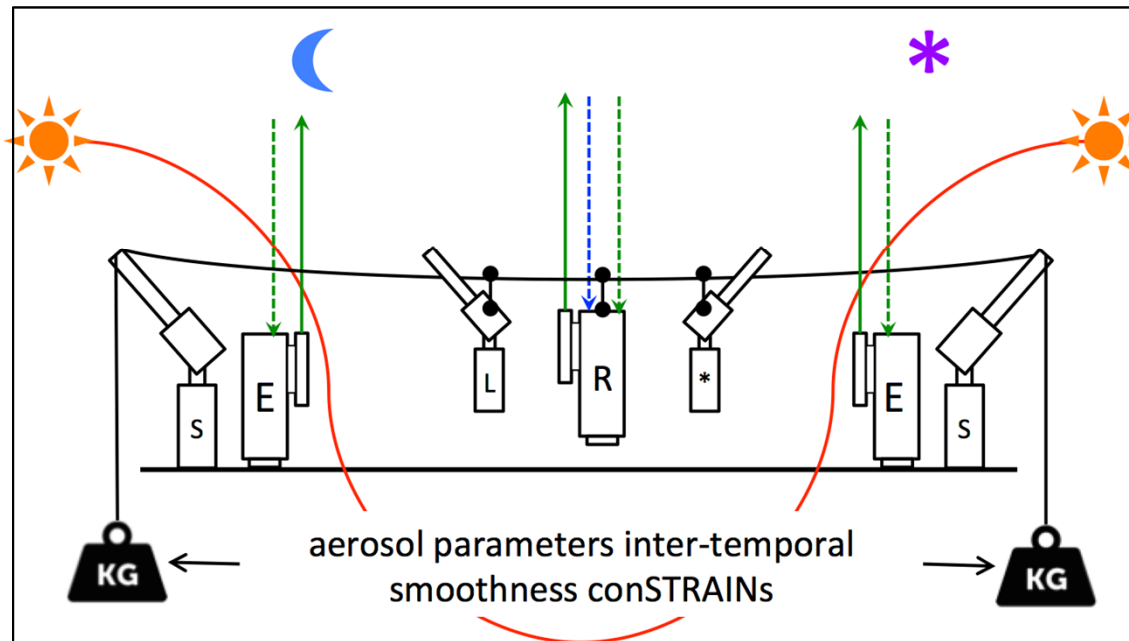
43 parameters

Priorities in GRASP development for ground-based and in situ observations:

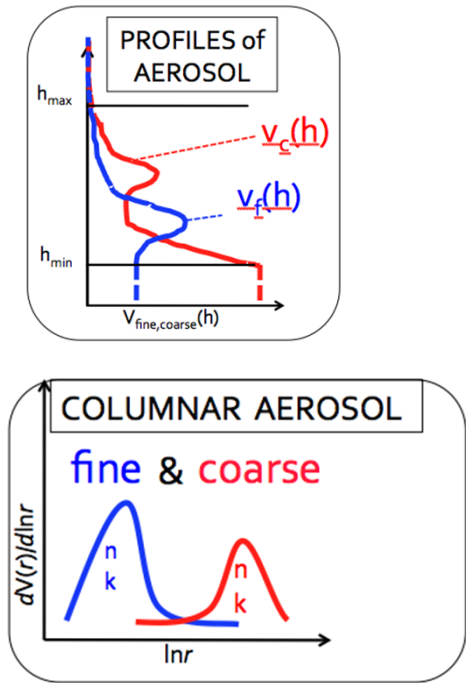
- *multi-instrument combination,*
- *diversity of observations,*
- *consistency of observations*



Multi-temporal multi-instrumental retrievals concept



ACTRIS Project



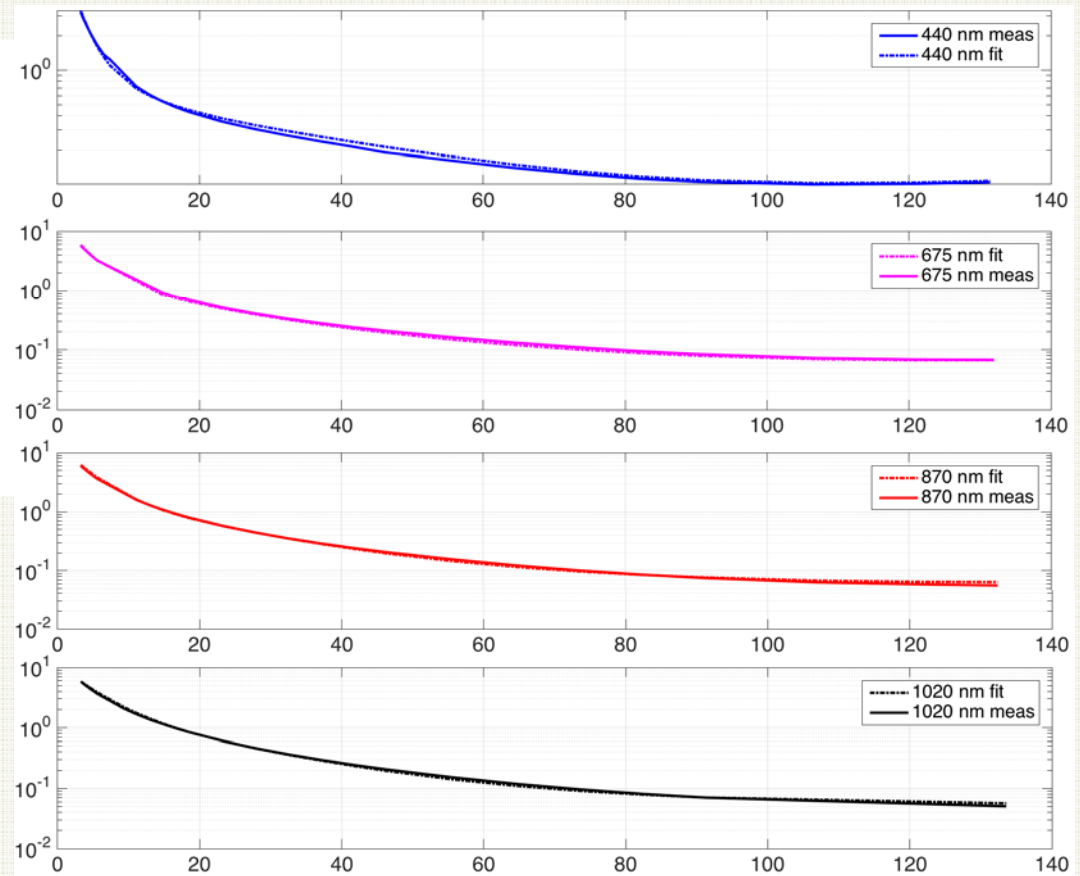
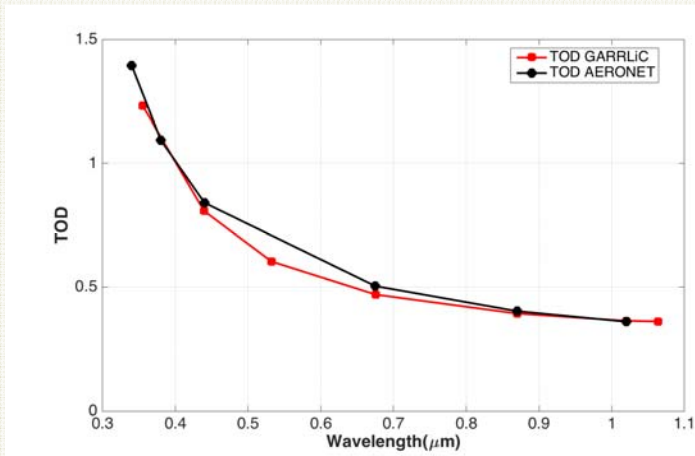
Advanced processing of ground-based observations using GRASP:

- combining observation during **several days**;
- combining **day and night** observations;
- combining **passive** (photometric) **and active** (lidar);
- combining **ground-based and satellite** observations;
- retrieving as many parameters as possible;

Expectations: more accurate and more complete validation data set

LIDAR + AERONET

Fitting AERONET by AERONET/lidar GRASP retrieval

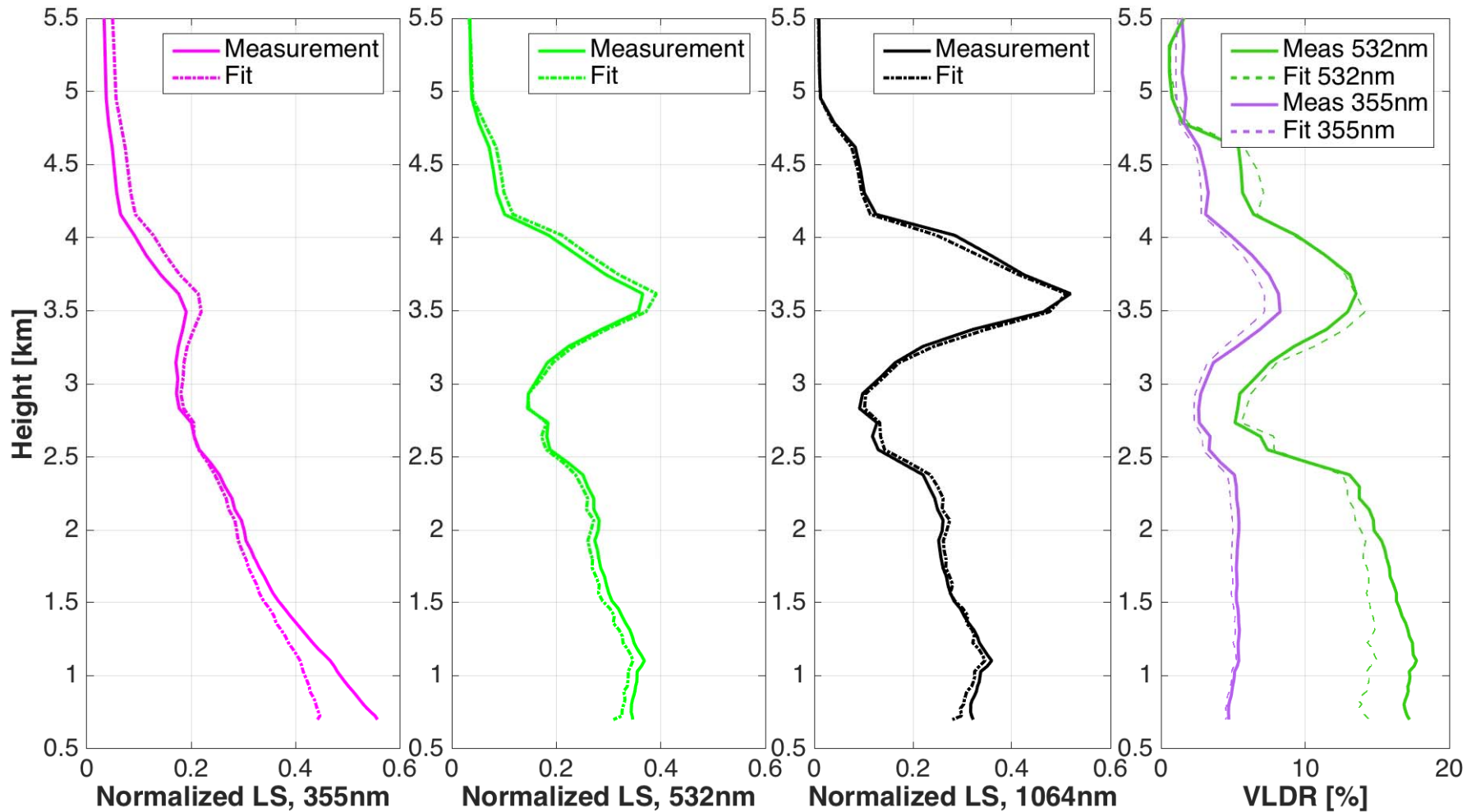


20 Jan 2016, M'bour

Qiaoyun HU, Anton Lopatin, etc.

LIDAR + AERONET

Fitting lidar observations by AERONET/lidar GRASP retrieval

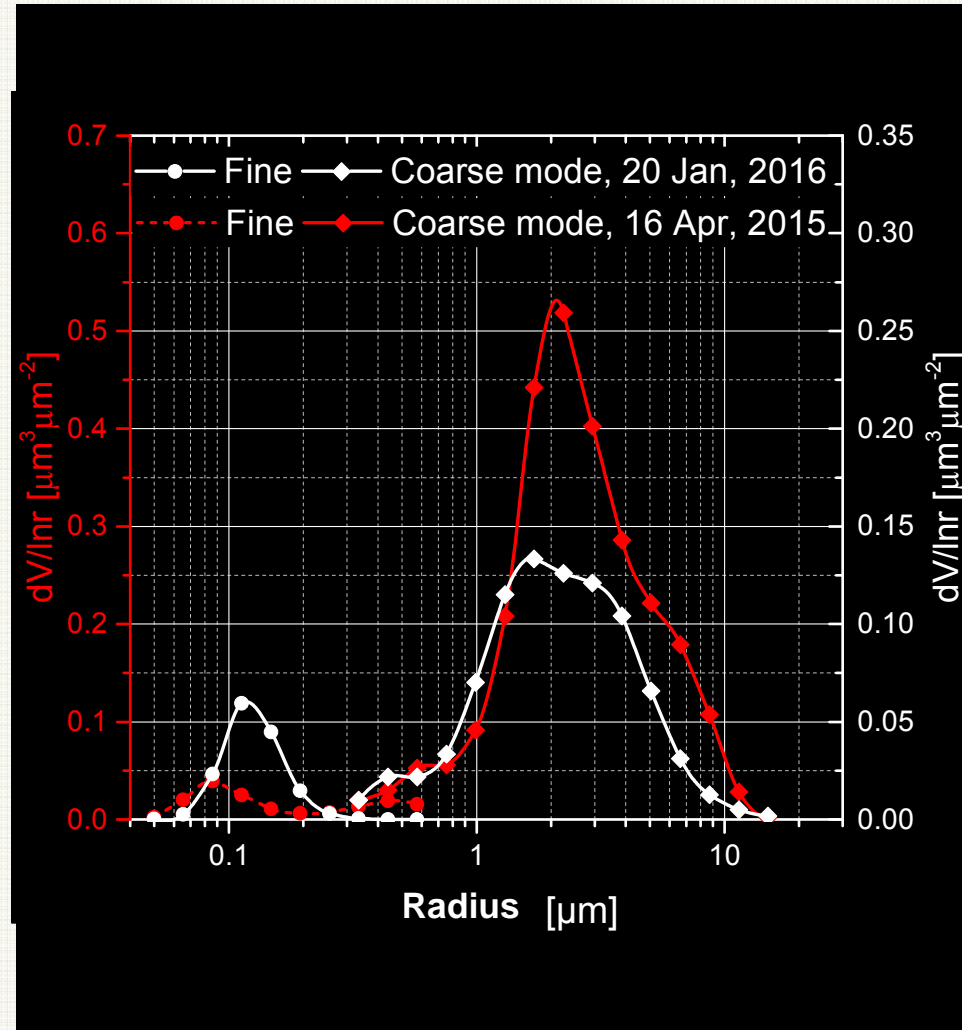
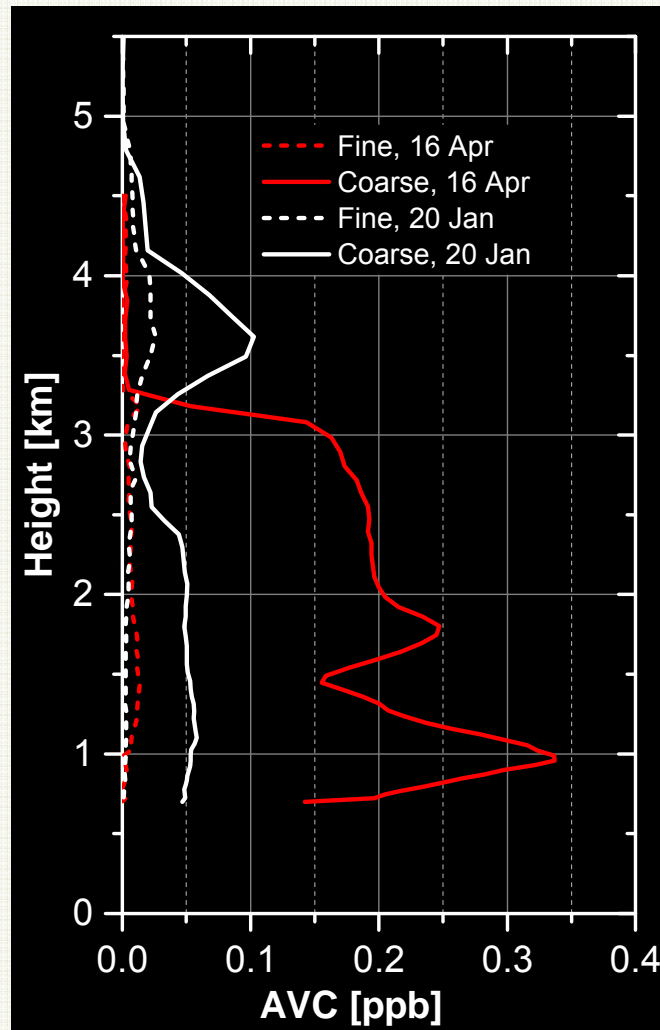


3 Backscattering + 2 Depolarizations

Qiaoyun HU, Anton Lopatin, etc.

LIDAR + AERONET – GRASP retrievals

• Vertical concentration



• Size distribution

Fig 3. Retrieval of aerosol vertical concentration and size distribution for 16 Apr, 2015 (09:04,) and 20 Jan, 2016 (09:15).

Qiaoyun HU, Anton Lopatin, etc.

Polar- Nephelometer (Martins et al.), GRASP

[Espinosa et al. 2017](#)

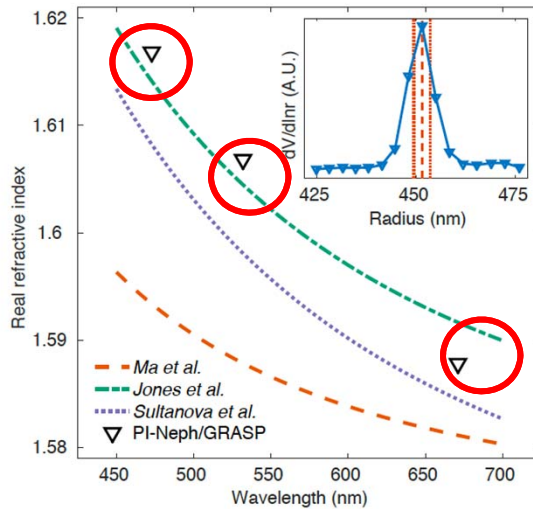


Figure 9. Retrieved real part of the refractive index for PSL spheres, alongside three previous, modern measurements of polystyrene refractive indices (Ma et al., 2003; Jones et al., 2013; Sultanova et al., 2003). The subplot shows the retrieved size distribution (blue) alongside the manufacturer's specified central radius (red dashes) and FW67 (red dots).

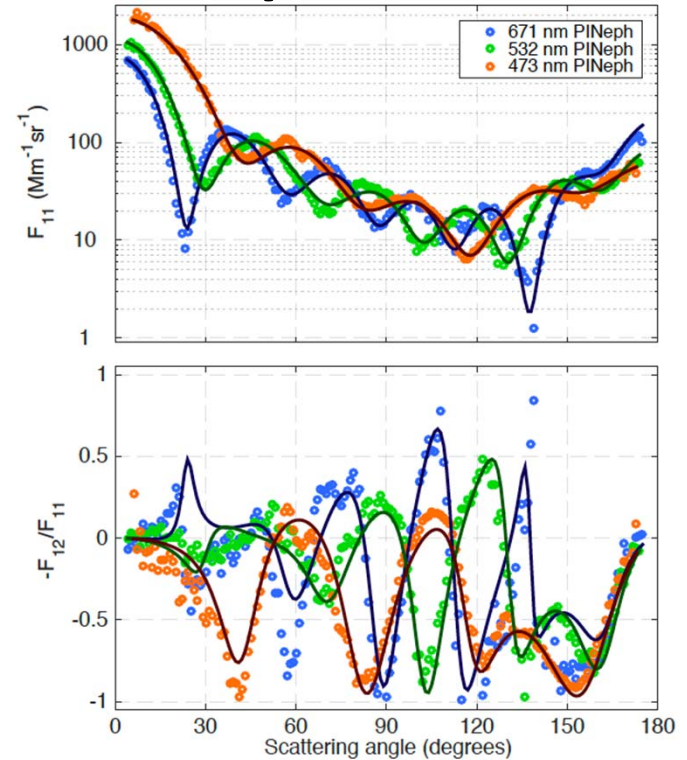


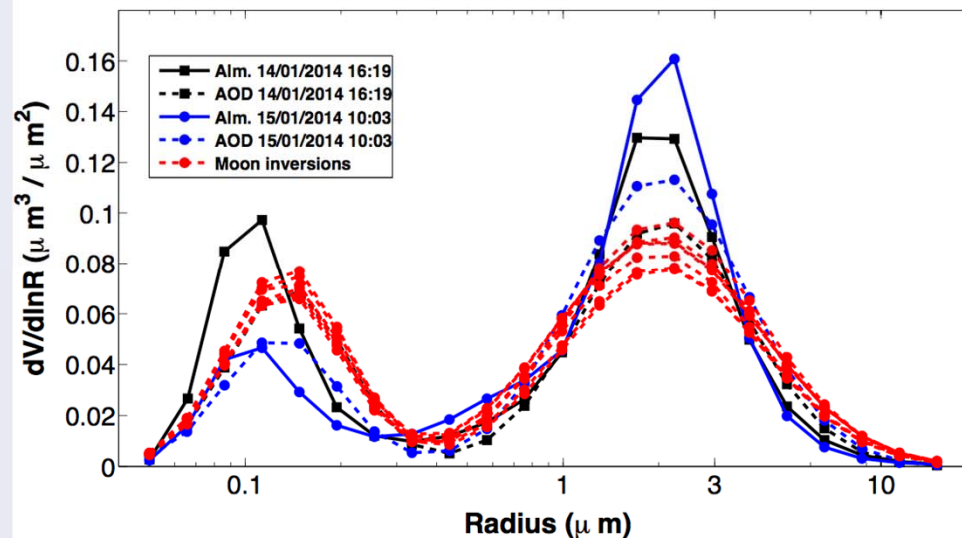
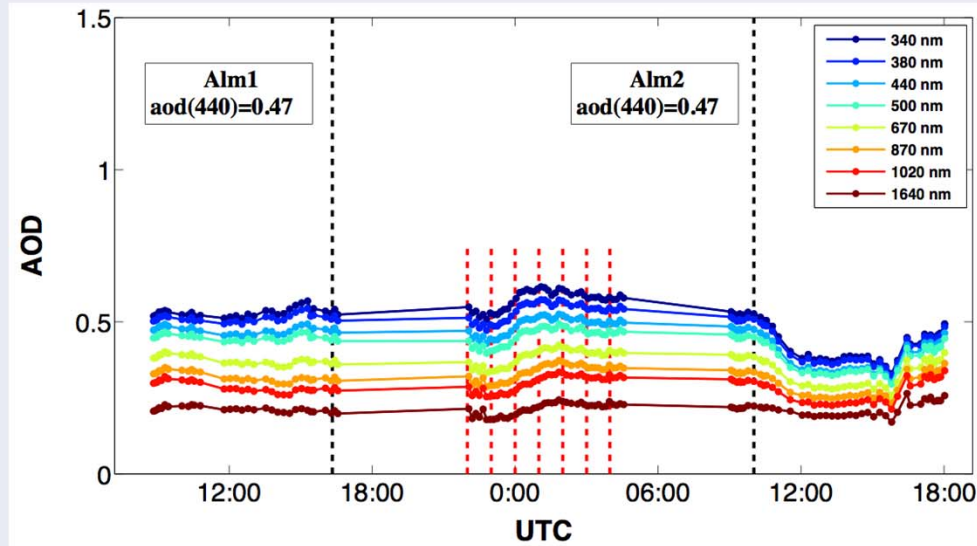
Figure 8. Scattering matrix elements at 473 nm (blue), 532 nm (green) and 671 nm (red) for 903 nm diameter PSL sample along with the corresponding GRASP fits (solid lines).

Compound	DRH (%)	Measured RH (%)	κ	r_{50}^{GRASP} (nm)	Sphere (%)	n_{dry}	$n_{\text{wet}}^{\text{GRASP}}$	$n_{\text{wet}}^{\kappa \text{Köhler}}$
NaCl	80	83.7 ± 2	0.91–1.33	144	100	1.544	1.395	1.353–1.372
$(\text{NH}_4)_2\text{SO}_4$	75	82.6 ± 2	0.33–0.72	120	100	1.530	1.383	1.370–1.414
NH_4NO_3	62	83.5 ± 2	0.58–0.75	129	54	1.554	1.392	1.371–1.393

Lunar Photometer: Night GRASP/AOD inversions

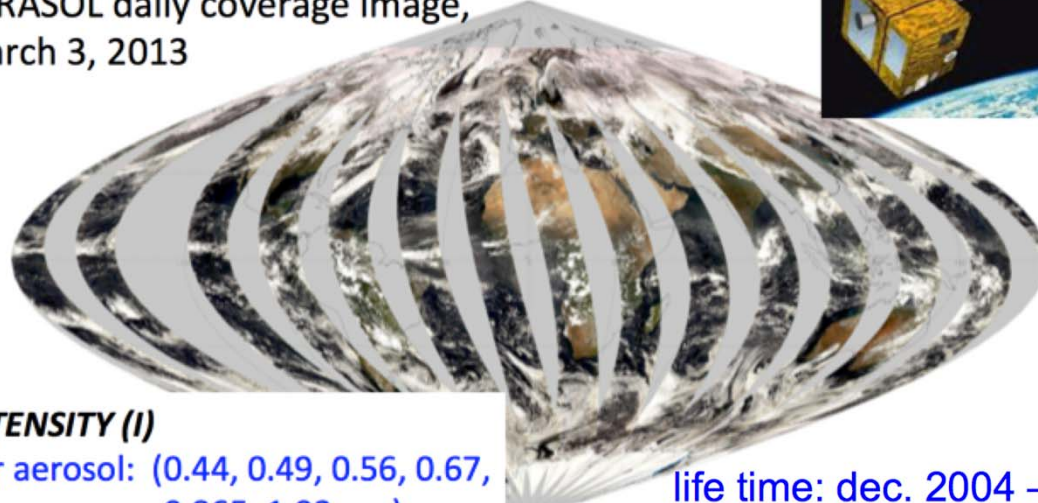
Dakar - 14/01/2014 and 15/01/2014 - Ph#714

*Torres et al.,
2017*



PARASOL: the space-borne instrument most suitable for enhanced aerosol/surface characterization

PARASOL daily coverage image,
March 3, 2013



INTENSITY (I)

for aerosol: (0.44, 0.49, 0.56, 0.67, 0.865, 1.02 μm)

for gas absorption: (0.763, 0.765, 0.910 μm)

POLARIZATION (Q, U): (0.49, 0.67, 0.865 μm)

life time: dec. 2004 – 2013

Swath: about 1600 km cross-track

Global coverage: every 2 days

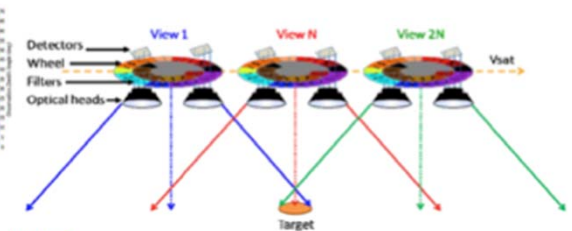
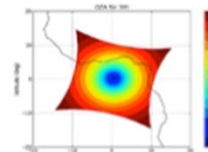
1 pixel spatial resolution: 5.3km \times 6.2km

Viewing directions: 16: (80 $^{\circ}$ – 180 $^{\circ}$)

Multi-Angular Polarimetric imagery:

What is a real value?

3MI:



Swath: ~ 2200 km

Global coverage: every :

Pixel spatial resolution: ~ 4 km

Viewing direction: 10 – 14 (80 $^{\circ}$ – 180 $^{\circ}$);

for aerosol (0.41, 0.44, 0.49, 0.56, 0.67, 0.87, 1.37, 1.65, 2.13);

for gas absorption (0.763, 0.765, 910);

polarization (0.41, 0.44, 0.49, 0.56, 0.67, 0.87, 1.37, 1.65, 2.13);

PARASOL:

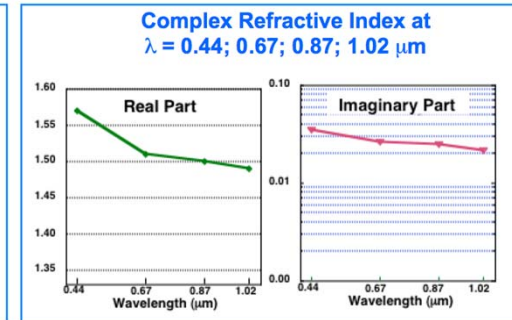
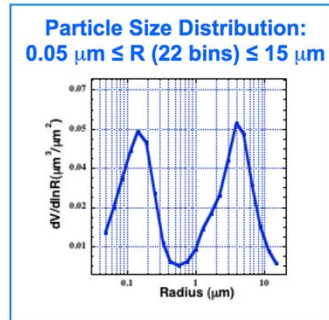
- radiances: (443, 490, 560, 670, 870, 1020 nm)
- polarization: (490, 670, and, 870 nm)
- up to 16 viewing directions



144 measurements

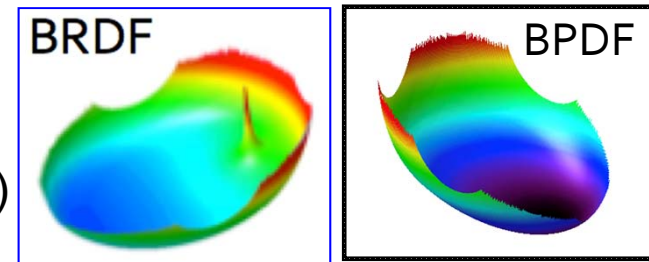
AEROSOL:

- size distribution (5 or more bins)
- spectral index of refraction (8λ)
- sphericity fraction;
- aerosol height



SURFACE:

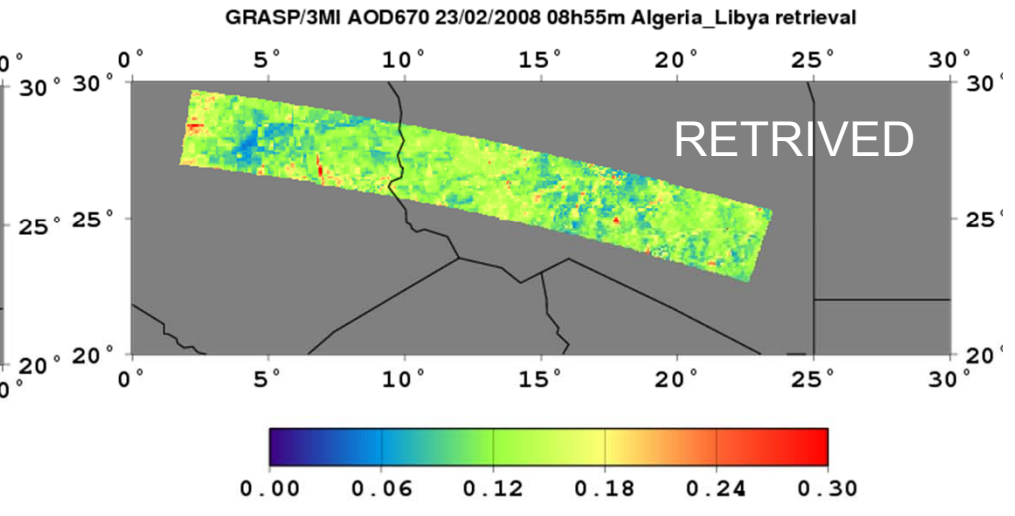
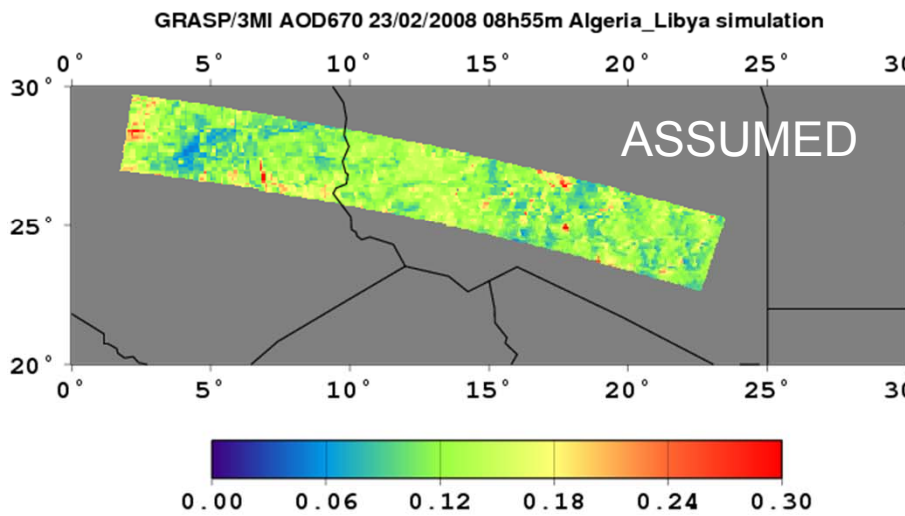
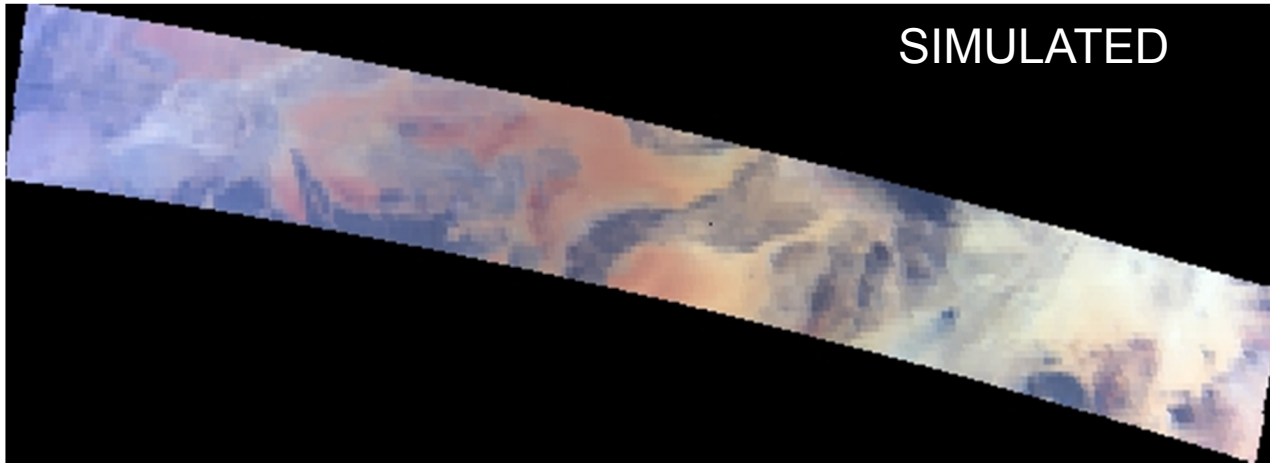
- BRDF (3 spectrally dependent parameters)
- BPDF (1 or 2 spectrally dependent parameters)



$$43 = (5 \text{ (SD)} + 12 \text{ (ref. ind.)} + 1 \text{ (nonsp.)} + 18 \text{ (BRDF)} + 6 \text{ (BPDF)} + 1 \text{ (height)})$$

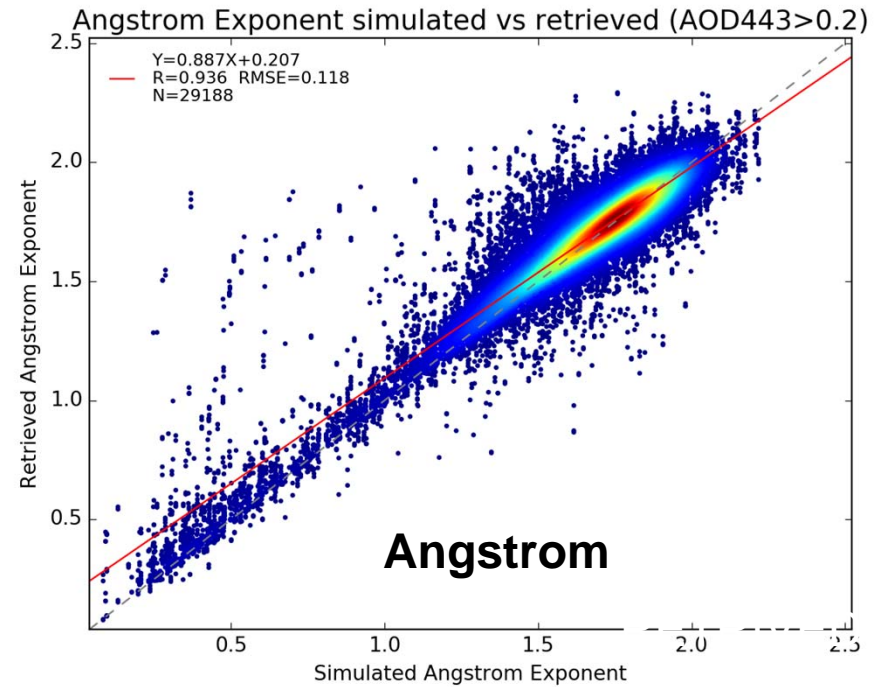
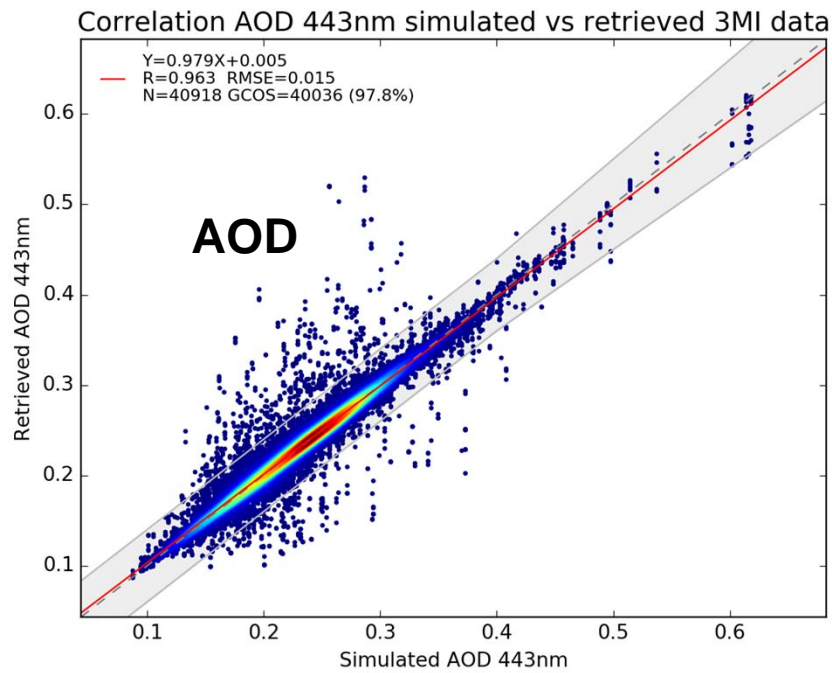


3MI / Metop



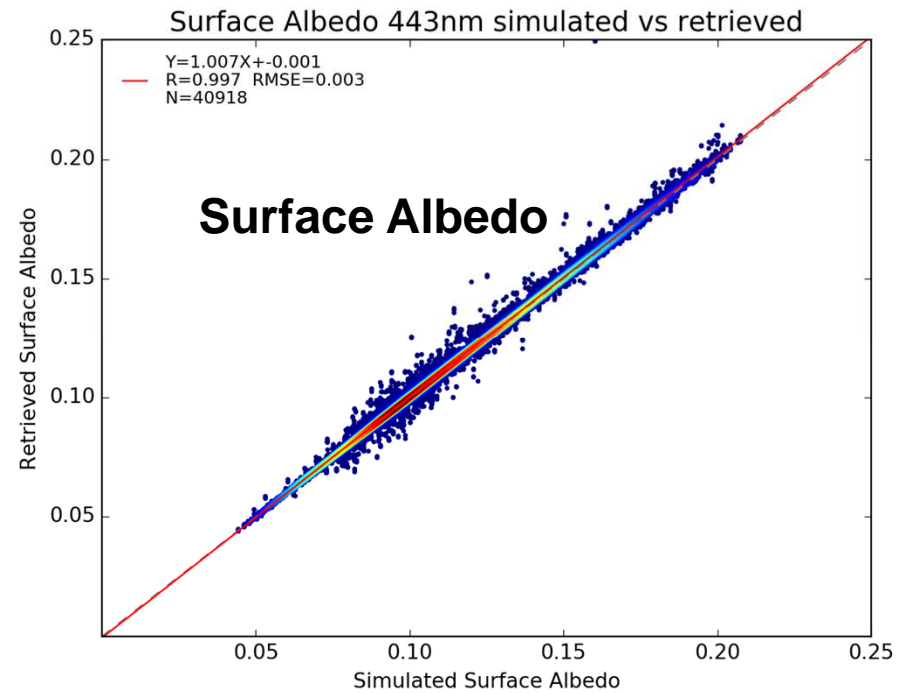
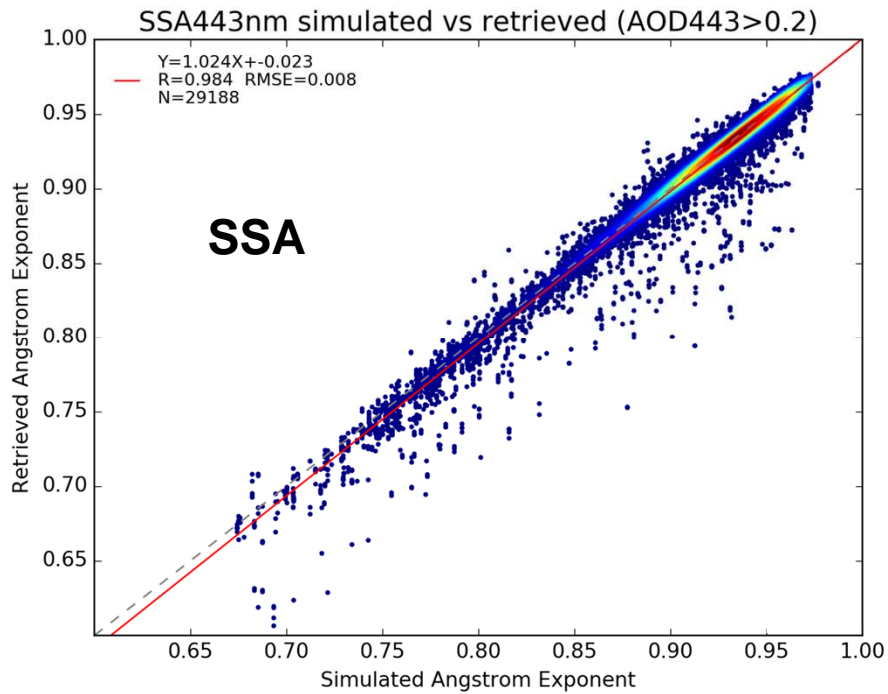


3MI / Metop





3MI / Metop



PARASOL:

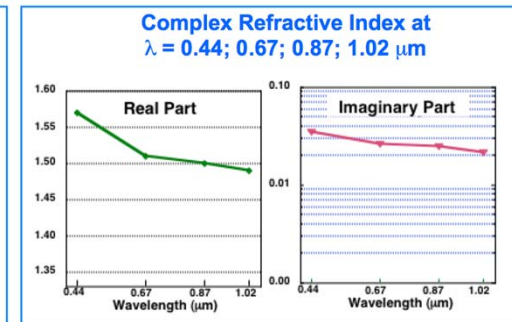
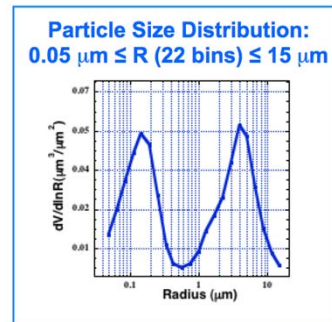
- radiances: (443, 490, 560, 670, 870, 1020 nm)
- polarization: (490, 670, and, 870 nm)
- up to 16 viewing directions



144 measurements

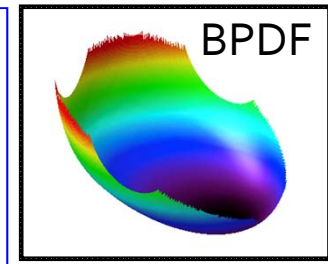
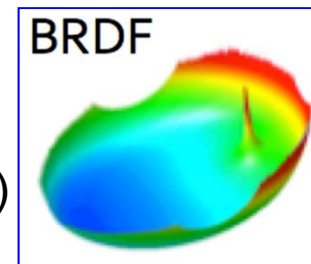
AEROSOL:

- size distribution (5 or more bins)
- spectral index of refraction (8λ)
- sphericity fraction;
- aerosol height



SURFACE:

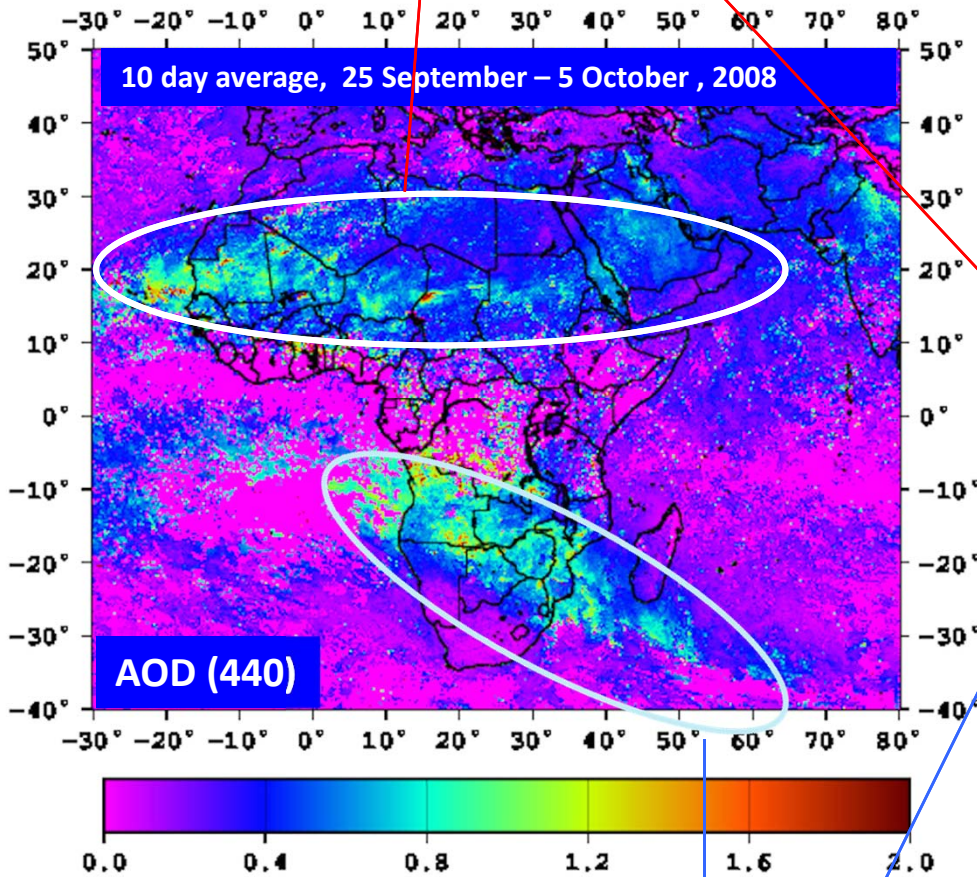
- BRDF (3 spectrally dependent parameters)
- BPDF (1 or 2 spectrally dependent parameters)



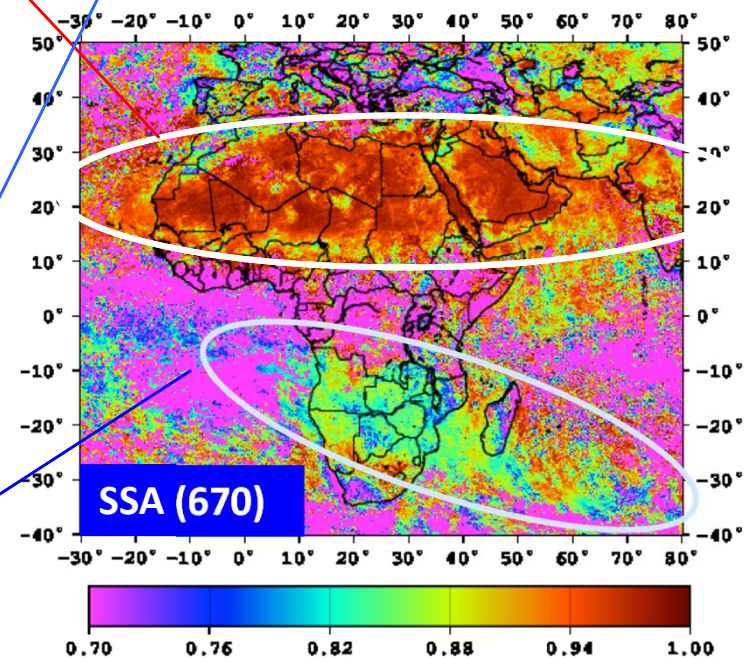
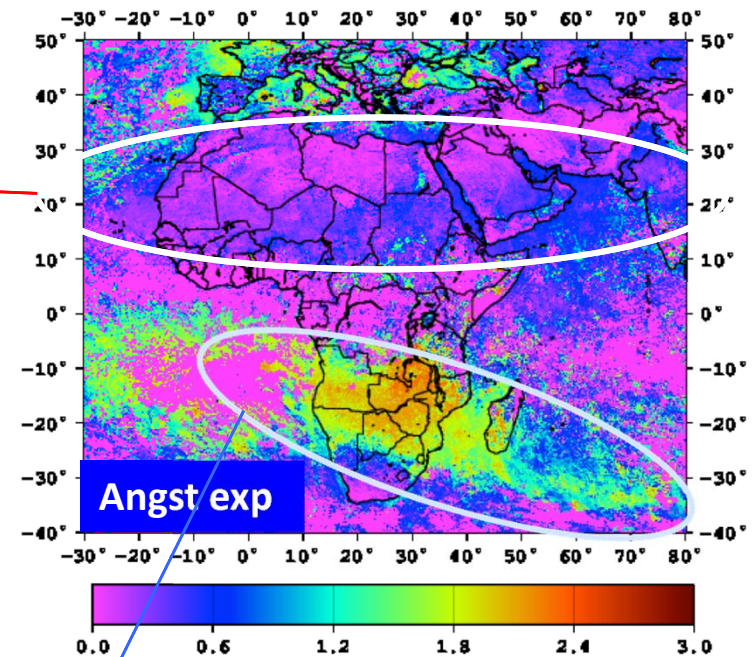
$$43 = (5 \text{ (SD)} + 12 \text{ (ref. ind.)} + 1 \text{ (nonsp.)} + 18 \text{ (BRDF)} + 6 \text{ (BPDF)} + 1 \text{ (height)})$$

GRASP: towards aerosol classification

Desert Dust

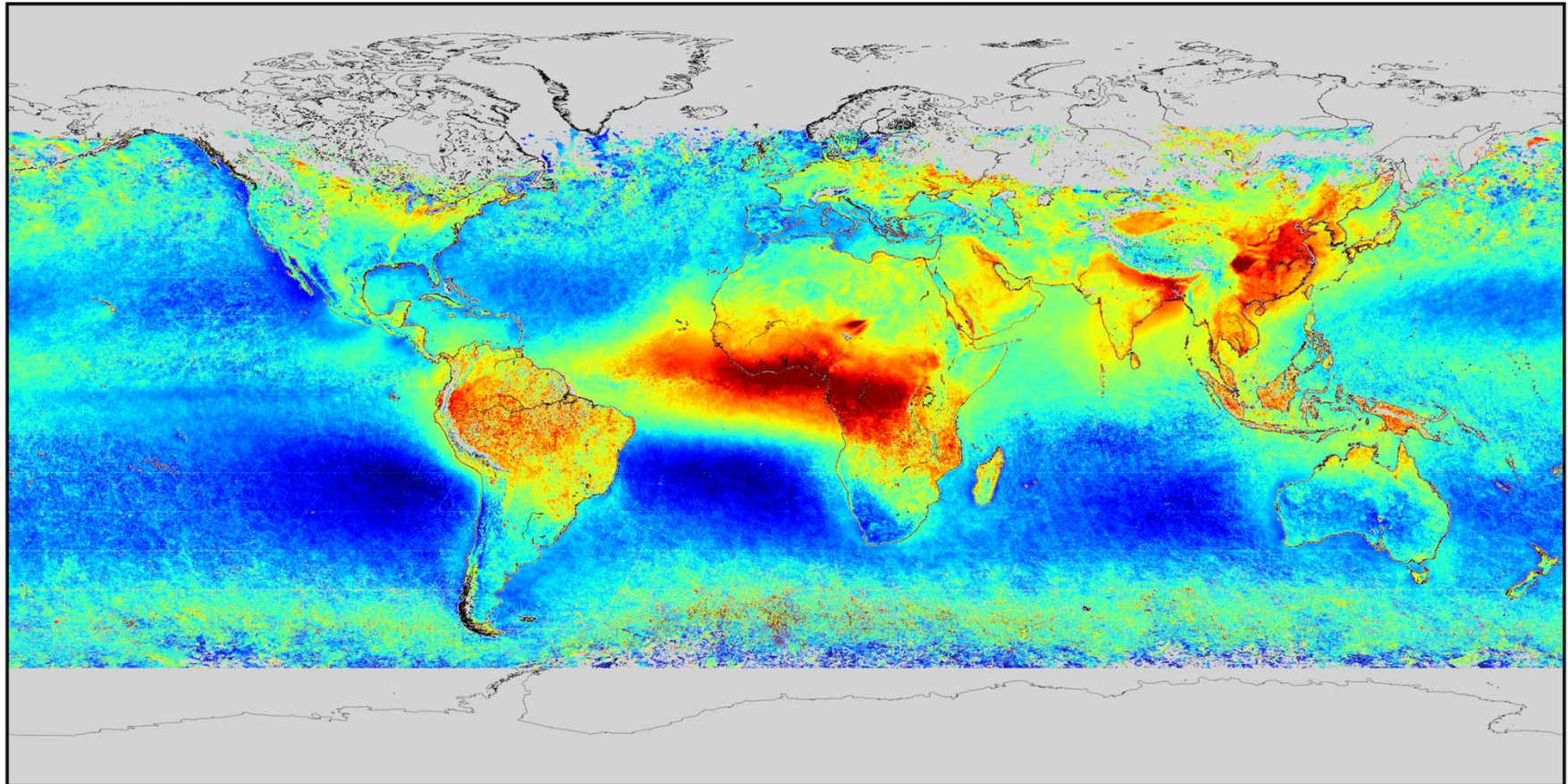


Biomass Burning



AOD (565), Winter (PARASOL archive average)

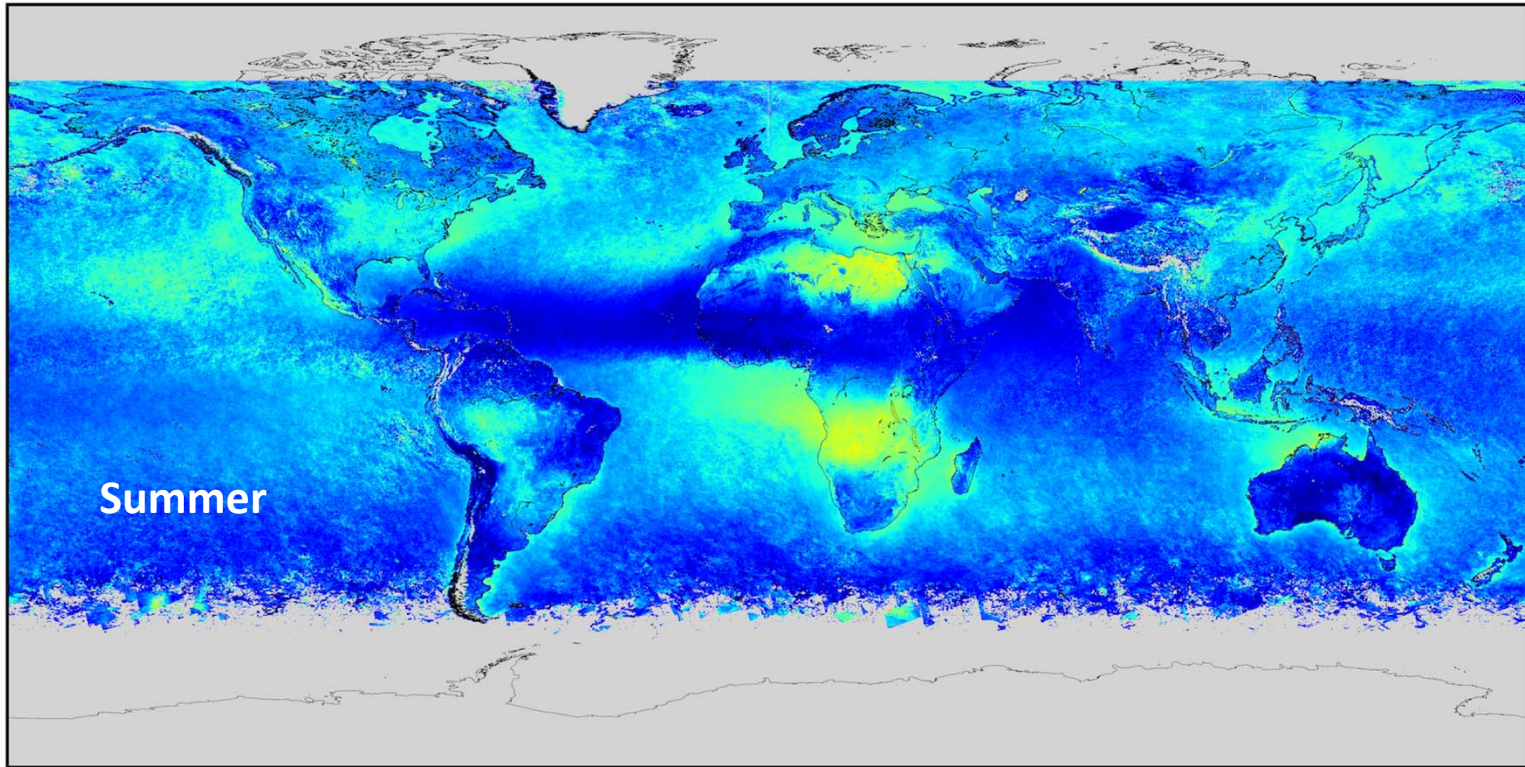
Averaged Winter data of POLDER Log AOD 565 (2005-2013)



Amount of aerosol

Angstrom exponent, Summer (PARASOL archive average)

Averaged Summer data of POLDER Angstrom Exponent 670-865 (2005-2013)



Large particles

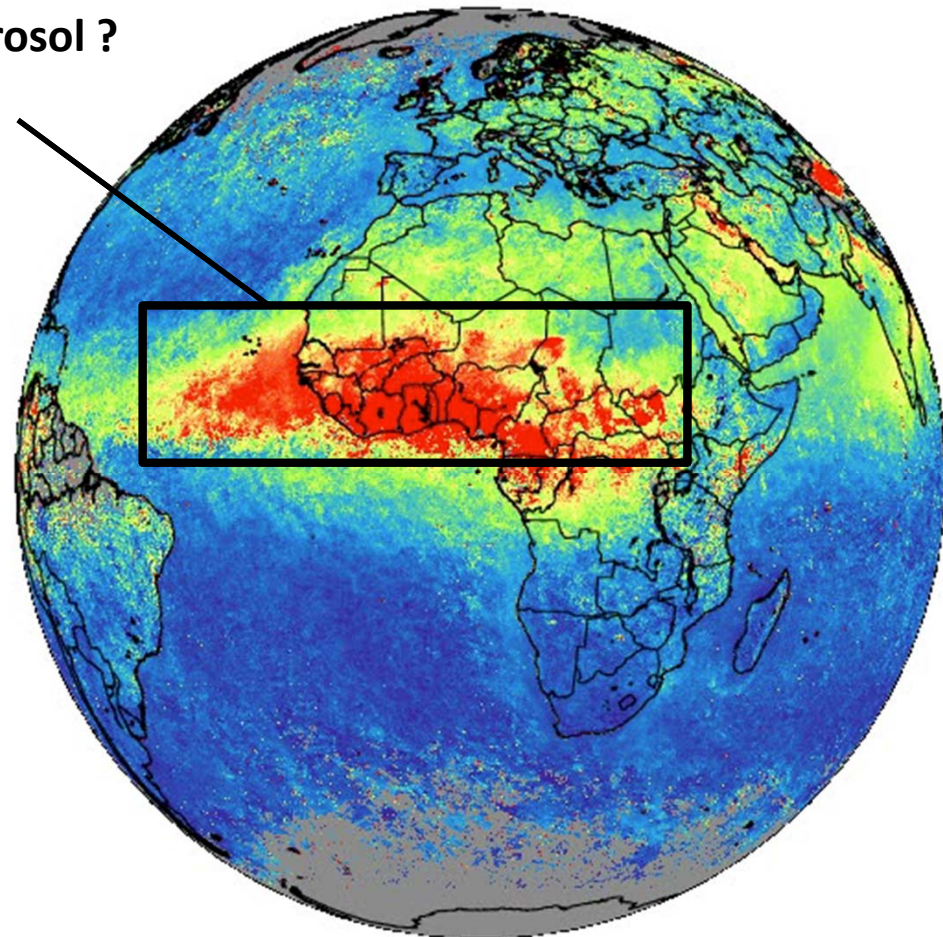
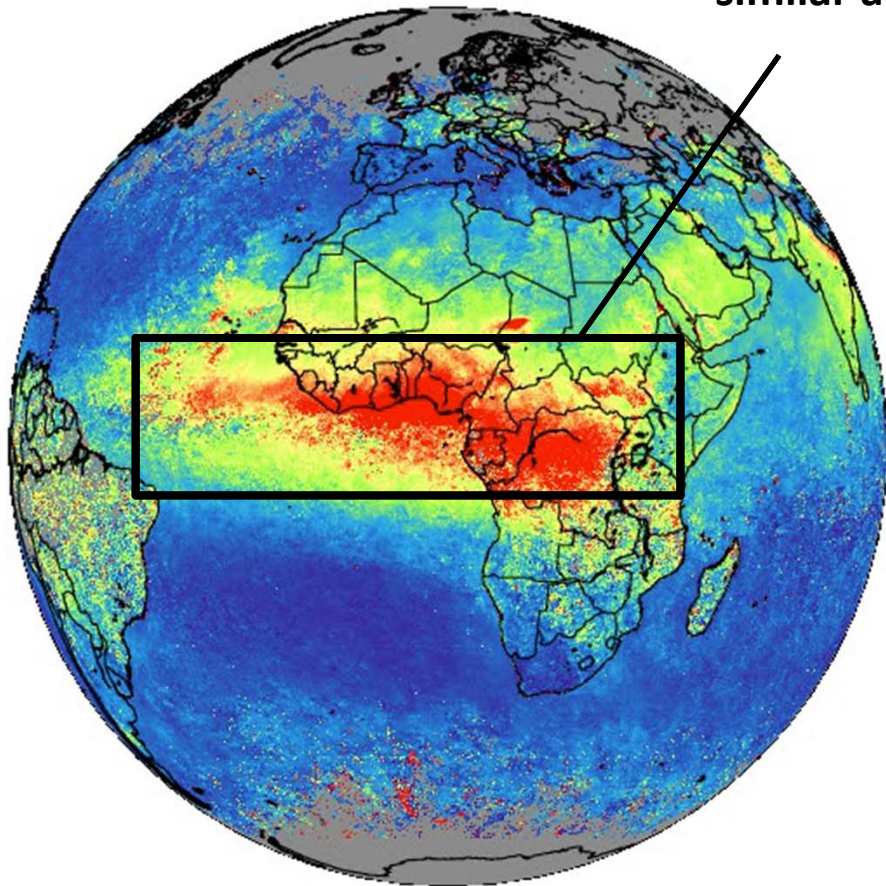
Small particles

AOD(565) – aerosol loading

2012 Winter

2012 Spring

similar aerosol ?



Biomass burning



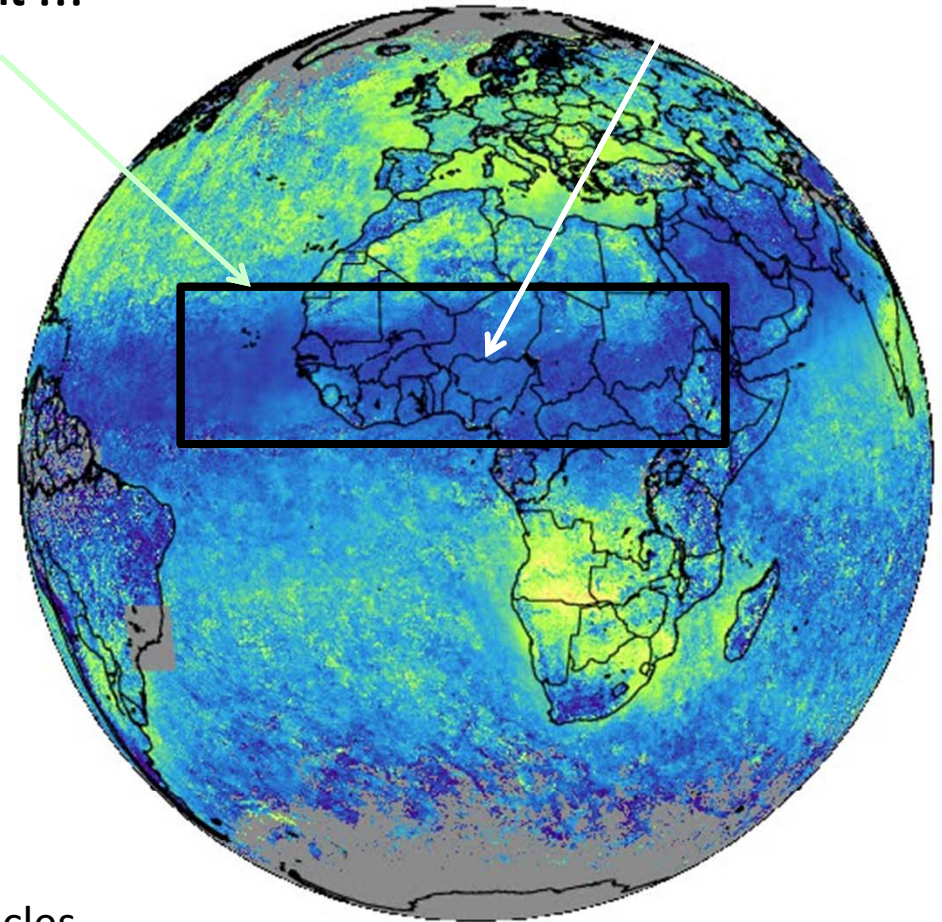
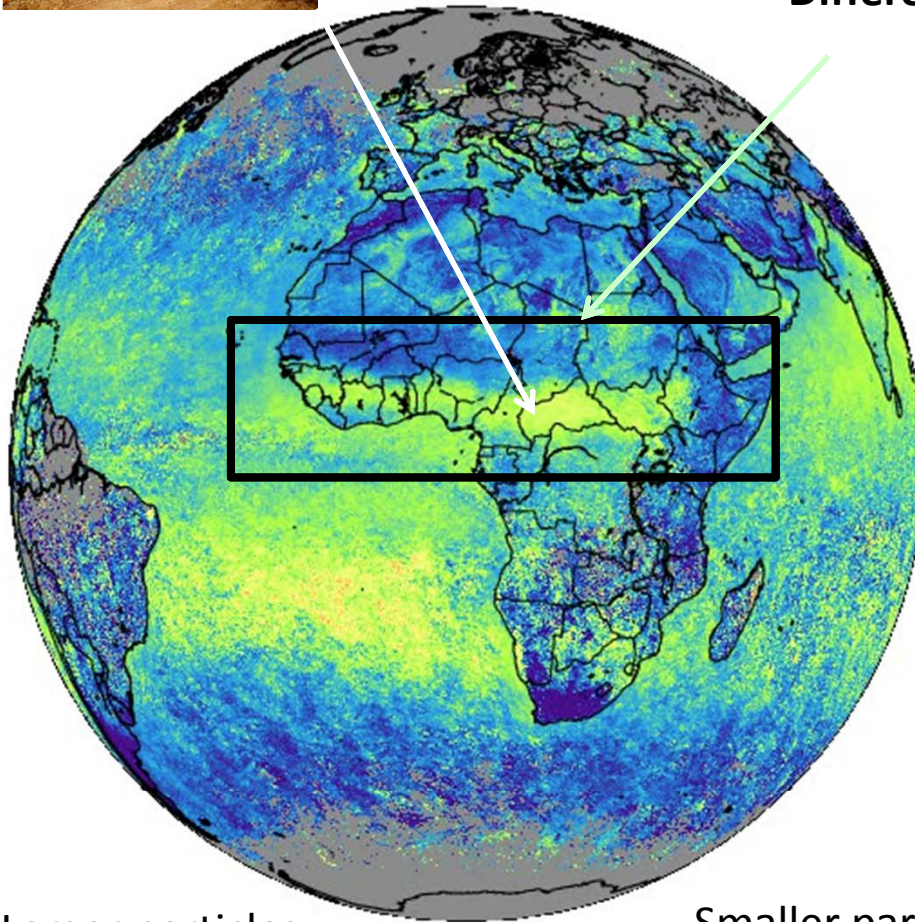
Angstrom exponent

2012 Winter

2012 Spring

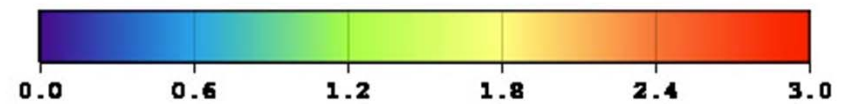
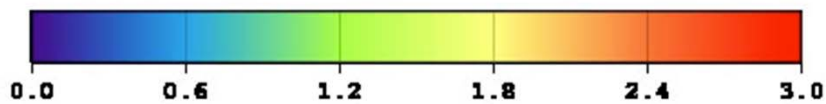


Different !!!



Larger particles

Smaller particles



Validation vs AERONET 2004 - 2013

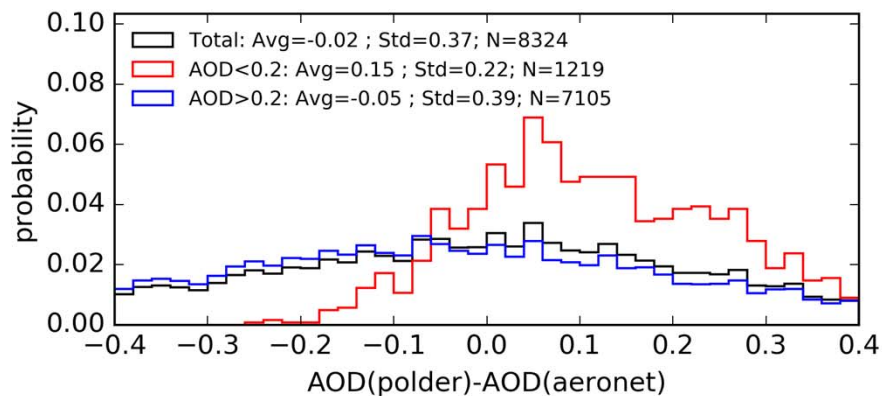
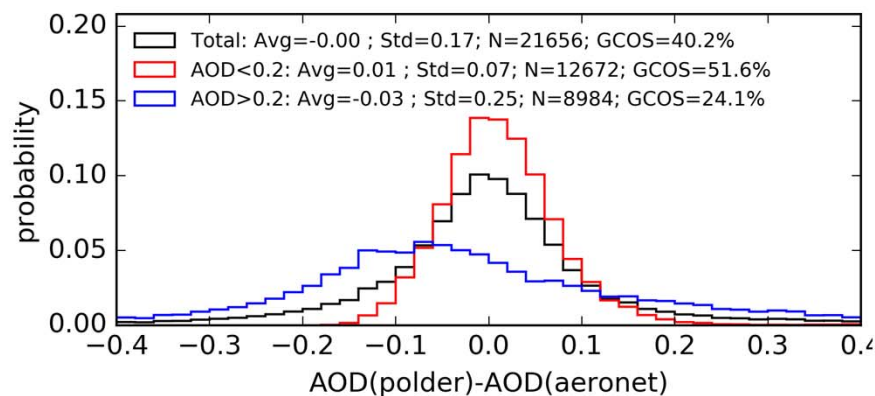
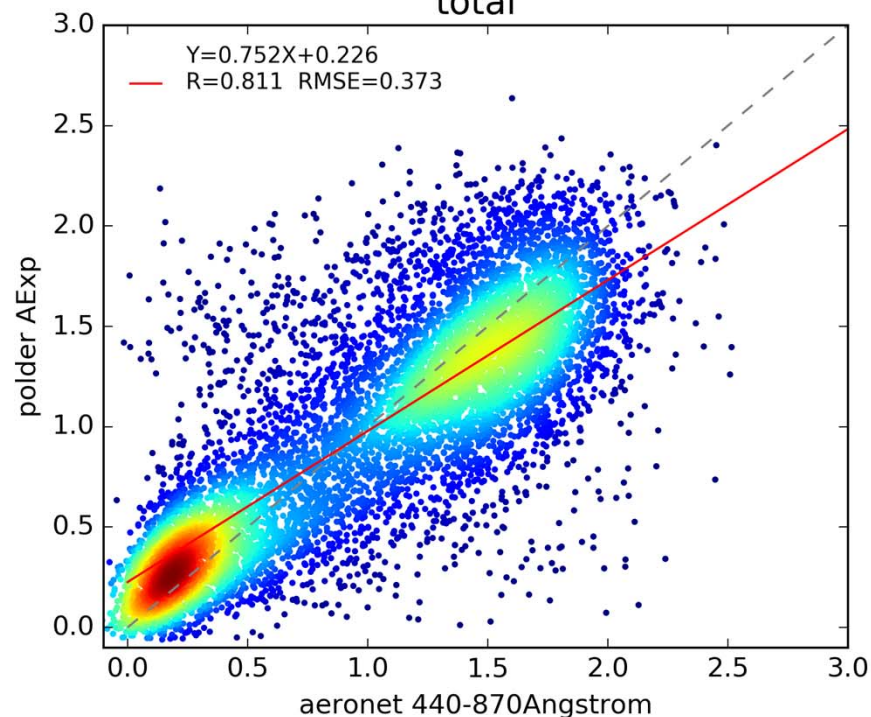
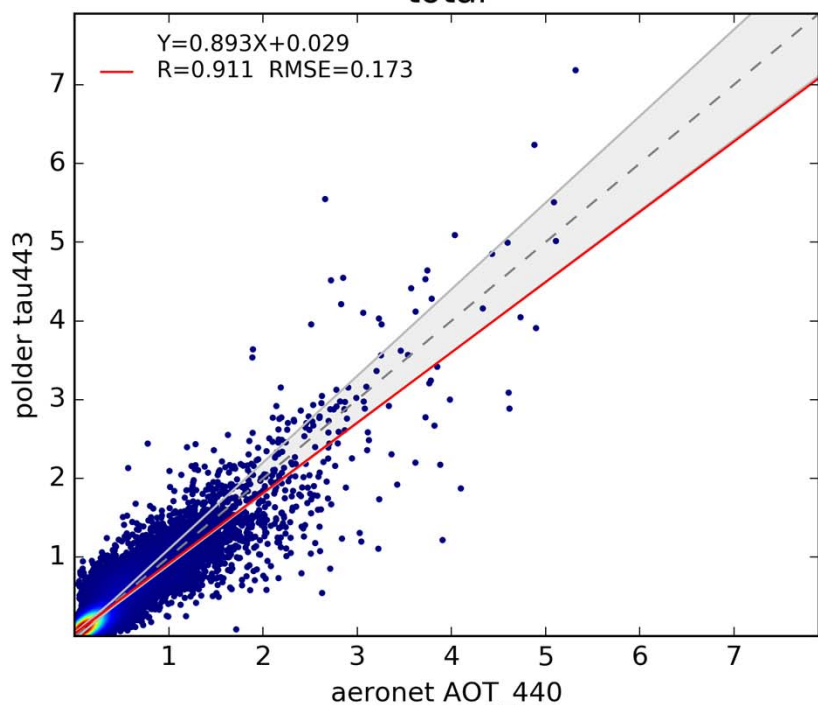
AOD

Land

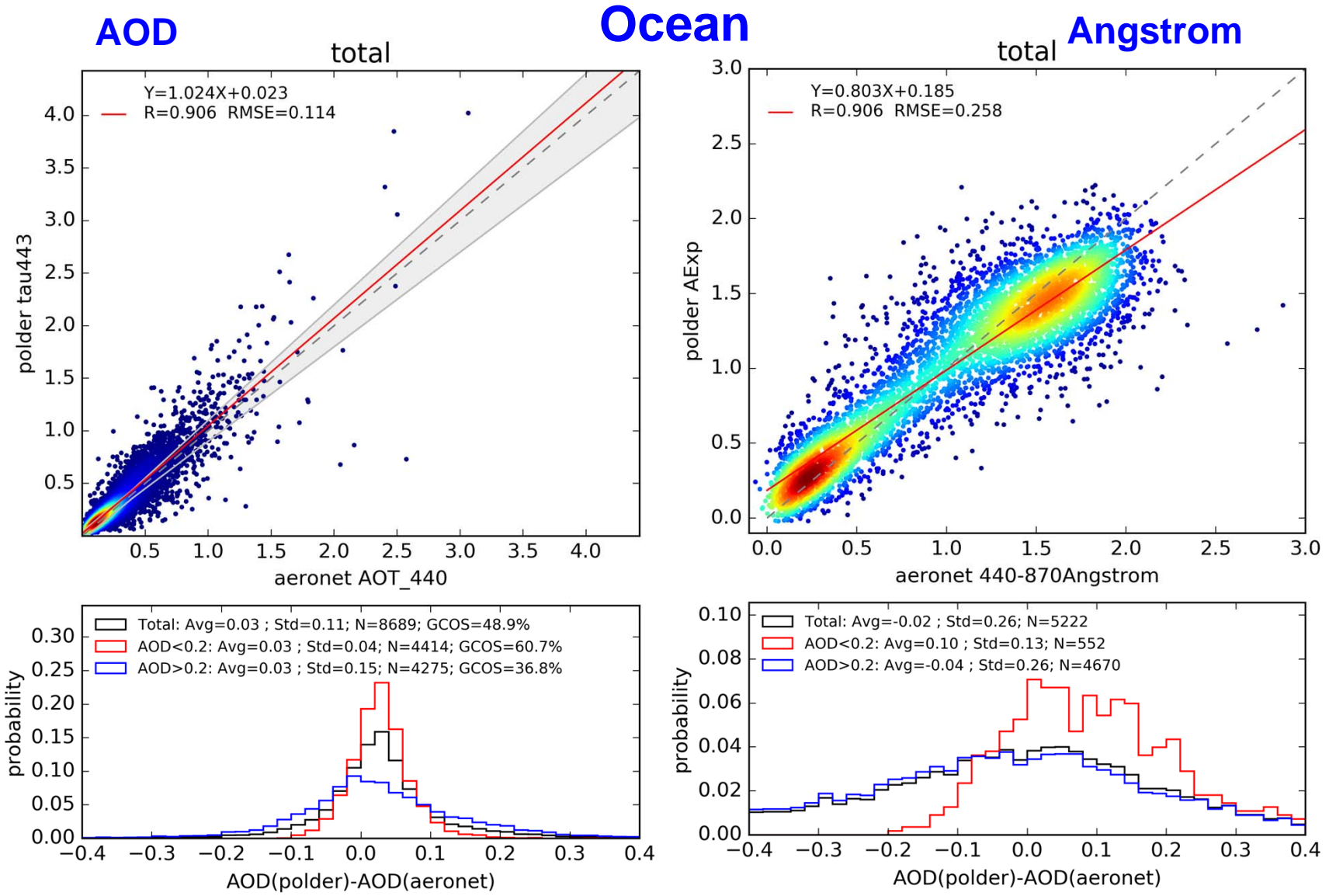
Angstrom

total

total



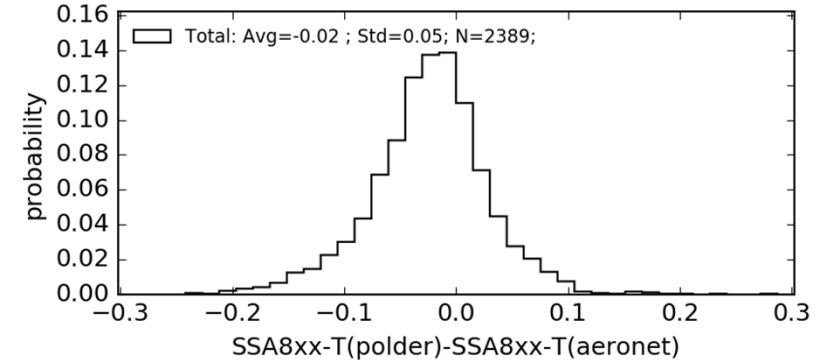
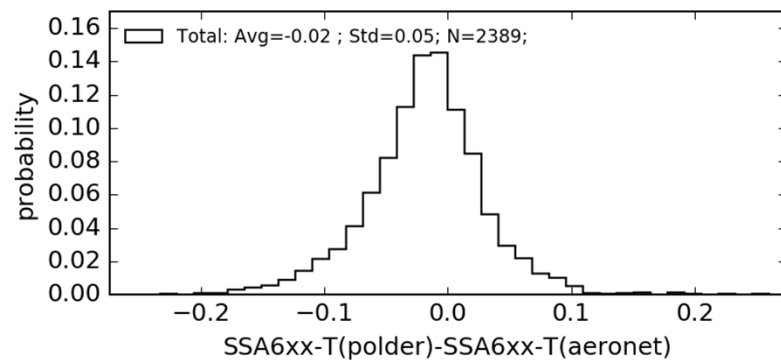
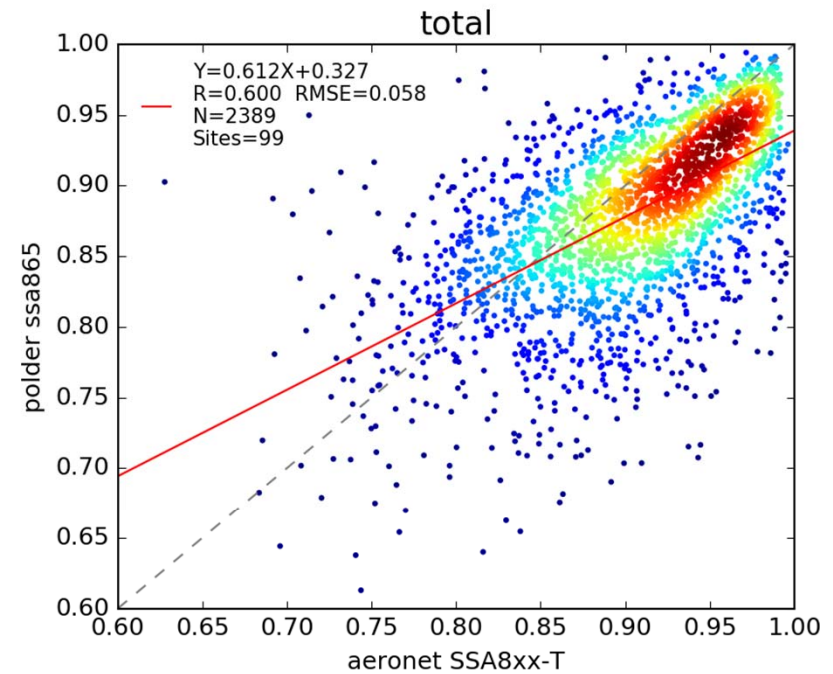
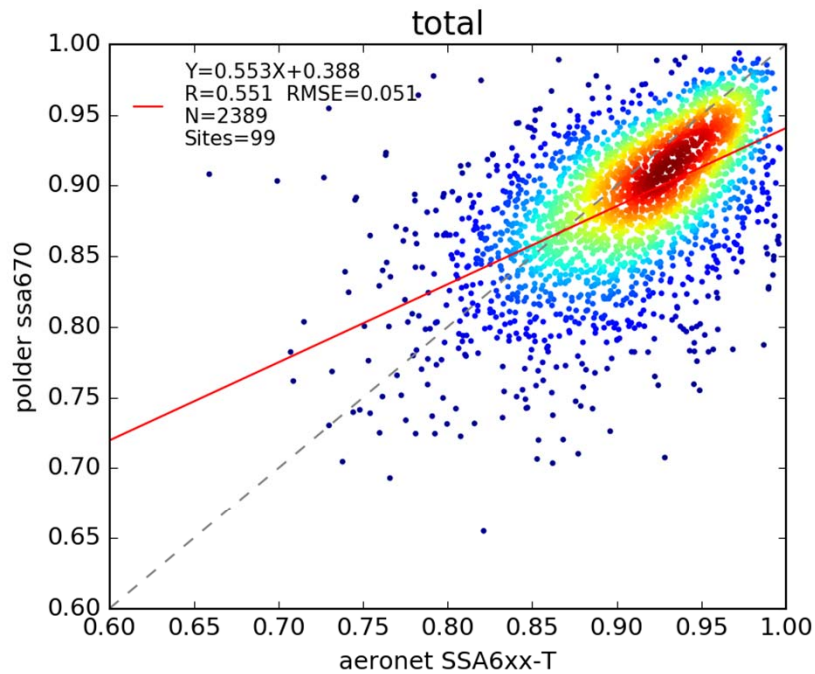
PARASOL Validation vs AERONET 2004 - 2013



PARASOL Validation vs AERONET 2004 - 2013

SSA(670) R=0.55 Land + Ocean

SSA(870) R=0.6

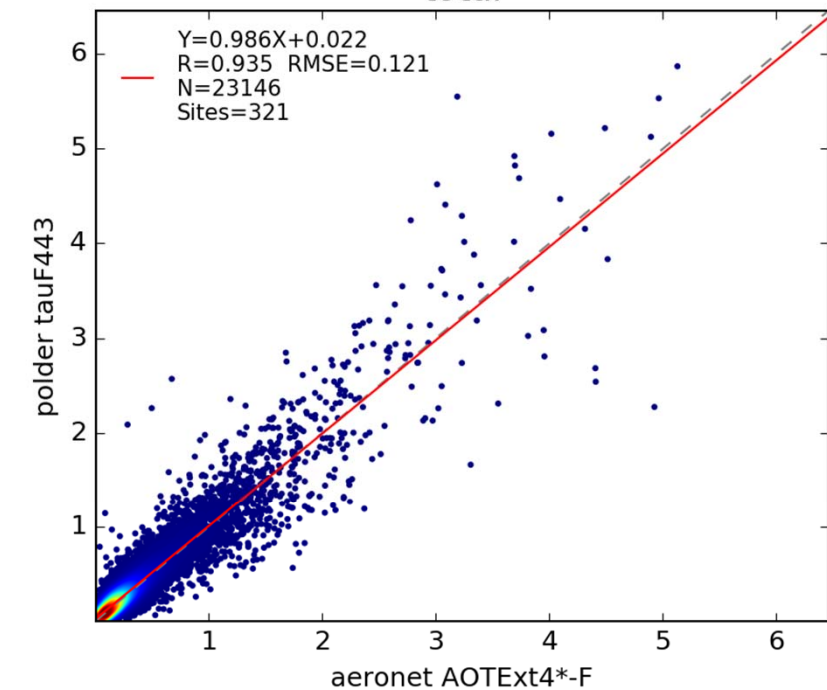


PARASOL Validation vs AERONET 2004 - 2013

Land + Ocean

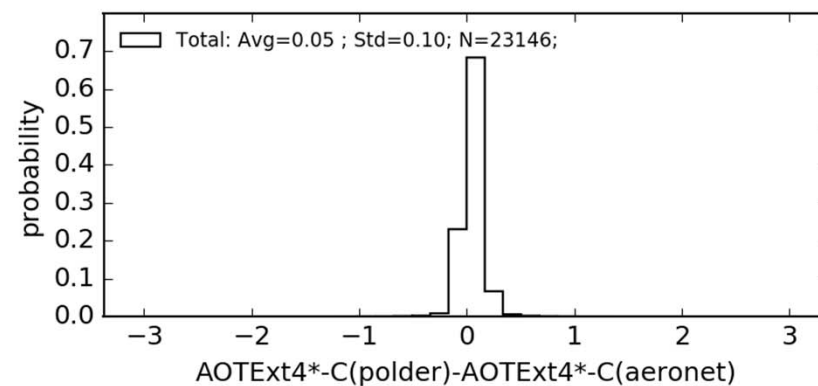
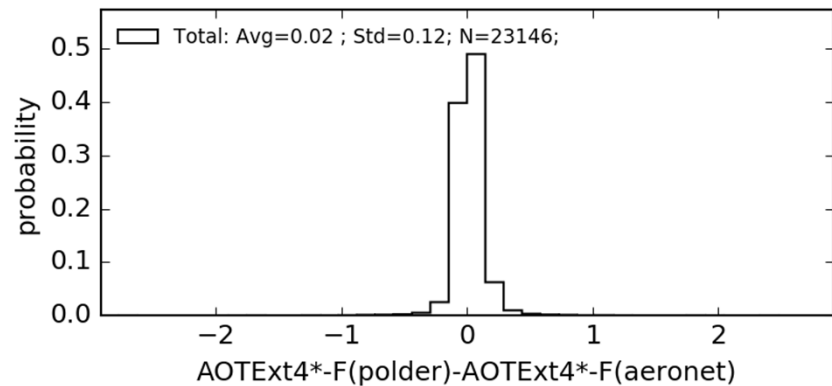
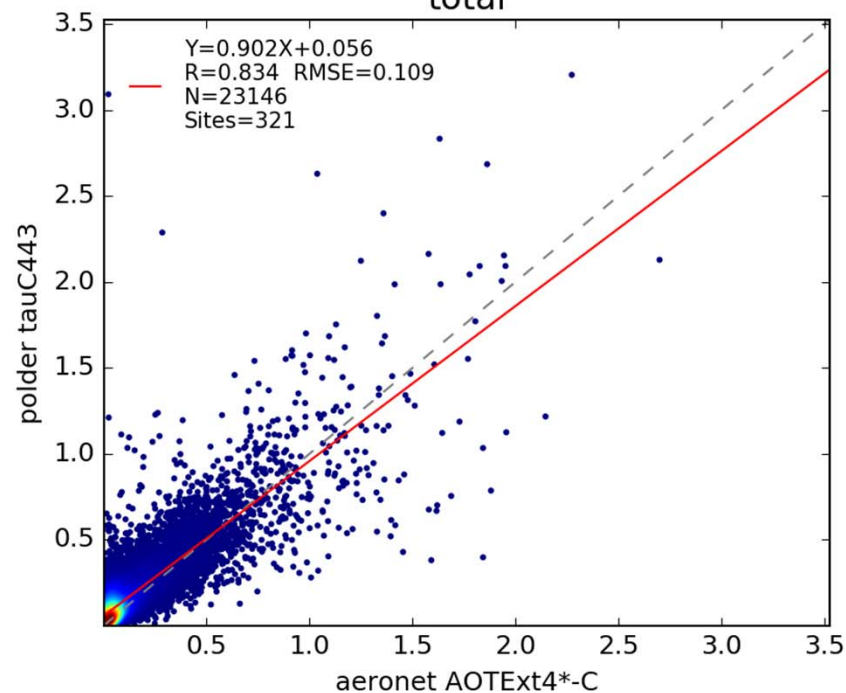
AOD Fine mode

total



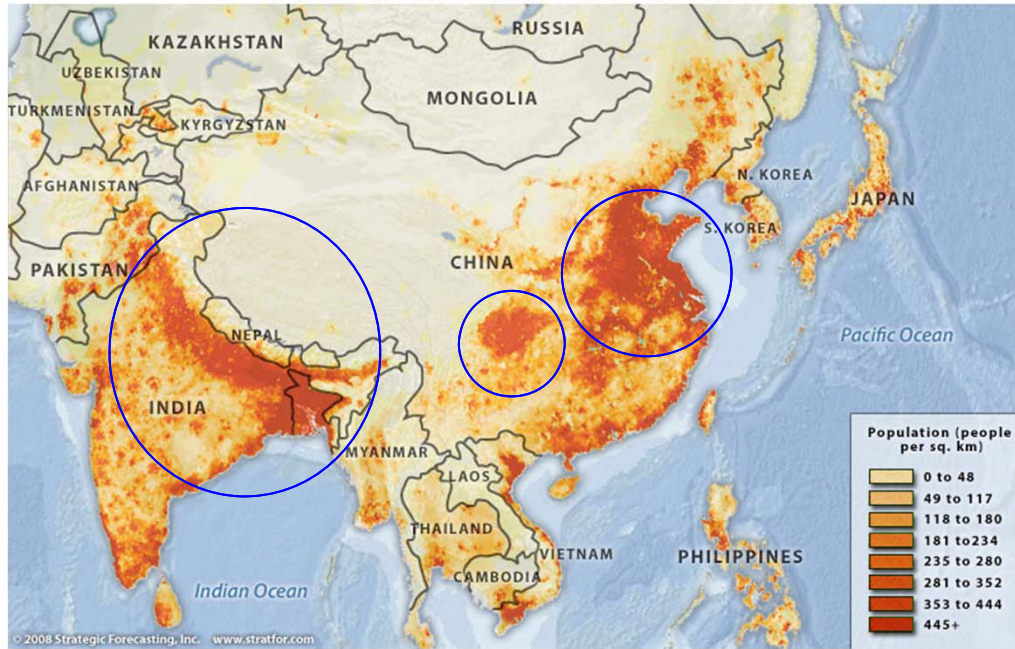
AOD Coarse mode

total



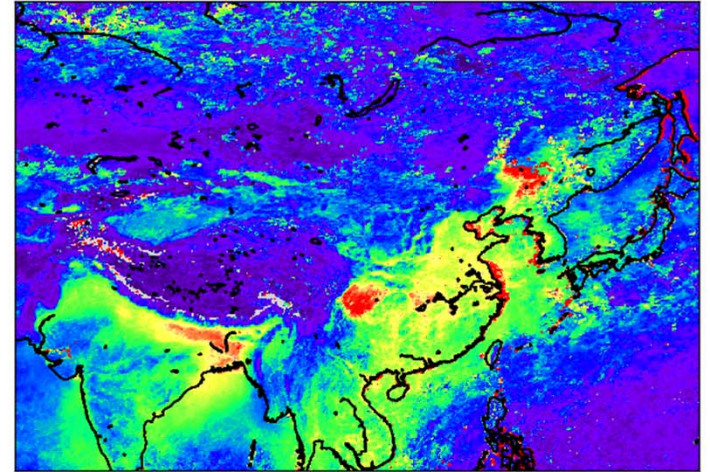
Correlation of population density and pollution

POPULATION DENSITY MAP OF ASIA

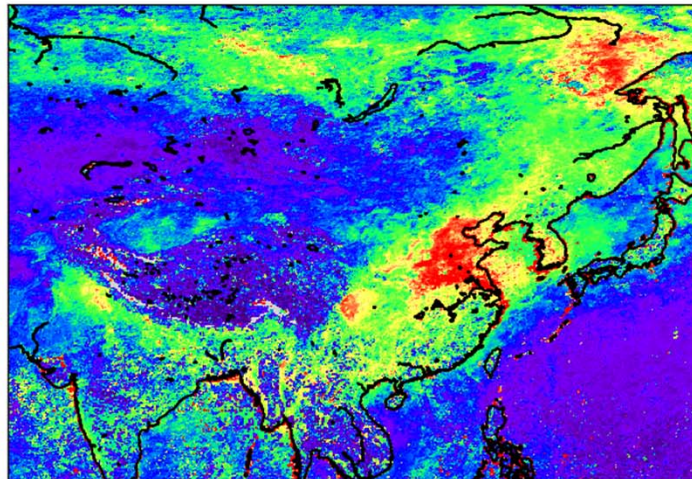


$AOD_{fine}(565)$

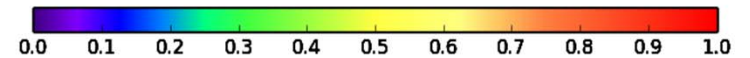
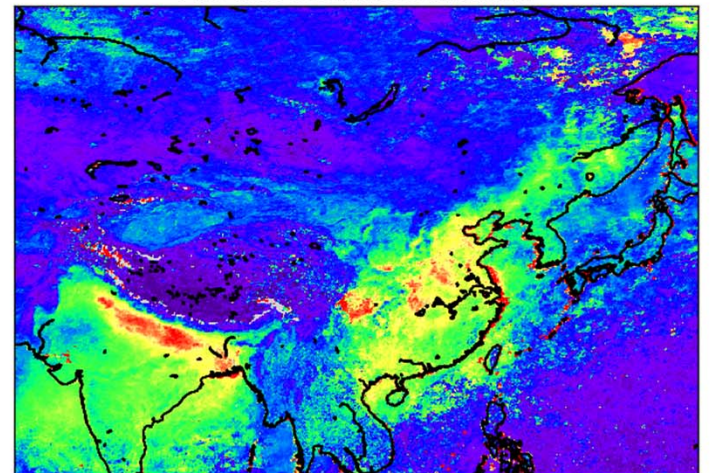
Fine AOD 565nm 2011 Winter



Fine AOD 565nm 2011 Summer

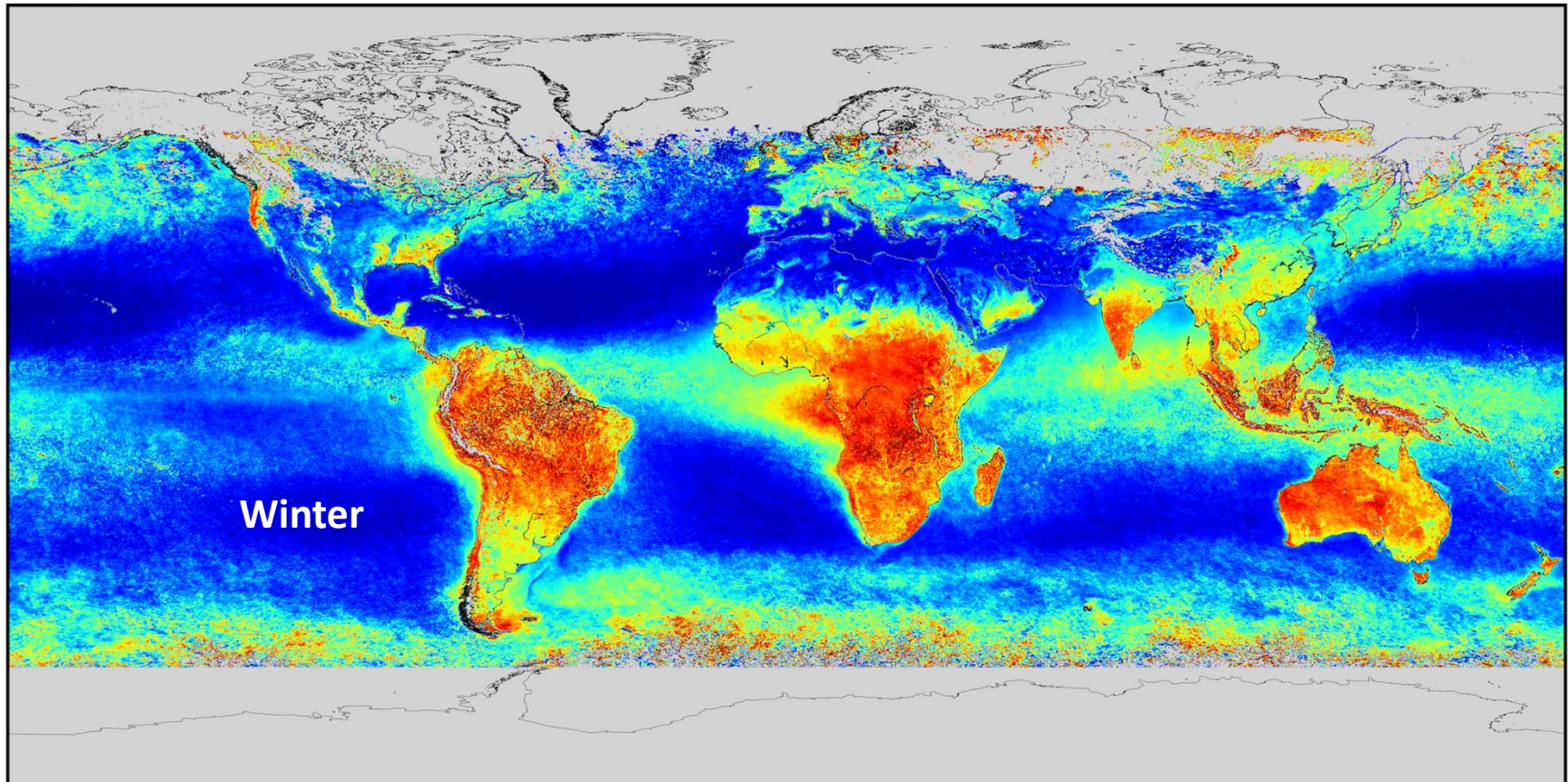


Fine AOD 565nm 2011 Autumn



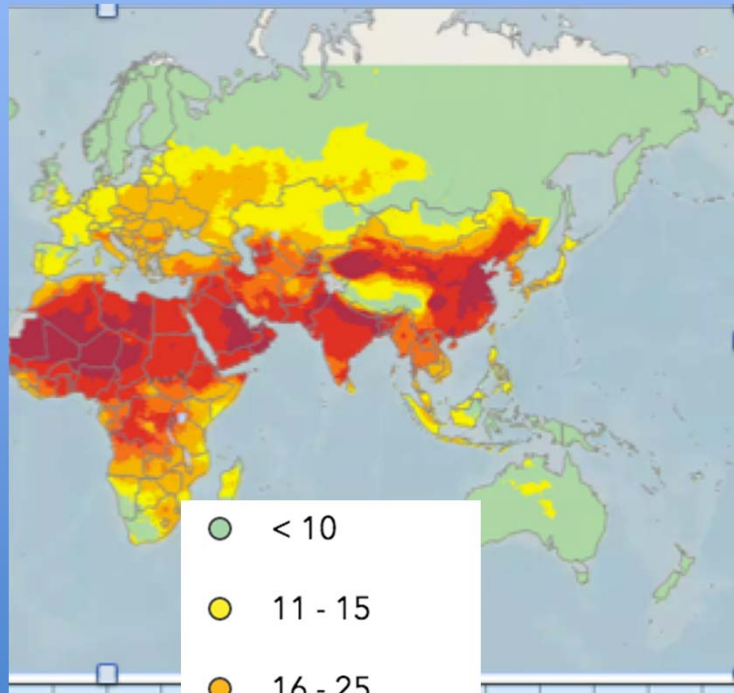
Scale height (m), Winter (PARASOL archive average)

Averaged Winter data of POLDER Vertical Profile Height (2005-2013)



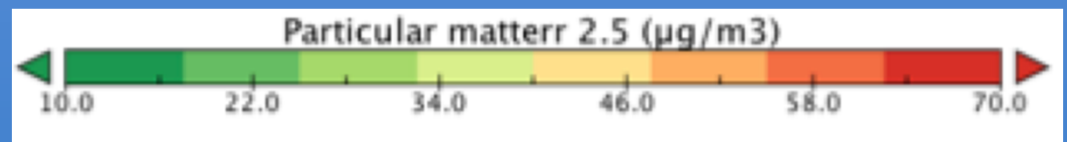
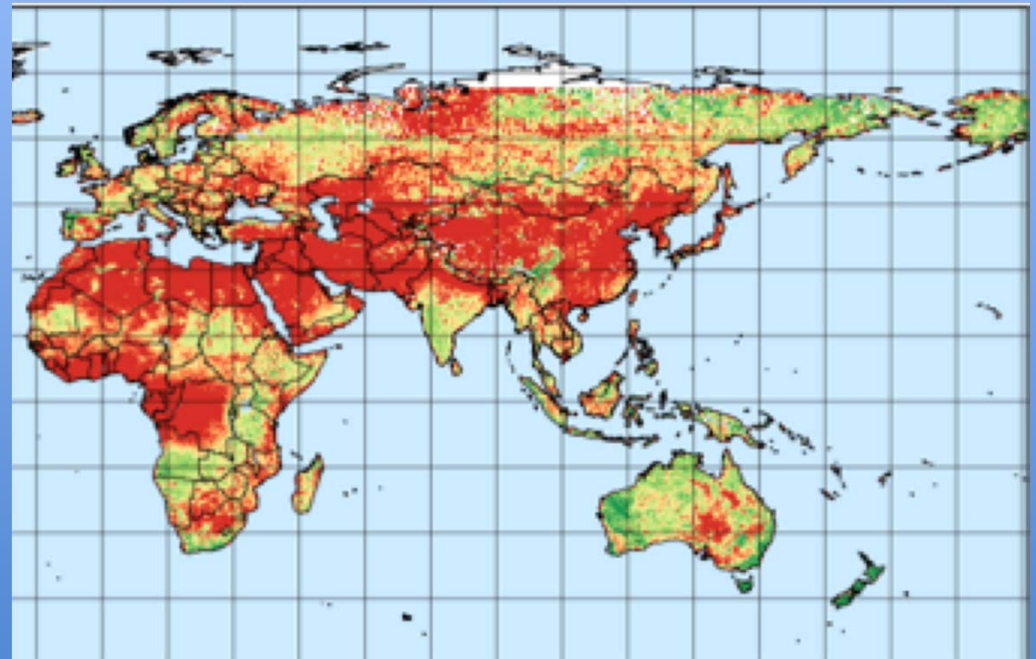
PM2.5 climatology

WHO Global Urban Ambient
Air Pollution Database



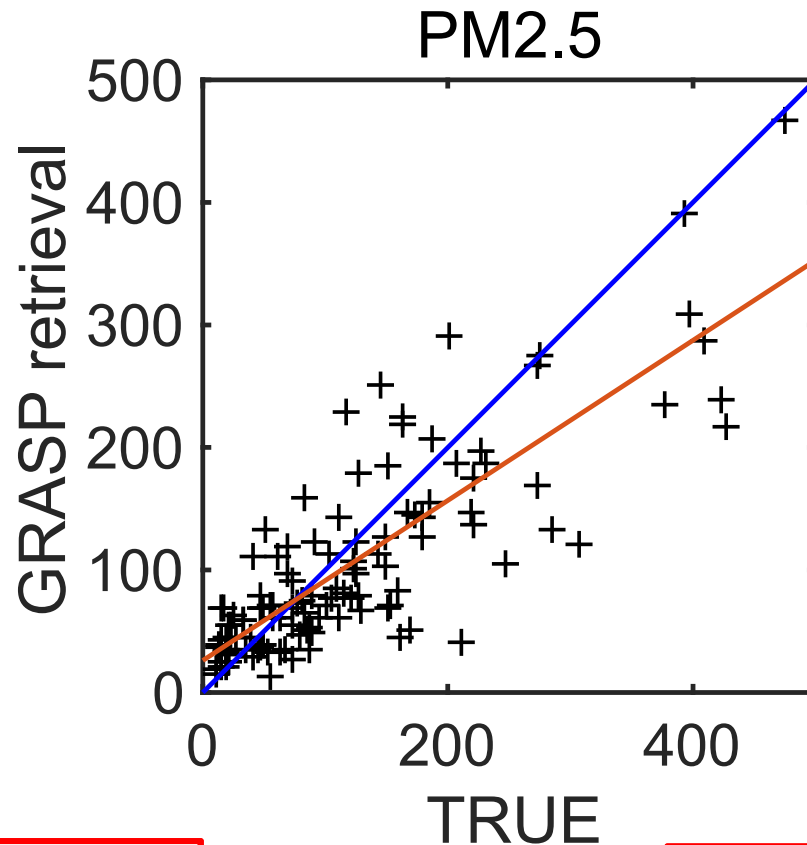
- < 10
- 11 - 15
- 16 - 25
- 26 - 35
- 36 - 69
- 70 or more

PARASOL/GRASP 2008



A. Lopatin

PARASOL/GRASP PM2.5 over Beijing 2009–2012



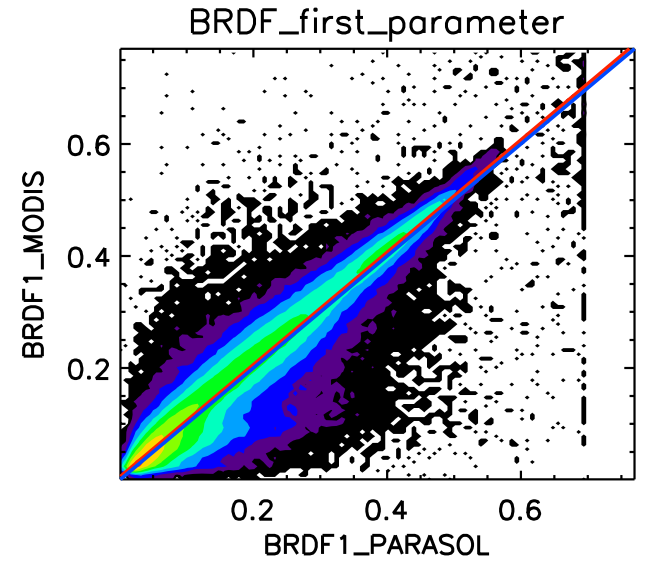
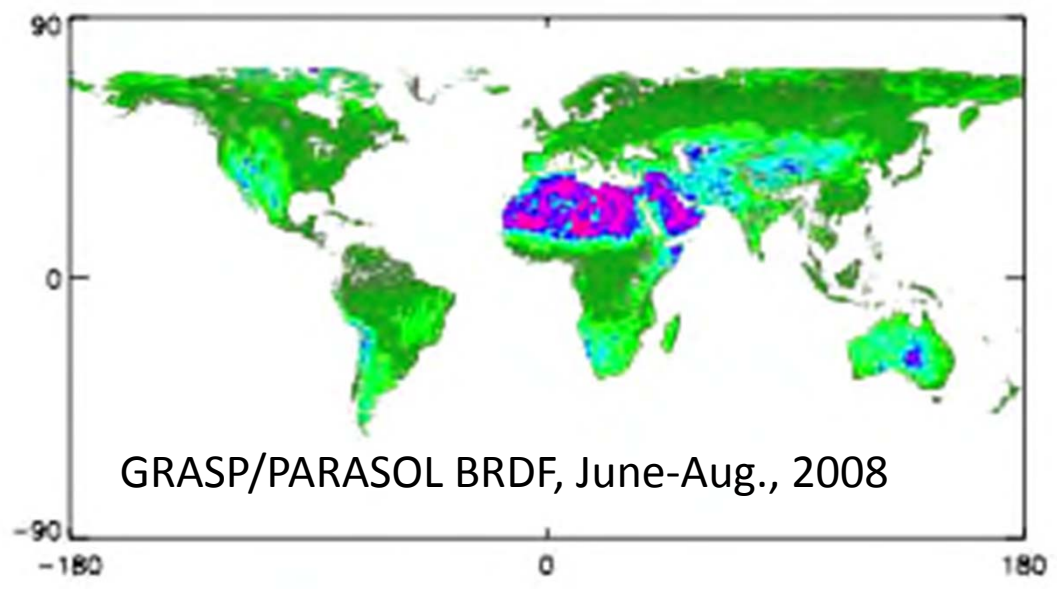
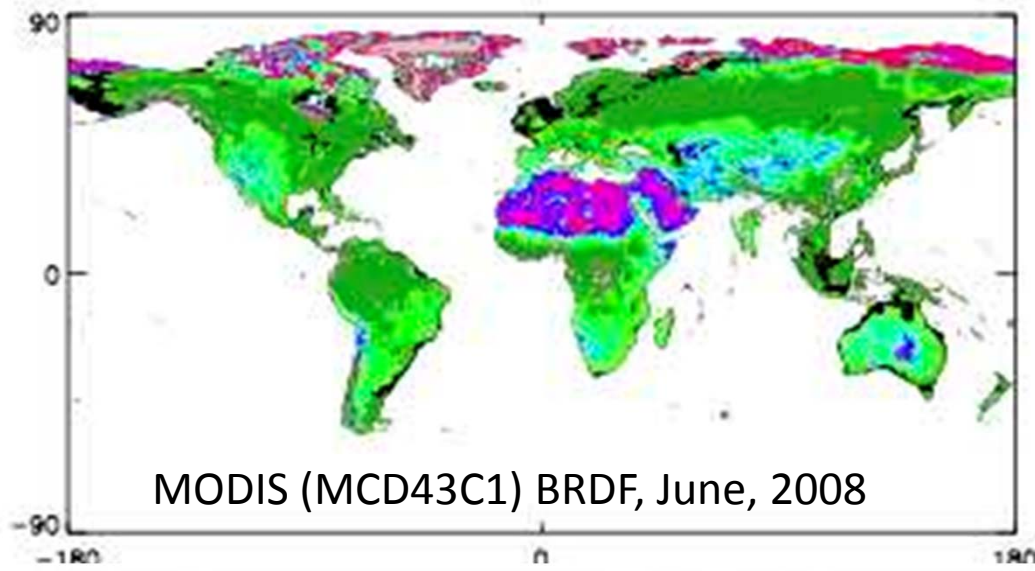
$K=0.821$ $a=0.65$ $b=26.00$ $RMSE=60.957$

$N=115$ $Aver.=121.513$

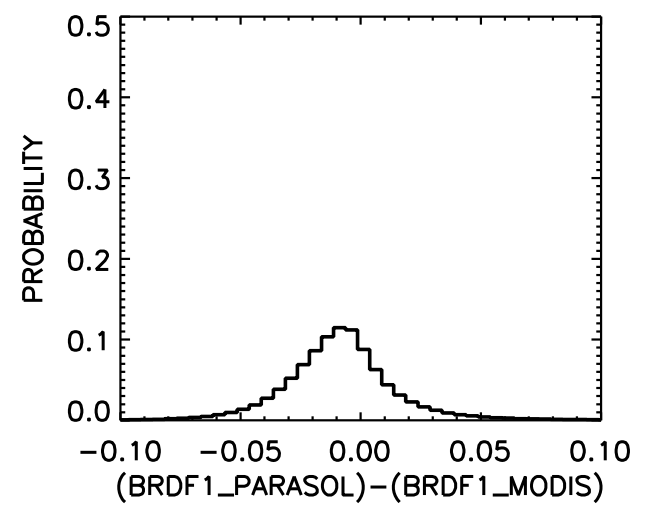
AOT>0.3, residual<3%

A. Lopatin

First parameter (670 nm) of Ross-Li BRDF, 2008



$K=0.965$ $a= 1.00$ $b= 0.01$ $RMSE= 0.030$



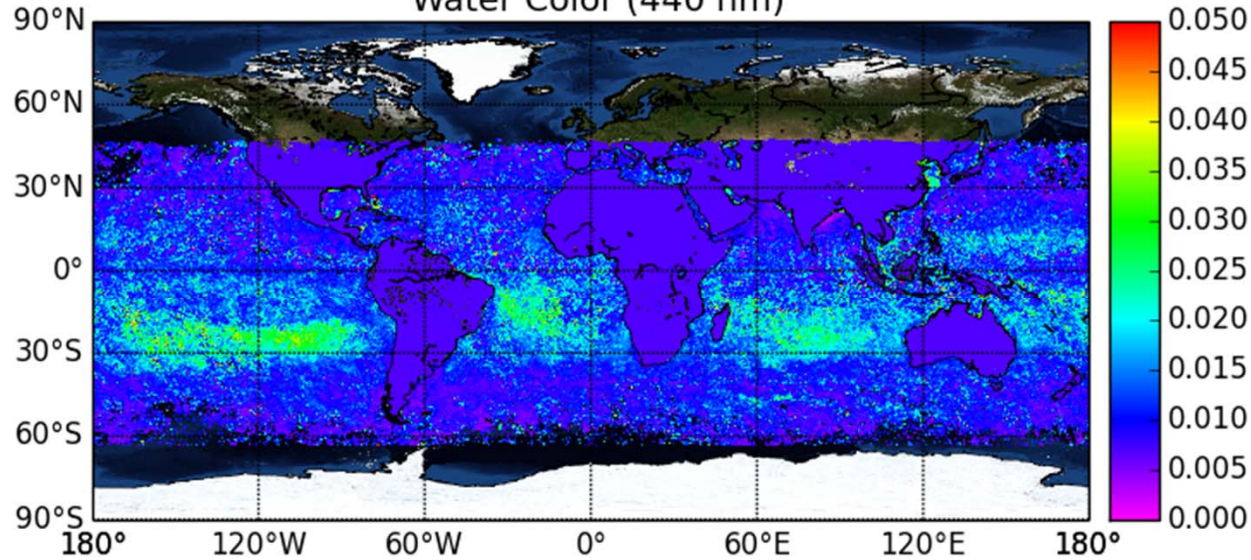
Aver. Value=-0.006 St.D.= 0.030 N=1222958

PARASOL water living radiance

December 2008,

GRASP_LAND_AND_OCEAN.Fast.WaterBRMCoxMunkIso_1.2008-12

Water Color (440 nm)

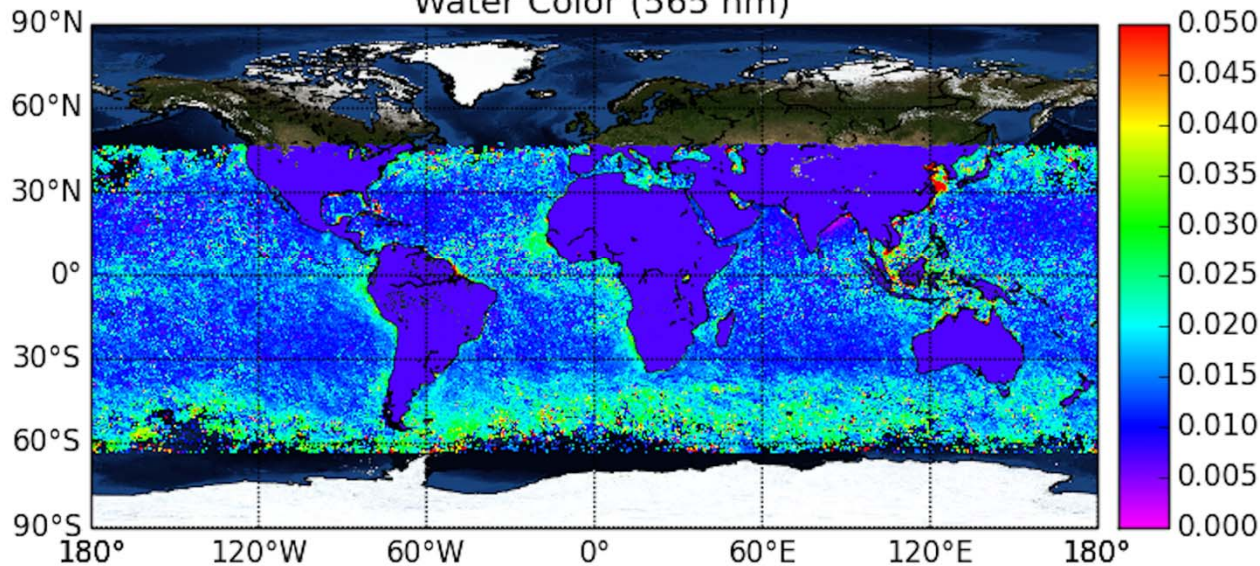


« Blue » water

« clean »

GRASP_LAND_AND_OCEAN.Fast.WaterBRMCoxMunkIso_1.2008-12

Water Color (565 nm)



« Green » water

« bio active »,
bio-active (phytoplankton), etc.

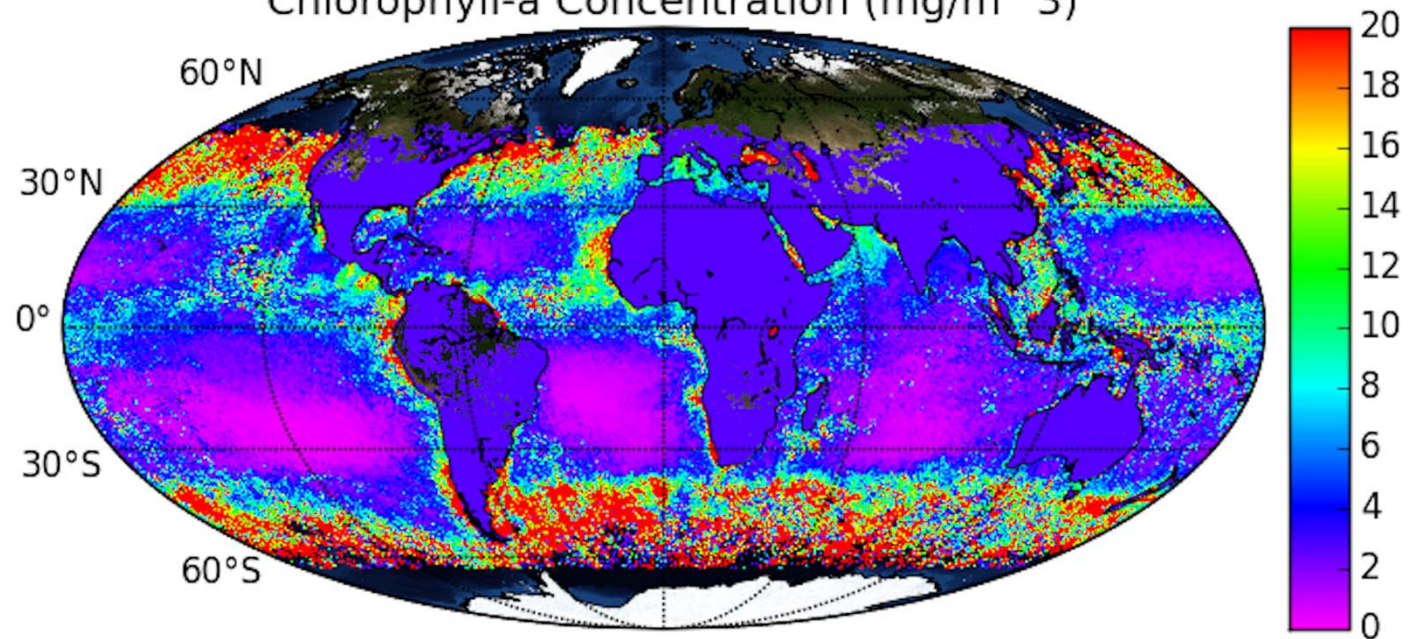
PARASOL 2008

Chlorophyll

Preliminary result...

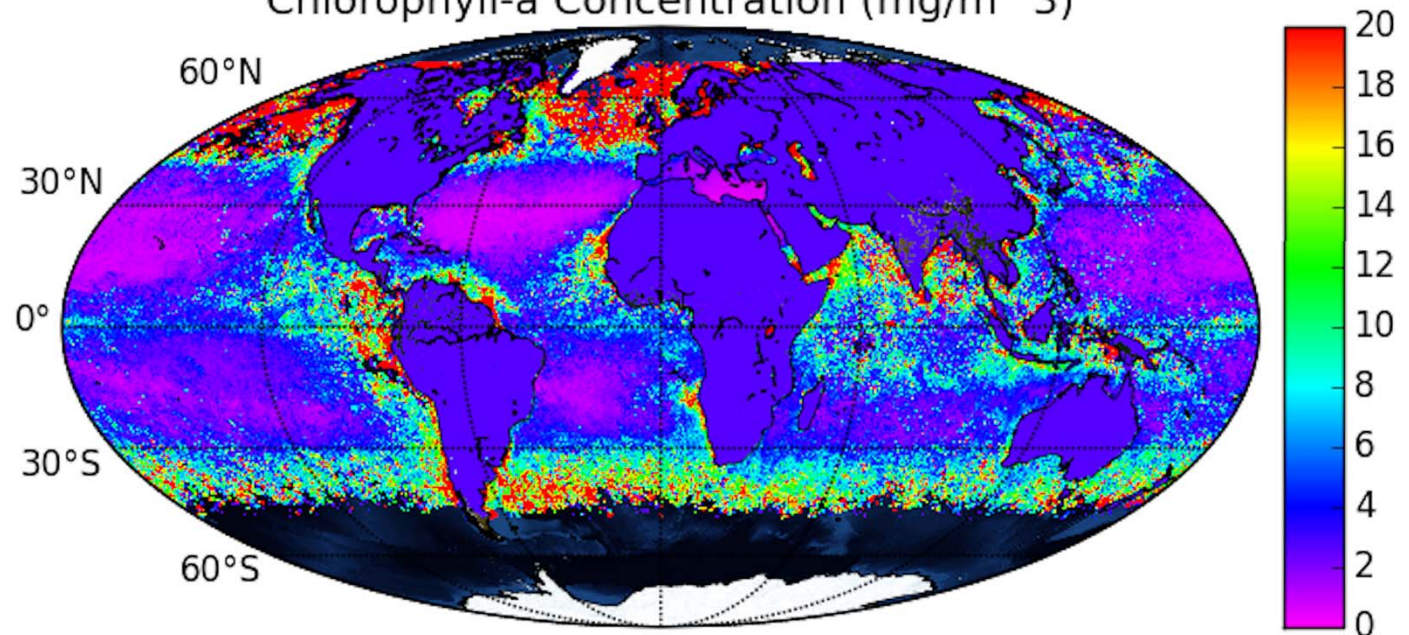
January

GRASP_LAND_AND_OCEAN.Fast.WaterBRMCoxMunkIso_1.2008-01
Chlorophyll-a Concentration (mg/m³)



GRASP_LAND_AND_OCEAN.Fast.WaterBRMCoxMunkIso_1.2008-07
Chlorophyll-a Concentration (mg/m³)

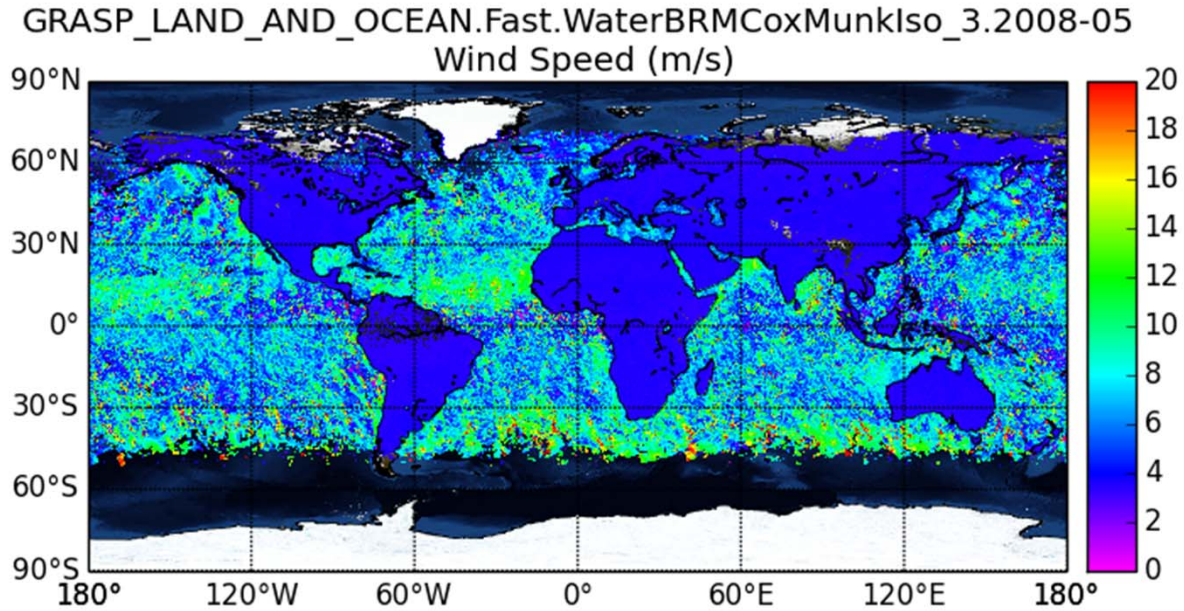
July



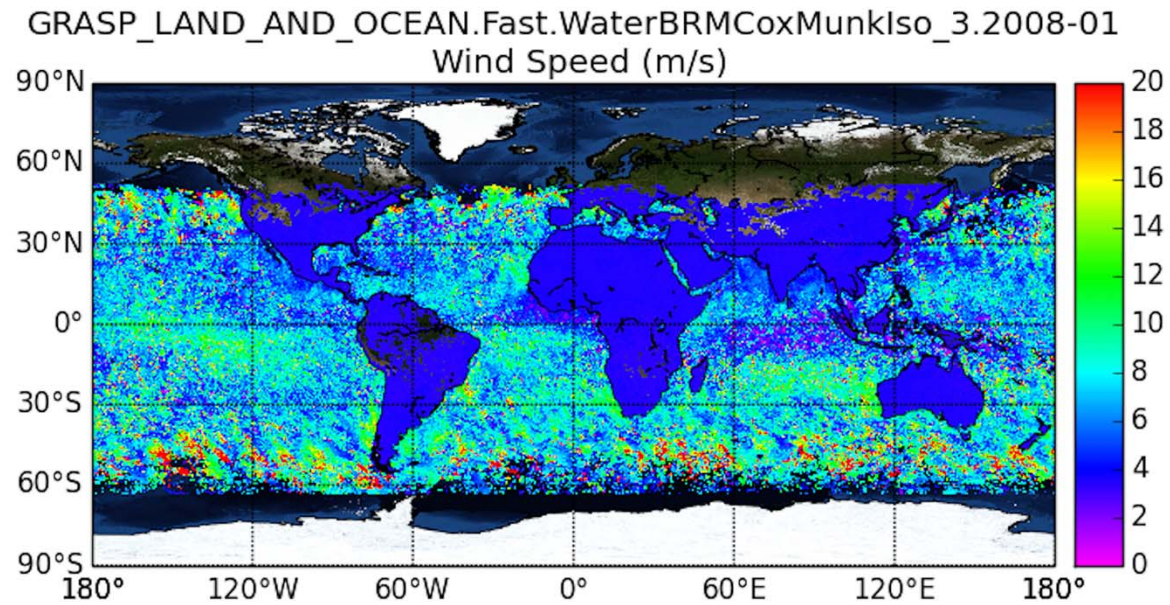
PARASOL

2008

May



January



PARASOL:

- radiances: (443, 490, 560, 670, 870, 1020 nm)
- polarization: (490, 670, and, 870 nm)
- up to 16 viewing directions

144 measurements



MERIS:

- radiances: (413, 443, 490, 510, 560, 665, 755, 870)
- 1 viewing direction

8 measurements



What are the differences in the results?



MERIS:

- radiances: (413, 443, 490, 510, 560, 665, 755, 870)
- 1 viewing direction

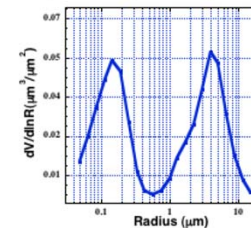


8 measurements

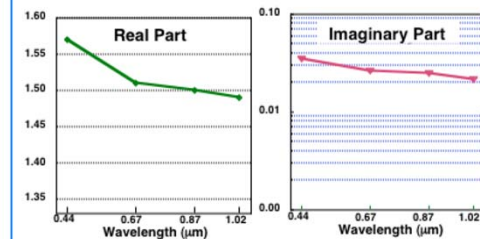
AEROSOL:

- size distribution (5 or more bins)
- spectral index of refraction (8 λ)
- sphericity fraction;

Particle Size Distribution:
0.05 $\mu\text{m} \leq R$ (22 bins) $\leq 15 \mu\text{m}$



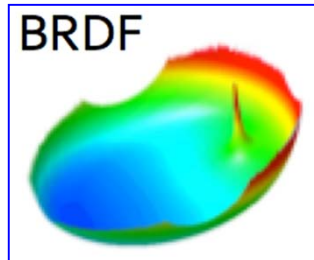
Complex Refractive Index at
 $\lambda = 0.44; 0.67; 0.87; 1.02 \mu\text{m}$



SURFACE:

- BRDF
(3 parameters)

BRDF



$$\tau^{aerosol}(\lambda) = C_i \sum_{i=1, \dots, 5} \int_{r_{\min}}^{r_{\max}} K_{\tau}^i(k_i; n_i; \epsilon_i; r) V_i(r) dr$$

$$43 = (5 \text{ (SD)} + 16 \text{ (r. ind.)} + 1 \text{ (nonsp.)} + 21 \text{ (BRDF)}) \longrightarrow 25 = (4 \text{ (aer. comp.)} + 21 \text{ (BRDF)})$$

GRASP/MERIS 2002- 2012 product has been generated



10 km resolution

GRASP/MERIS:
year 2008 averages

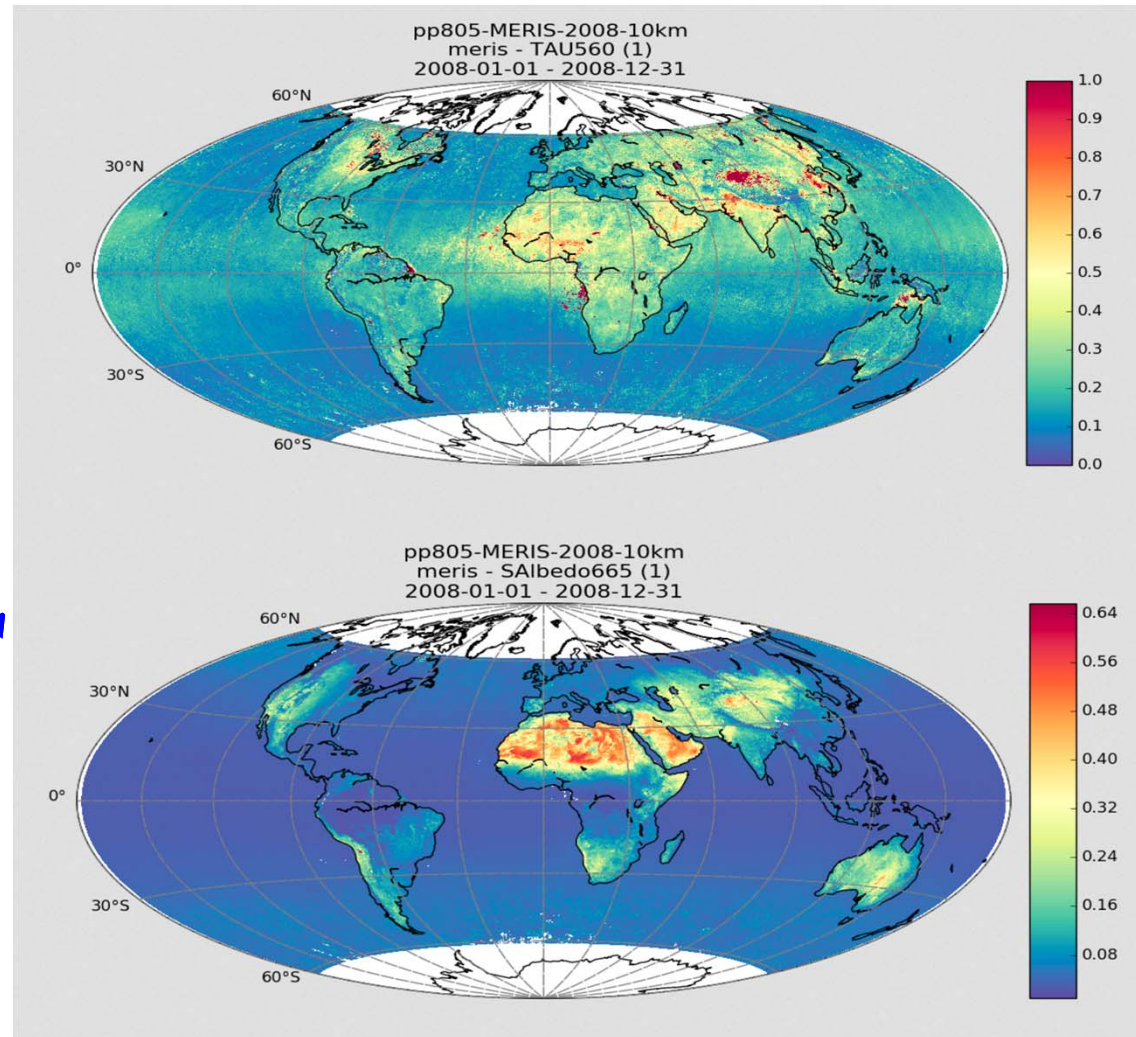
AOD(560 nm)

No location specific assumptions !!!

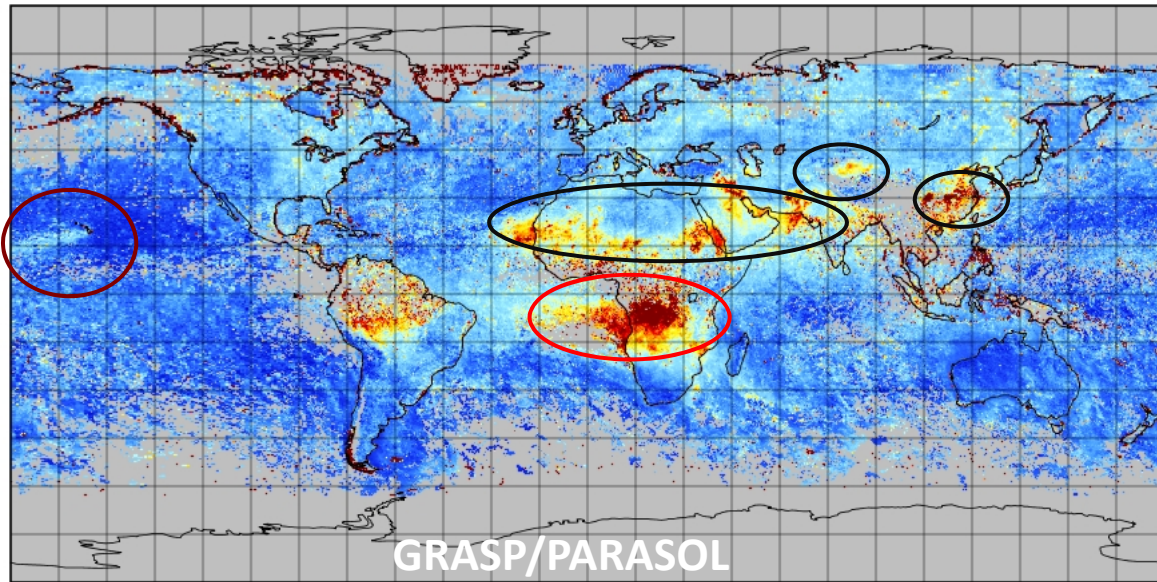
No climatologies!

Surface Albedo (670 nm)

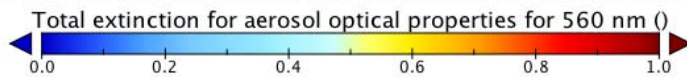
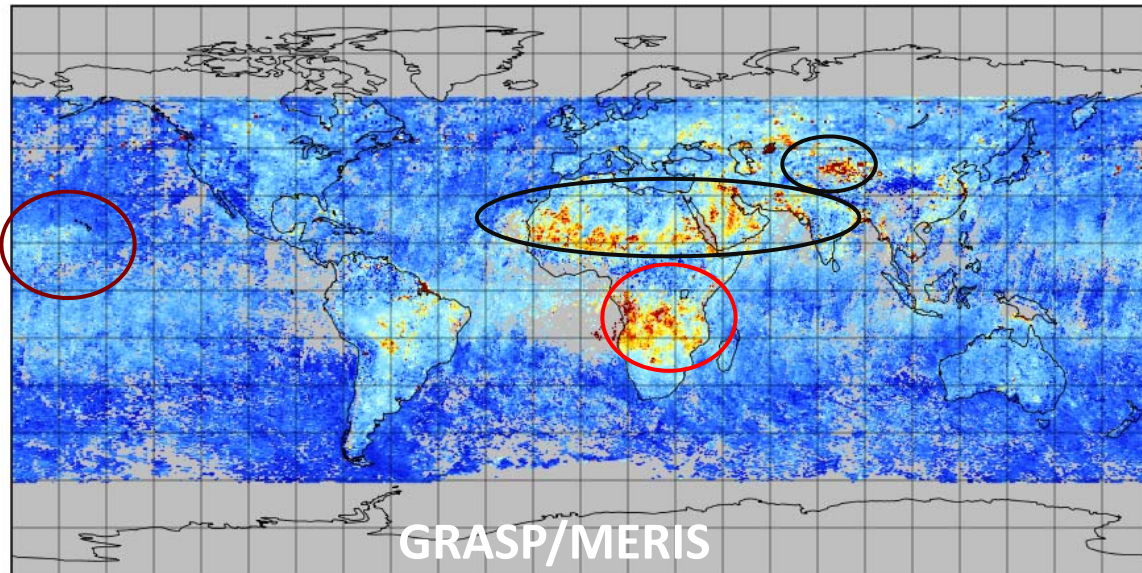
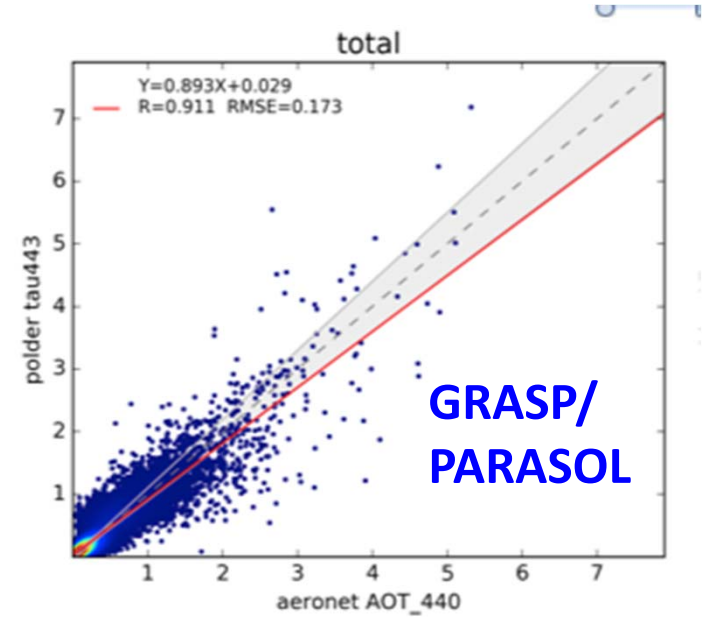
ESA CAWA project



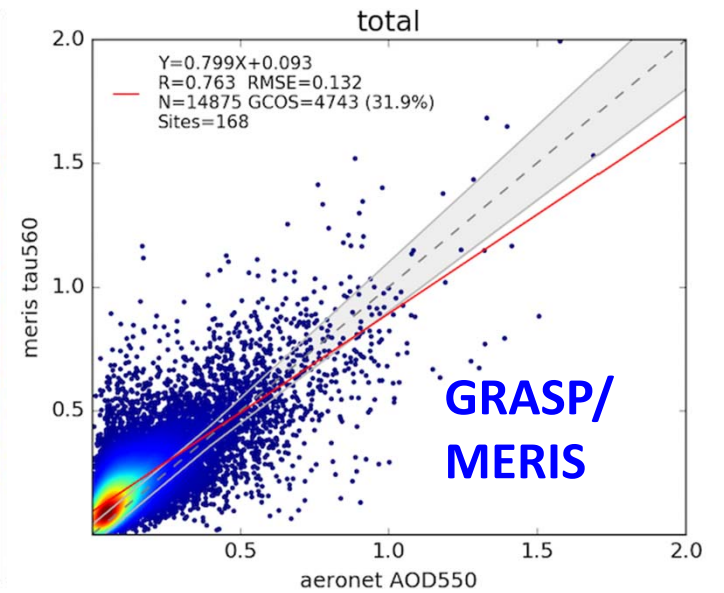
September, 2008



Total extinction for aerosol optical properties for 560 nm

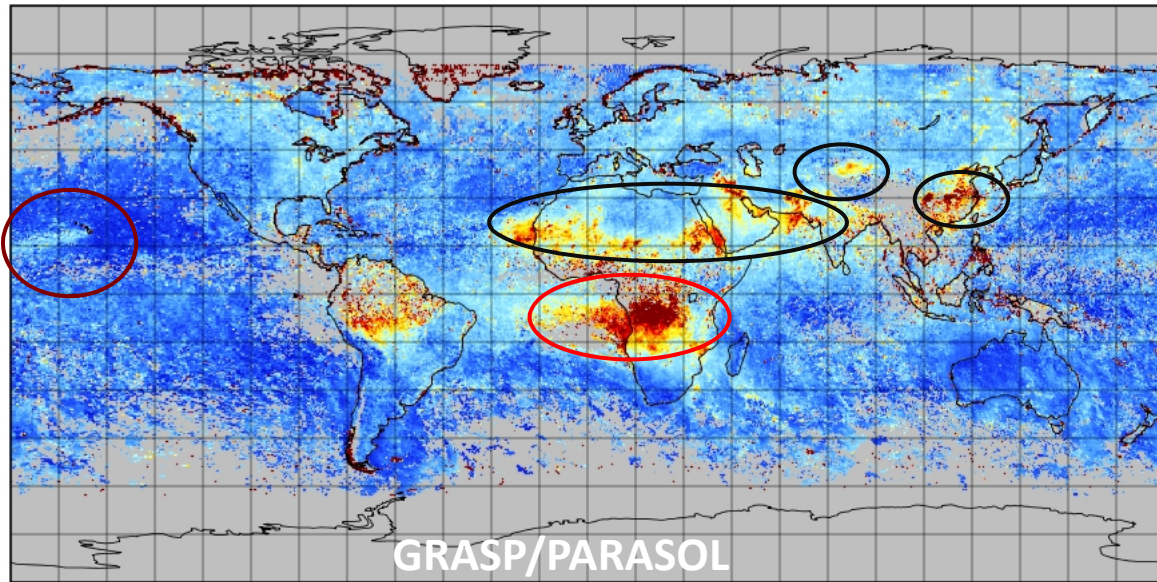


Data Min = 0.0, Max = 28.5, Mean = 0.2

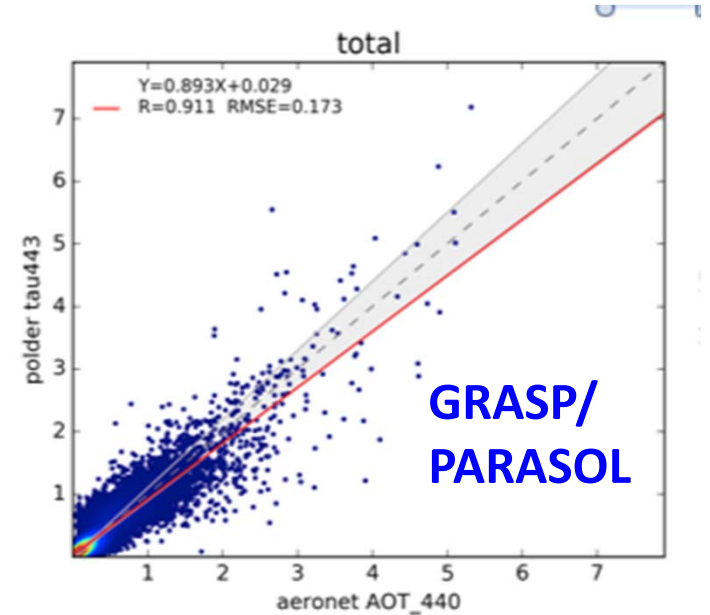
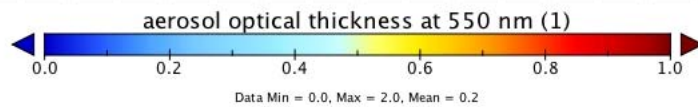
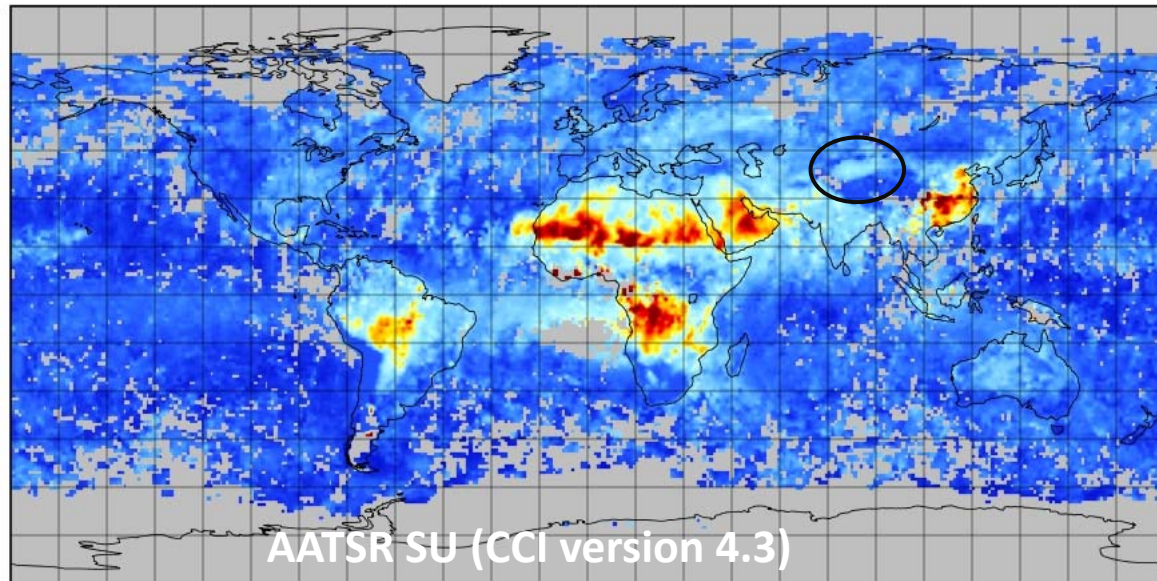


September, 2008

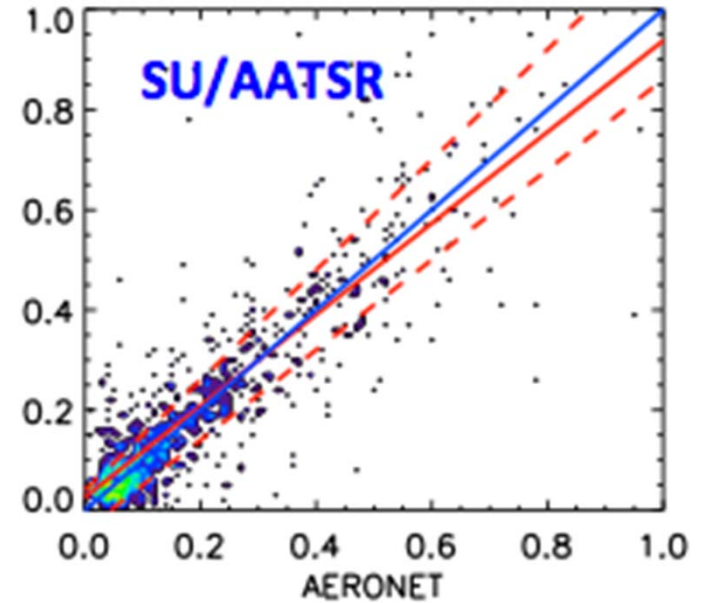
September, 2008



aerosol optical thickness at 550 nm



AOD,550nm

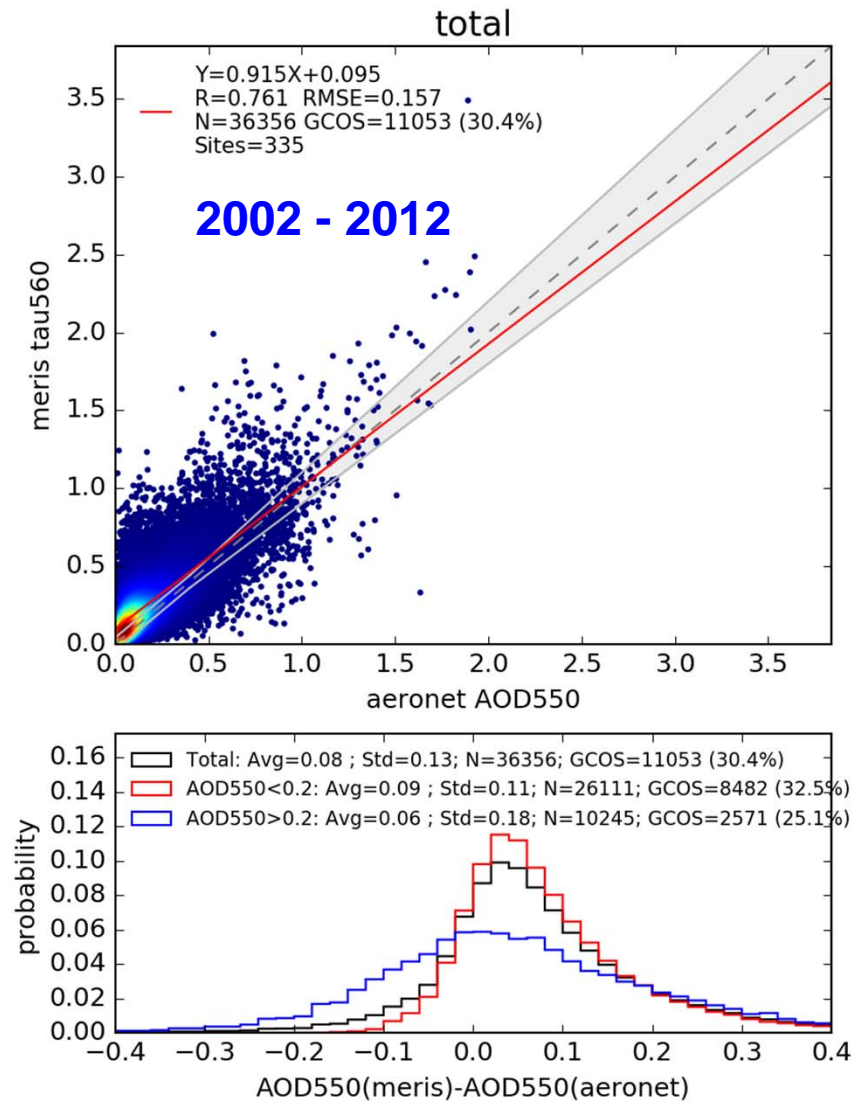
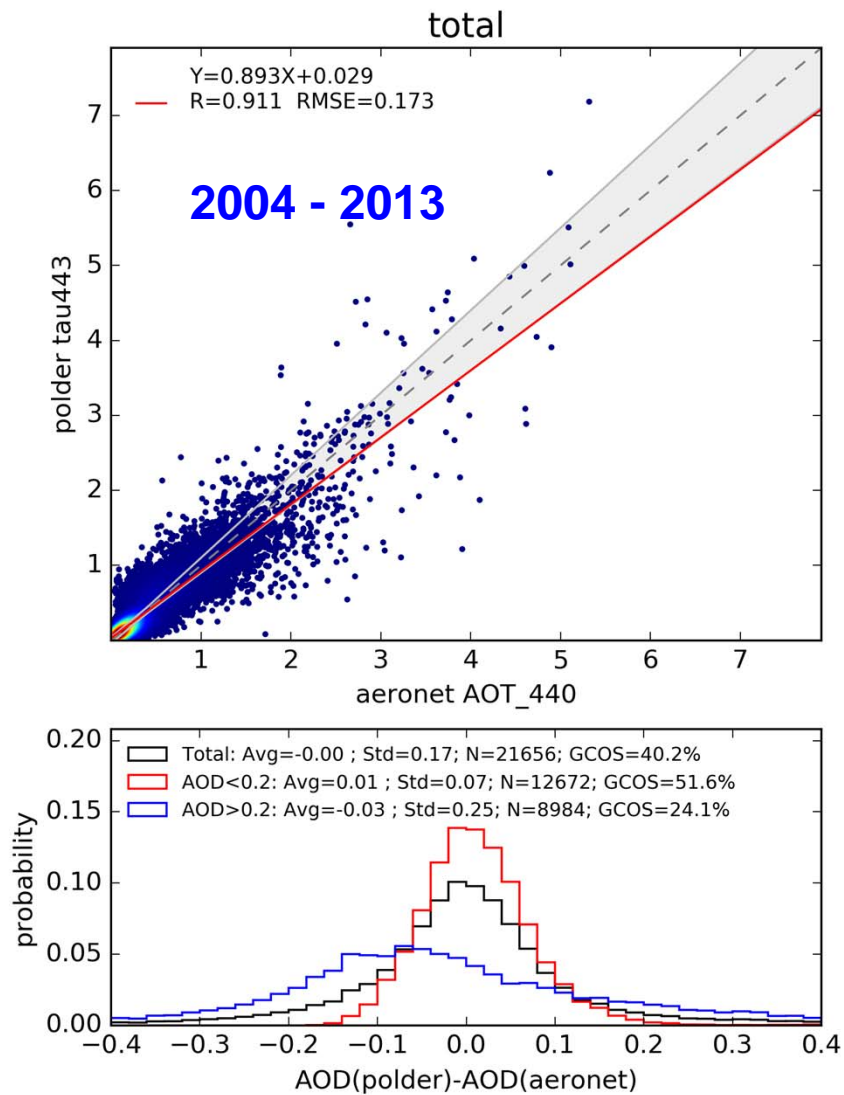


$K=0.860$ $\sigma=0.91$ $b=0.03$ RMSE= 0.119

Validation vs AERONET, AOD over land

PARASOL/GRASP, $R=0.91$

MERIS/GRASP, $R=0.76$

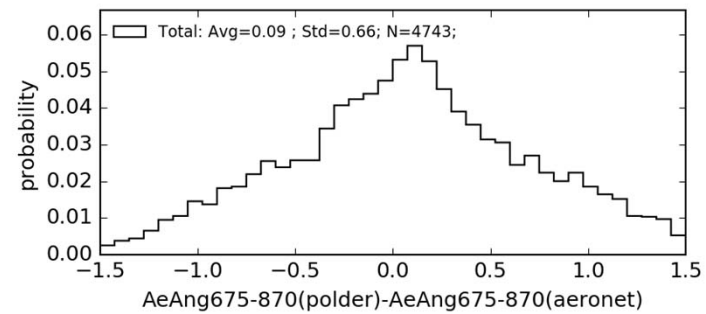
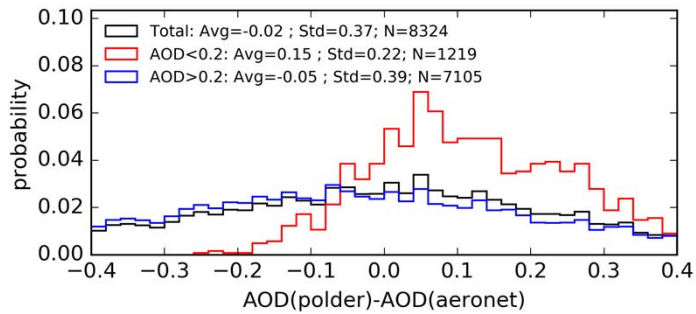
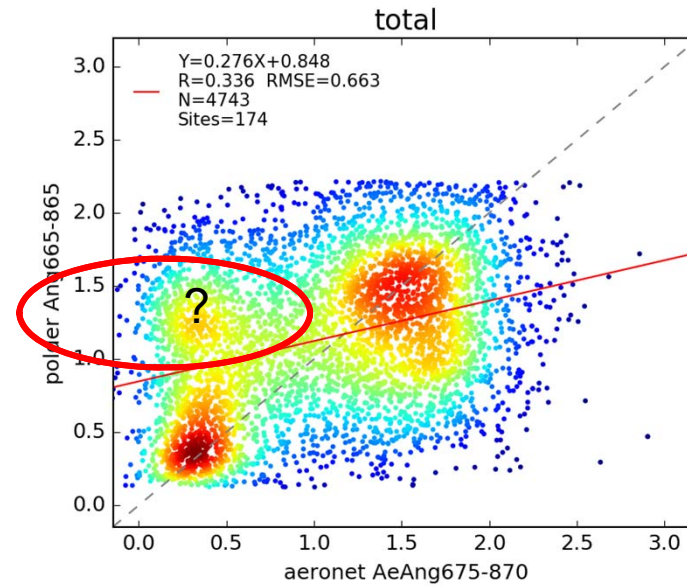
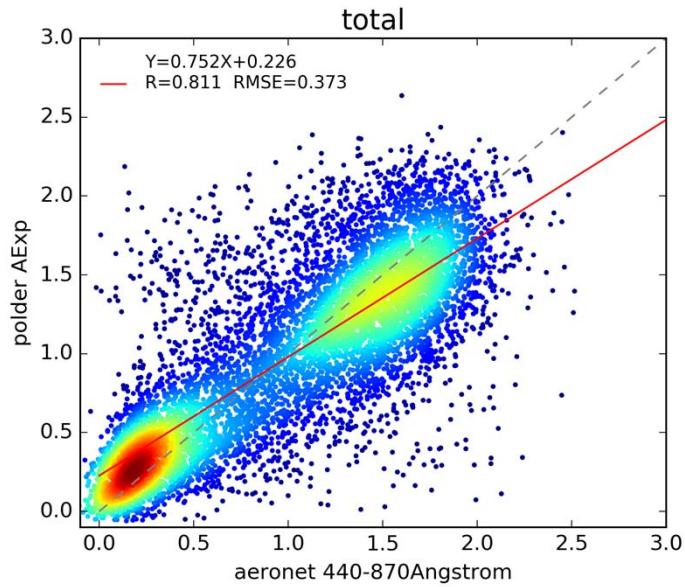


Validation vs AERONET over land

Angstrom

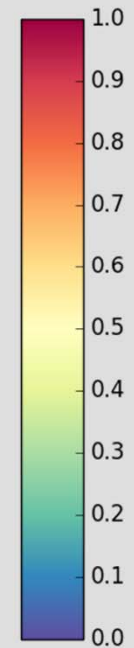
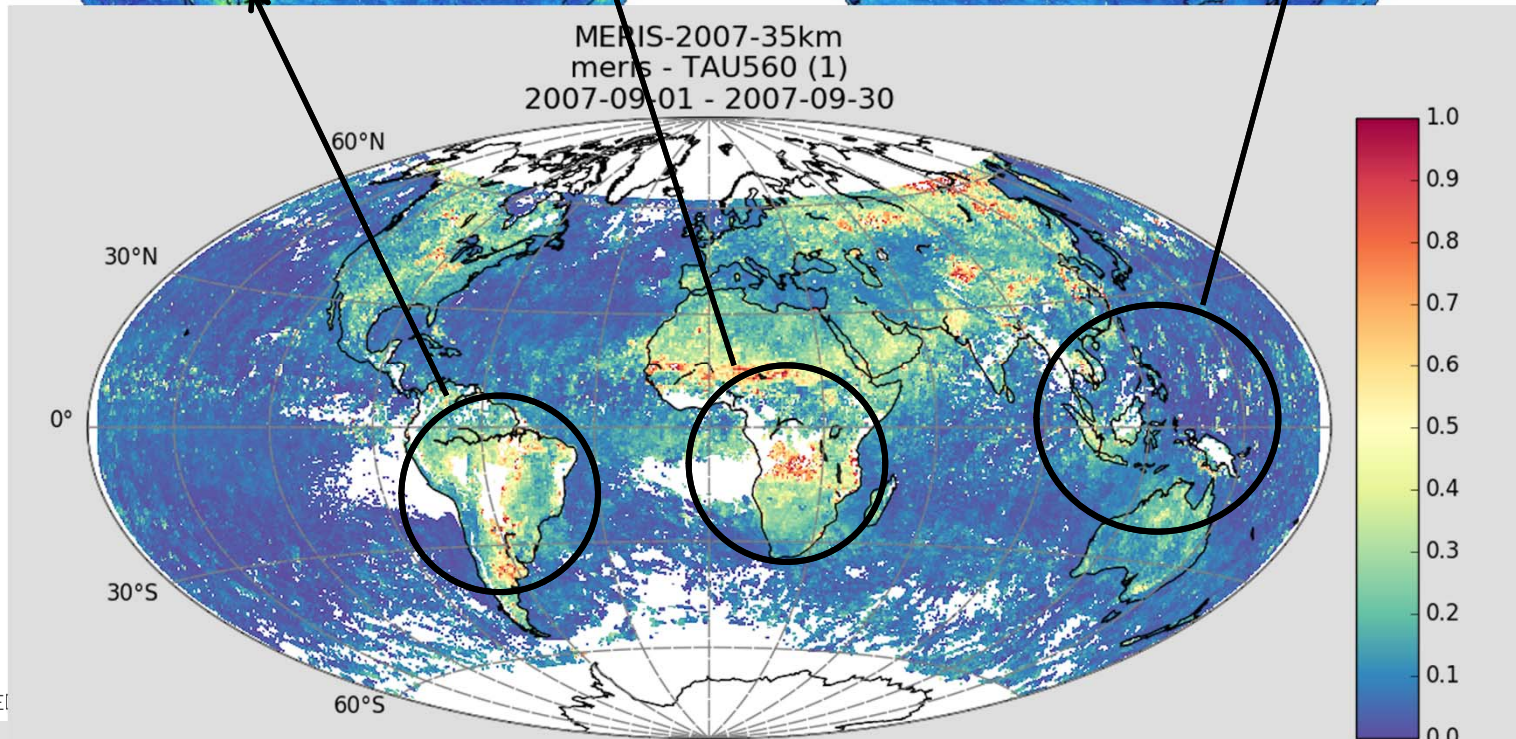
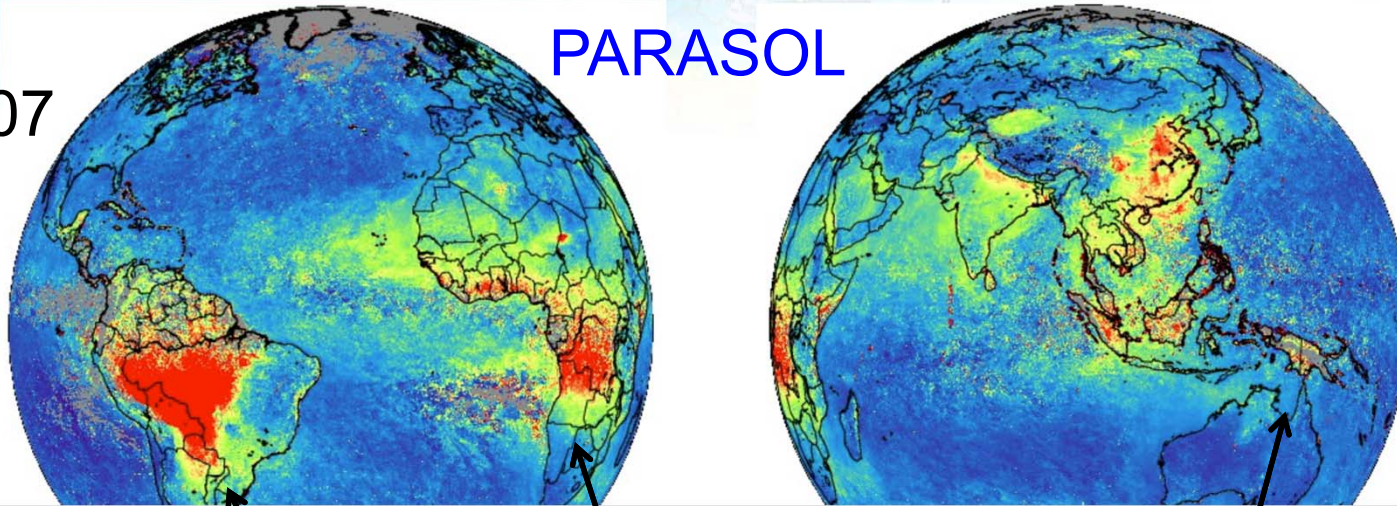
GRASP/PARASOL

GRASP/MERIS



PARASOL

Fall, 2007



Mongu, 1200x 1200 zone.

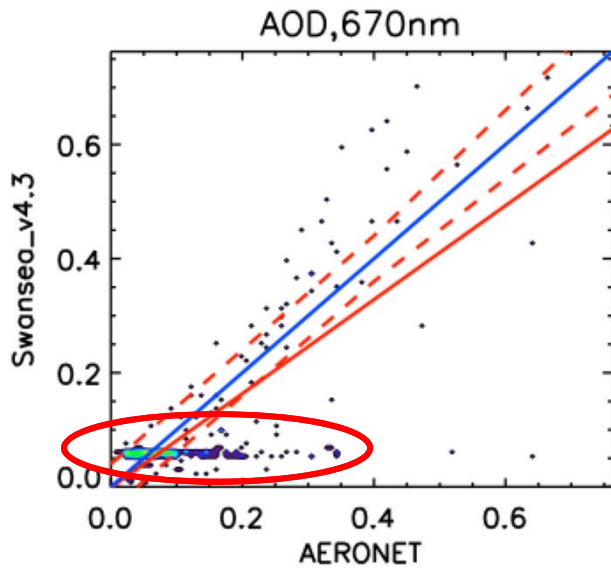
2002-2012

AATSR / SU, R=0.76

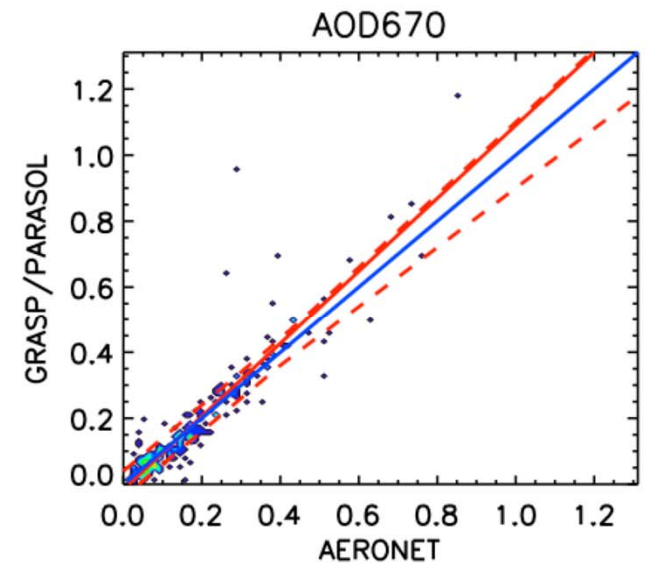
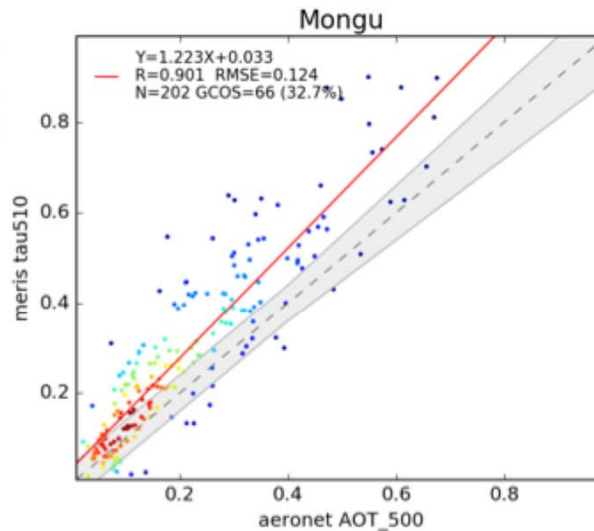
MERIS / GRASP, R=0.91

2004-2013

PARASOL / GRASP, R=0.91



K=0.760 $\alpha = 0.82$ $b = -0.00$ RMSE= 0.101



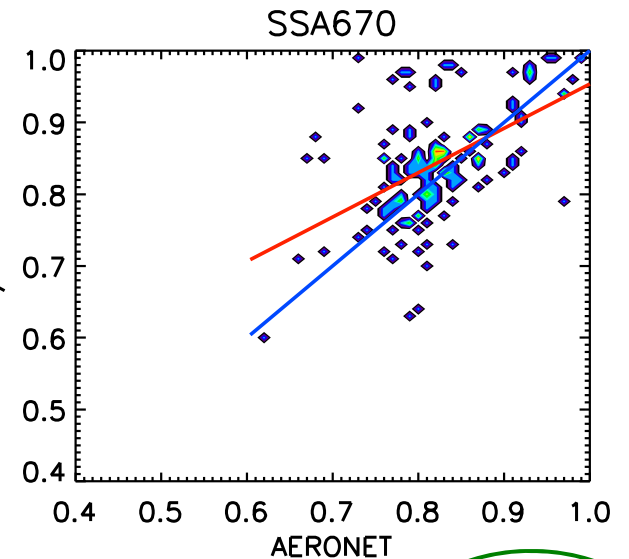
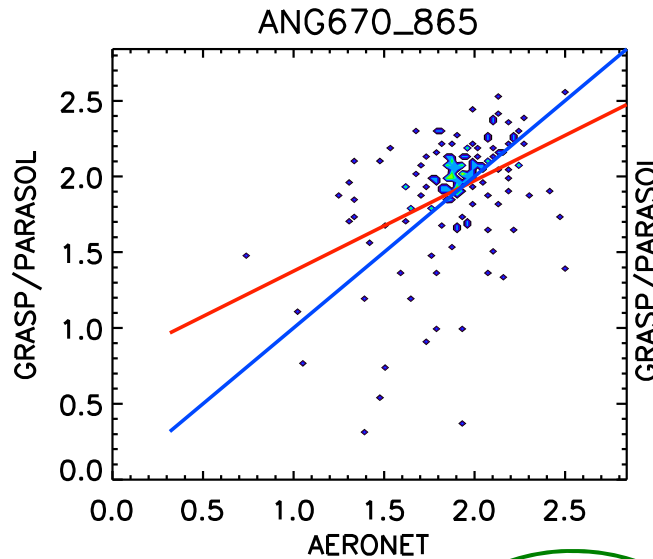
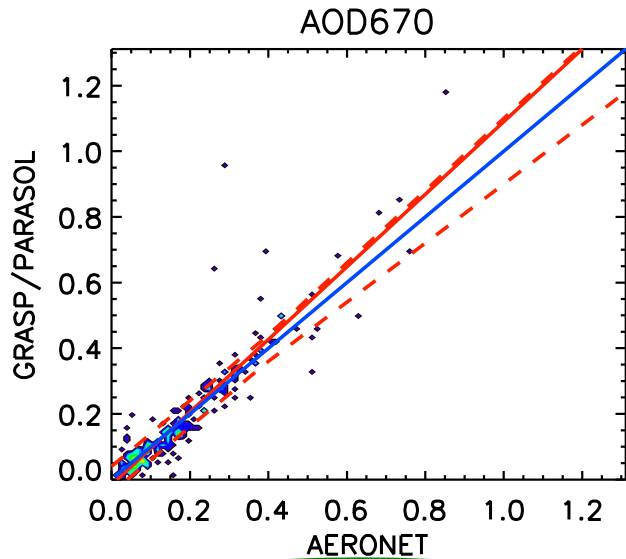
K=0.914 $\alpha = 1.11$ $b = -0.02$ RMSE= 0.076

AATSR - fails with aerosol model ???

MERIS is surprisingly good with R, but slope is wrong ???

PARASOL could be better???

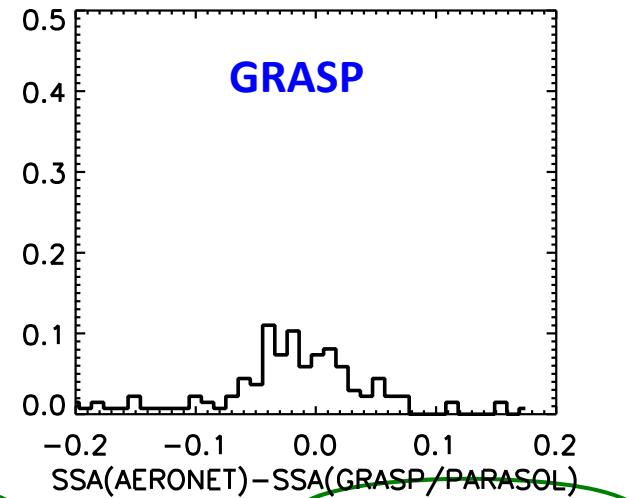
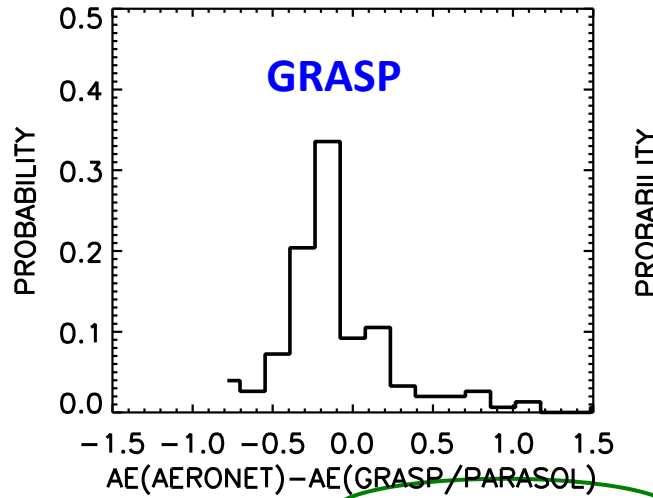
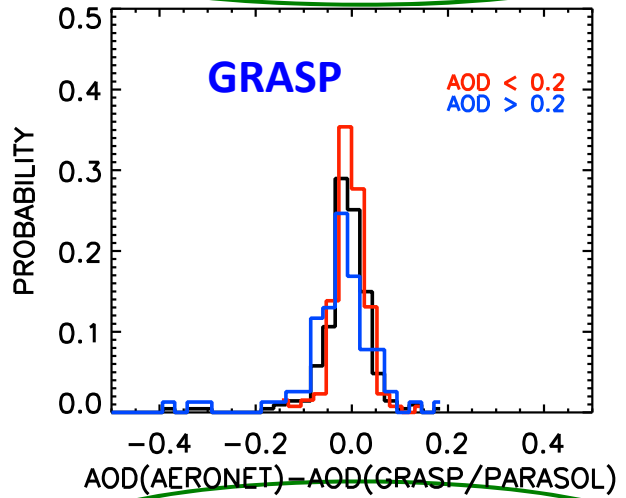
Mongu, 1200x 1200 zone. 2005-2013. 2 sites. GRASP



$K=0.914$ $a= 1.11$ $b=-0.02$ $RMSE= 0.076$
GCOS fraction:72%

$K=0.423$ $a= 0.60$ $b= 0.78$ $RMSE= 0.366$

$K=0.523$ $a= 0.62$ $b= 0.34$ $RMSE= 0.075$



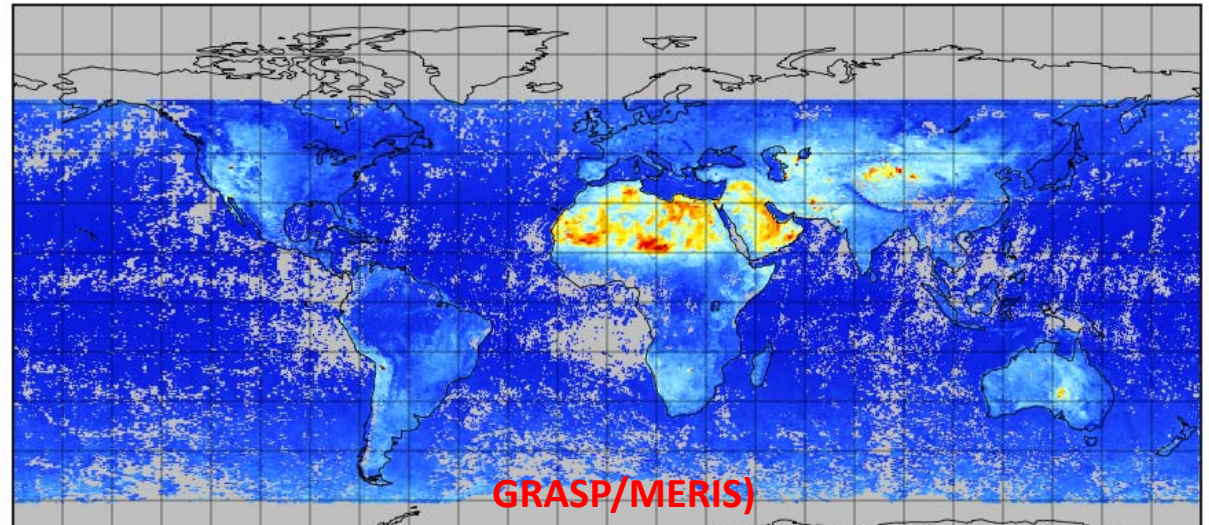
Aver. Value=-0.005 St.D.= 0.076 N=207
Aver. Value= 0.007 St.D.= 0.037 N=130
Aver. Value=-0.026 St.D.= 0.112 N= 77

Aver. Value=-0.013 St.D.= 0.366 N=152

Aver. Value=-0.020 St.D.= 0.072 N=136

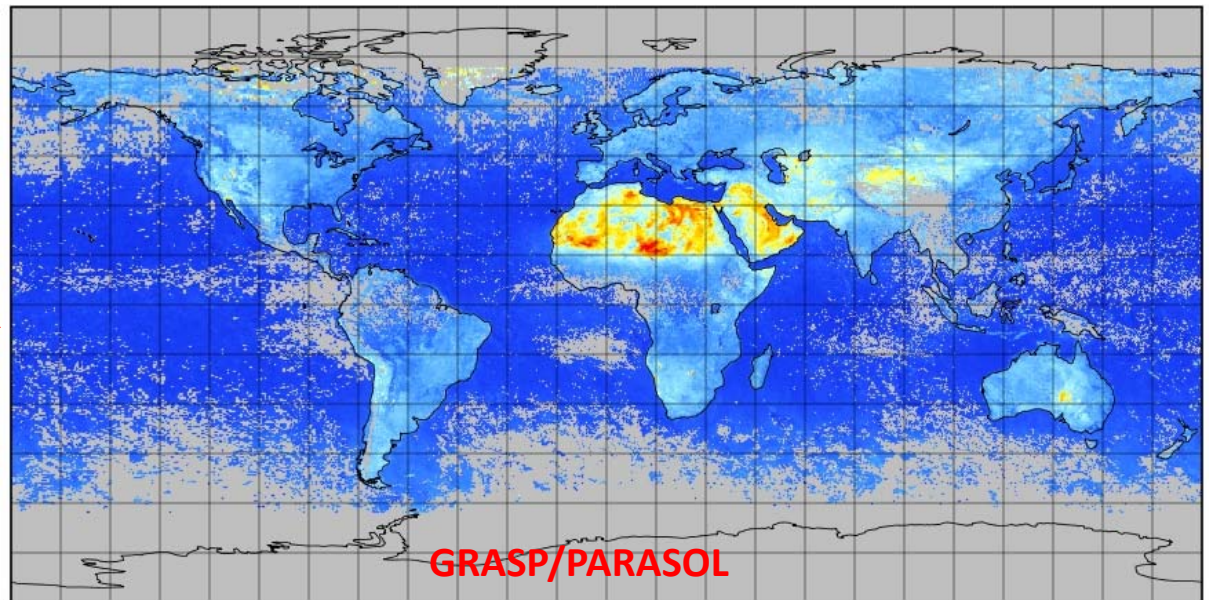
September, 2008

Comparison of surface reflectance

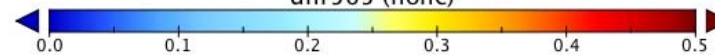


dhr565

Good agreement !

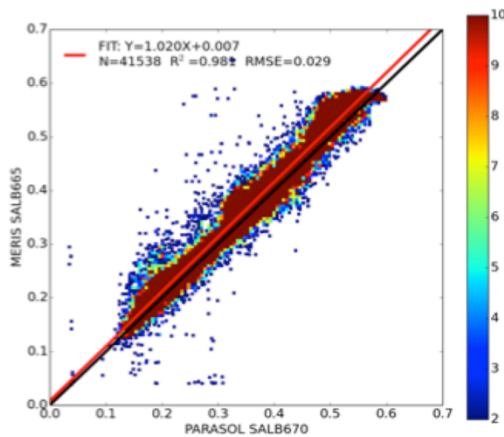


dhr565 (none)

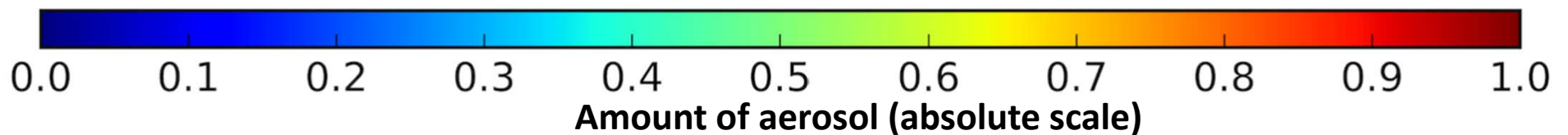
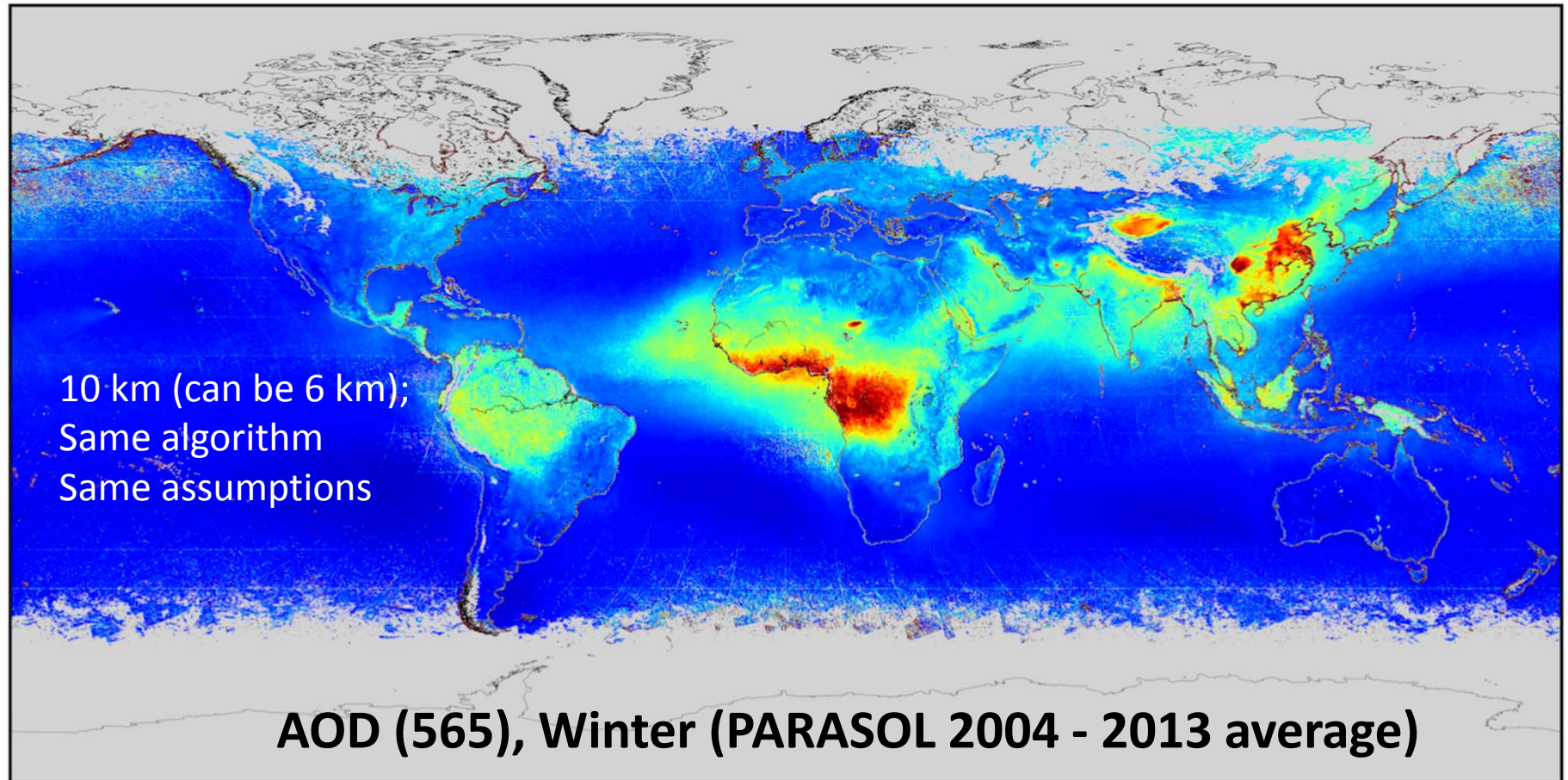


Data Min = 0.0, Max = 0.6, Mean = 0.1

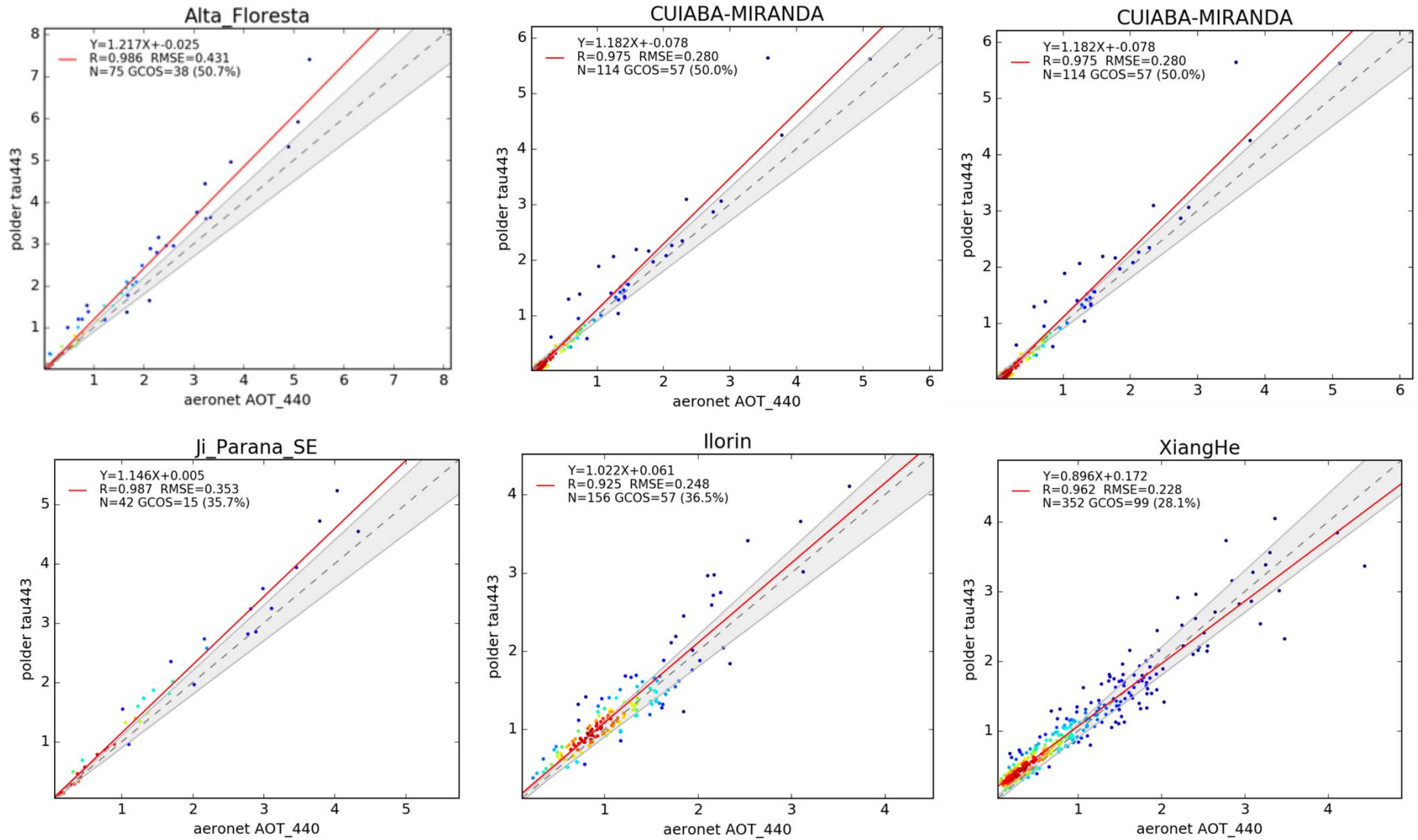
MERIS vs. PARASOL



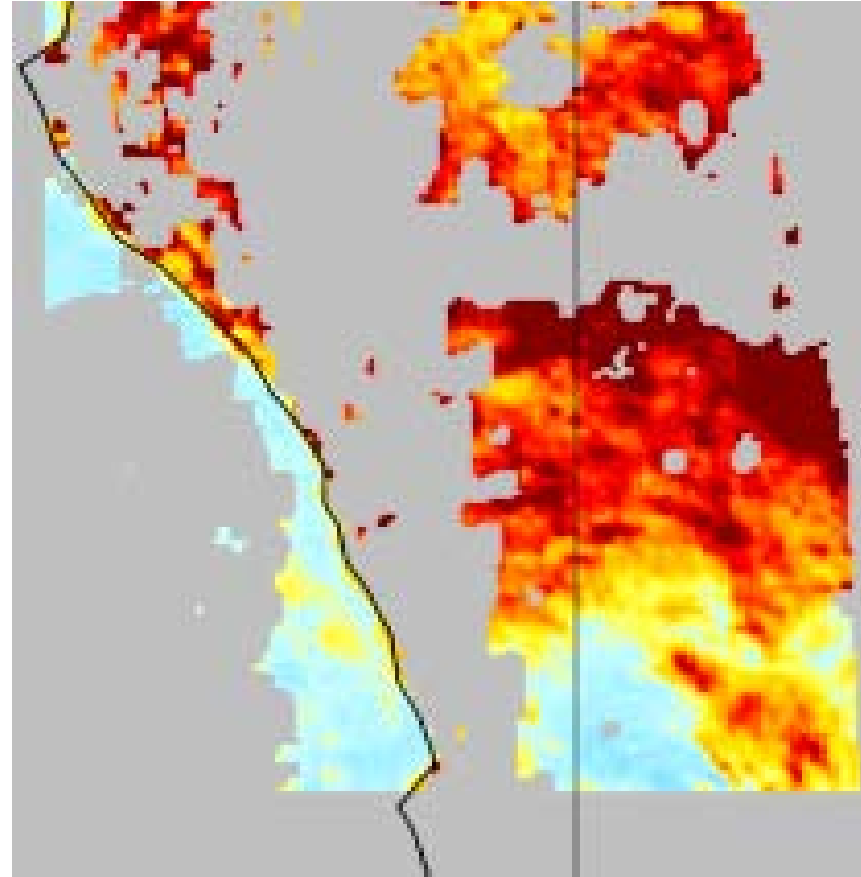
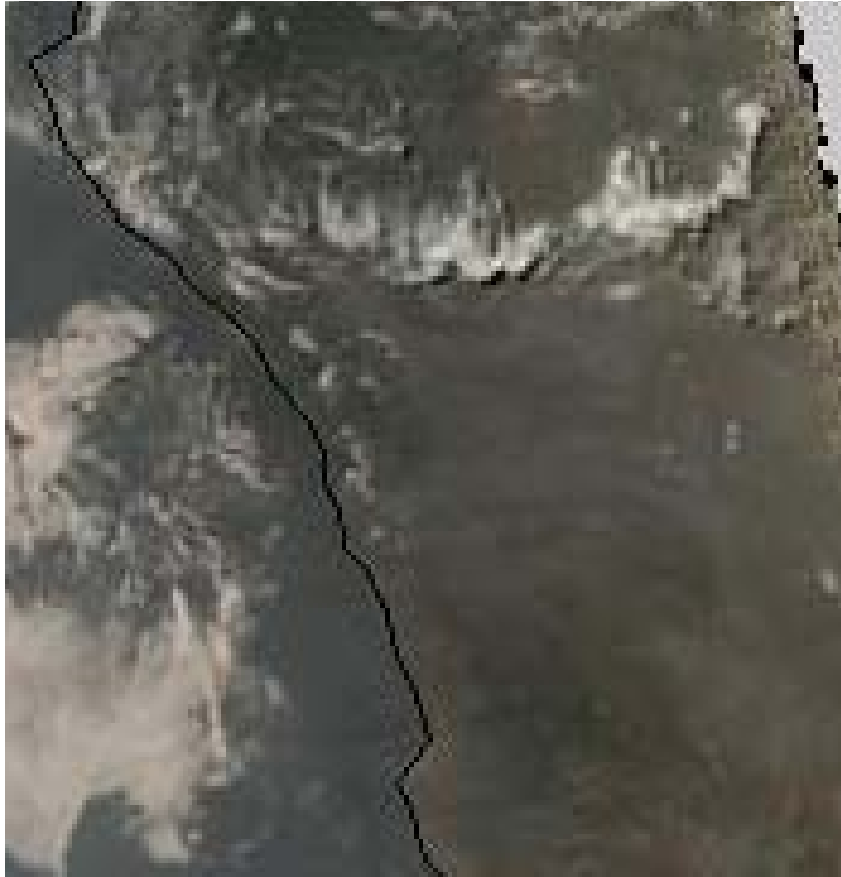
PARASOL/GRASP 2004- 2013 product has been generated



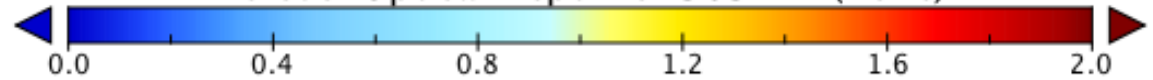
Validation against AERONET for high AOD biomass cases



Biomass burning. Mongu region, August, 3, 2013



Aerosol Optical Depth for 565 nm (none)



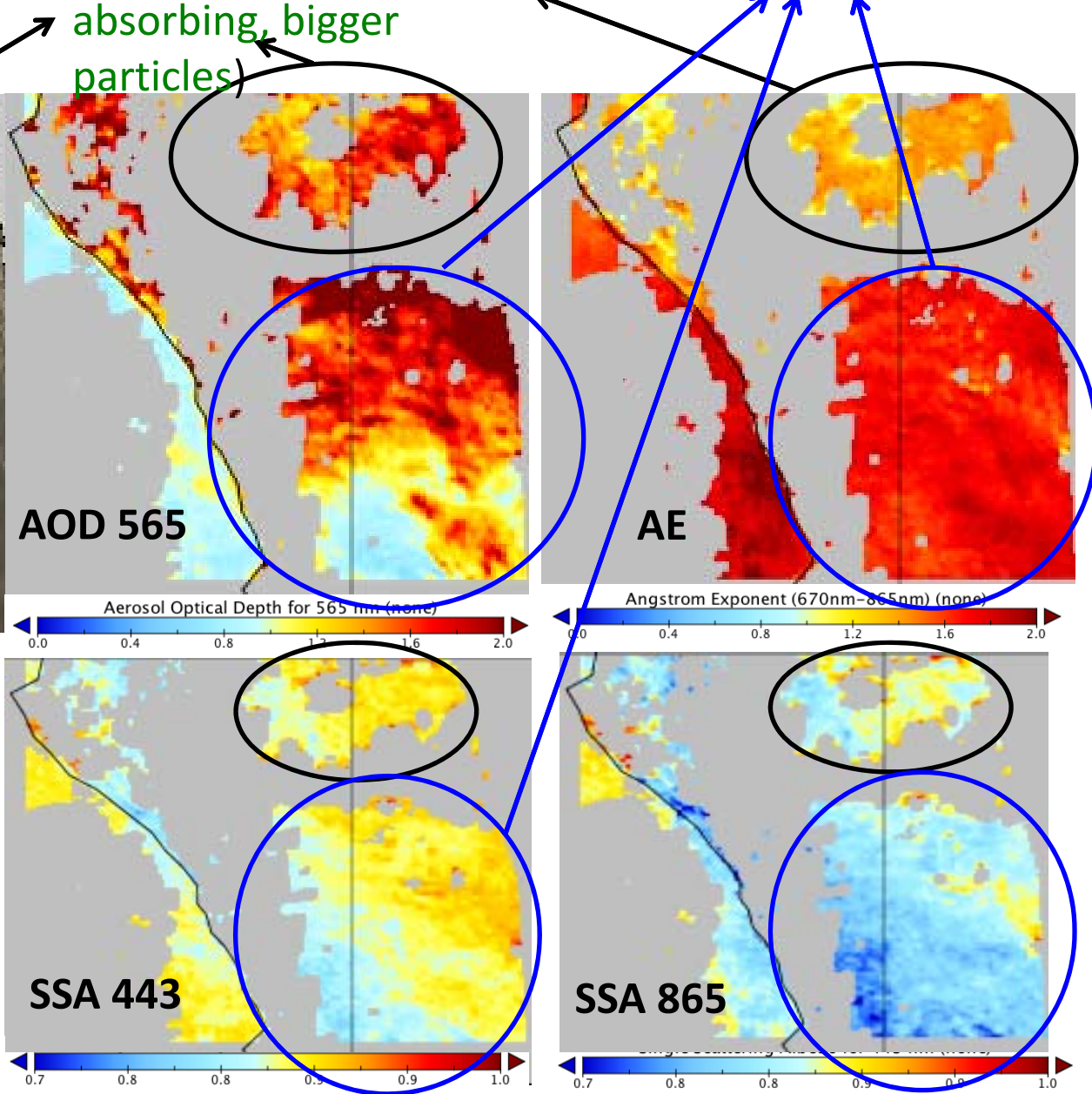
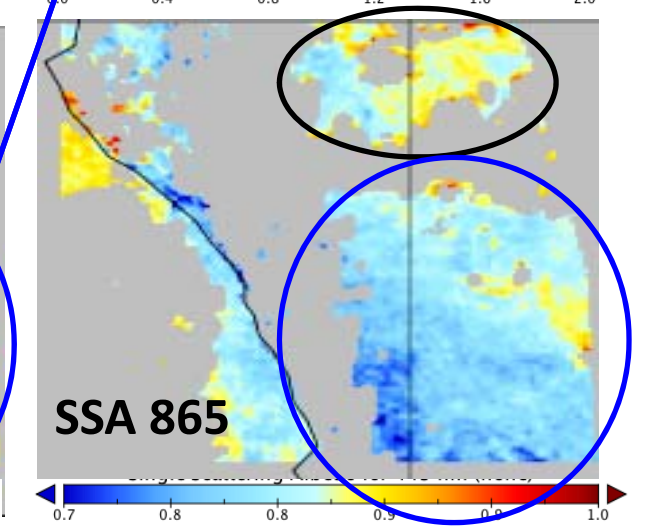
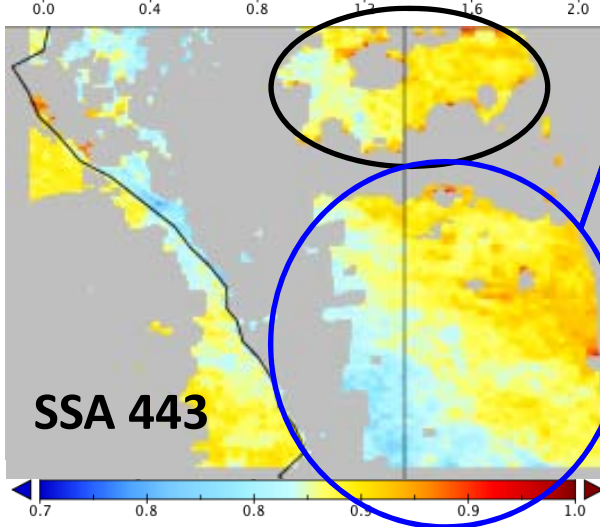
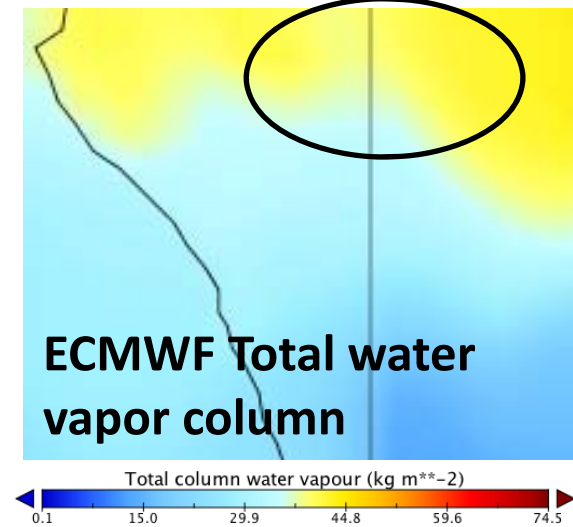
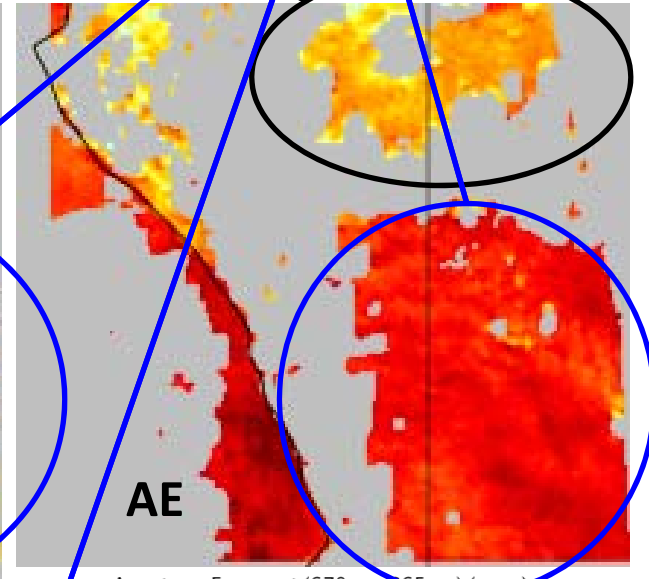
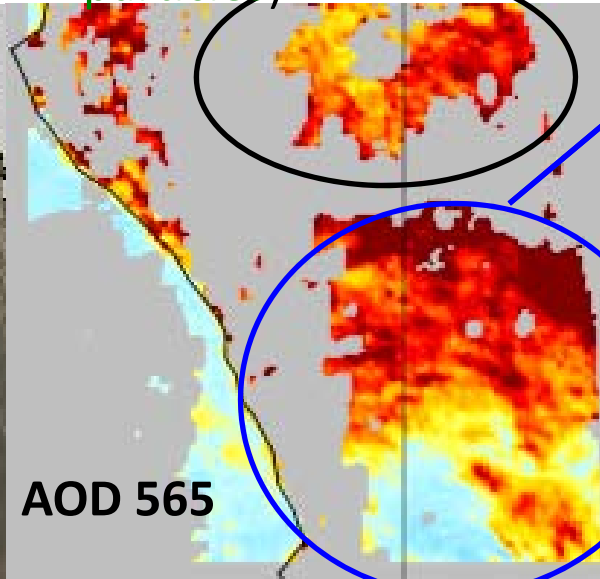
Data Min = 0.4, Max = 23.6

9-th ICAP, Lille, France, 26 – 28 June, 2017

Biomass burning. Africa, August, 3, 2013

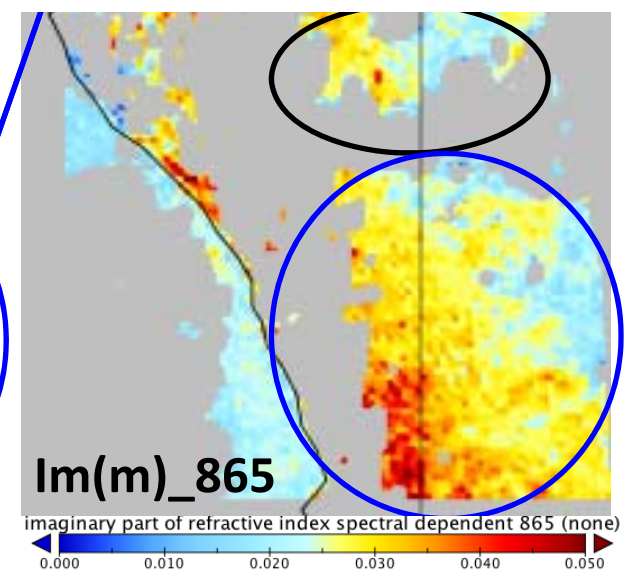
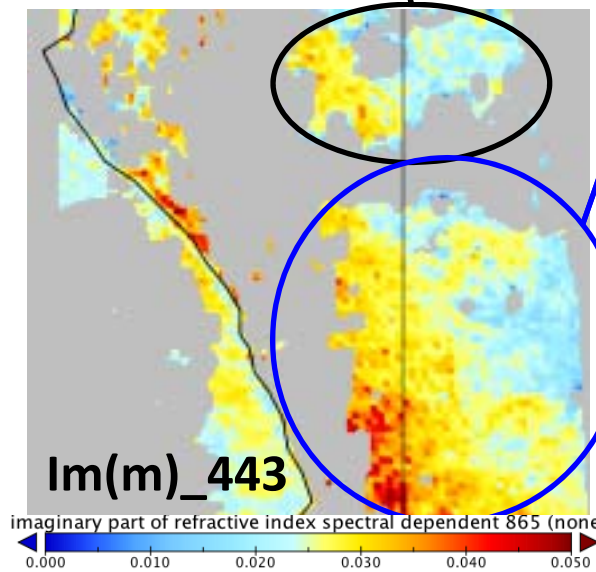
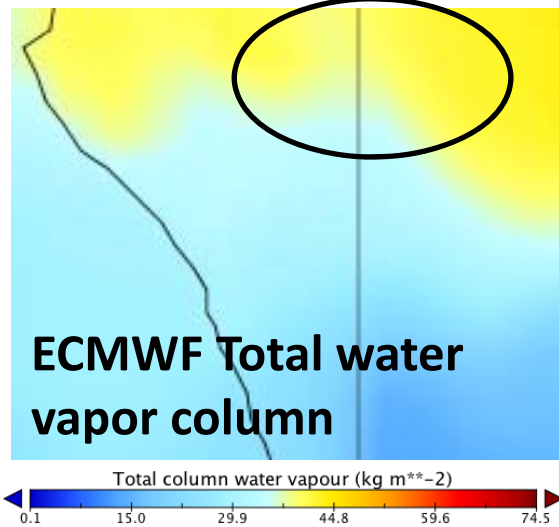
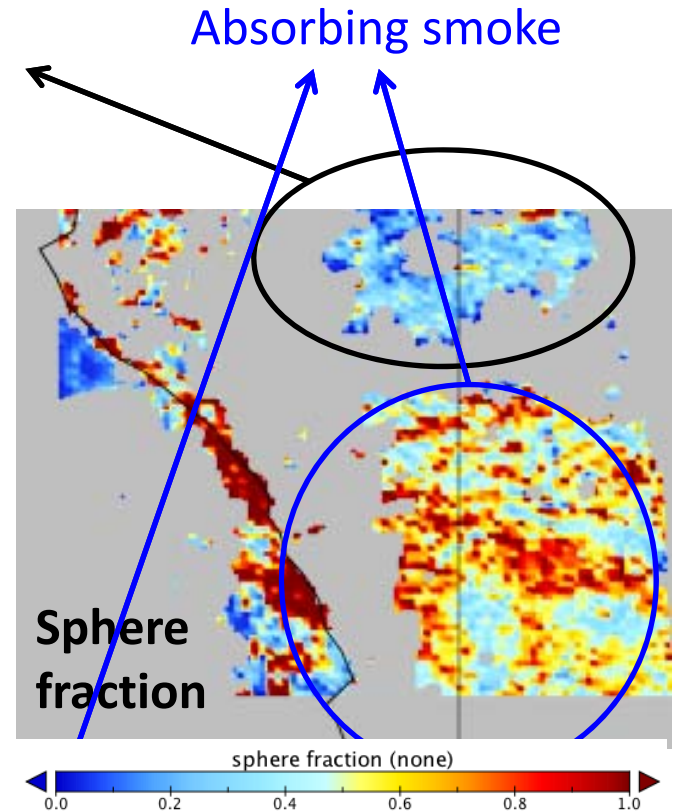
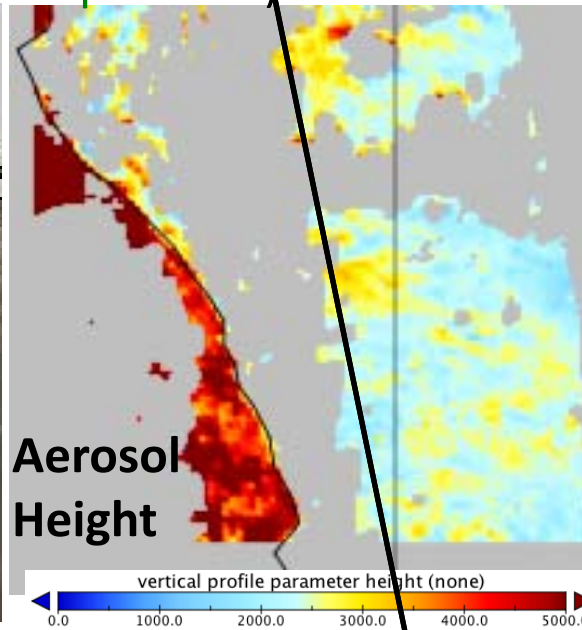
Aged soot-containing Particles (less absorbing, bigger particles)

Absorbing smoke

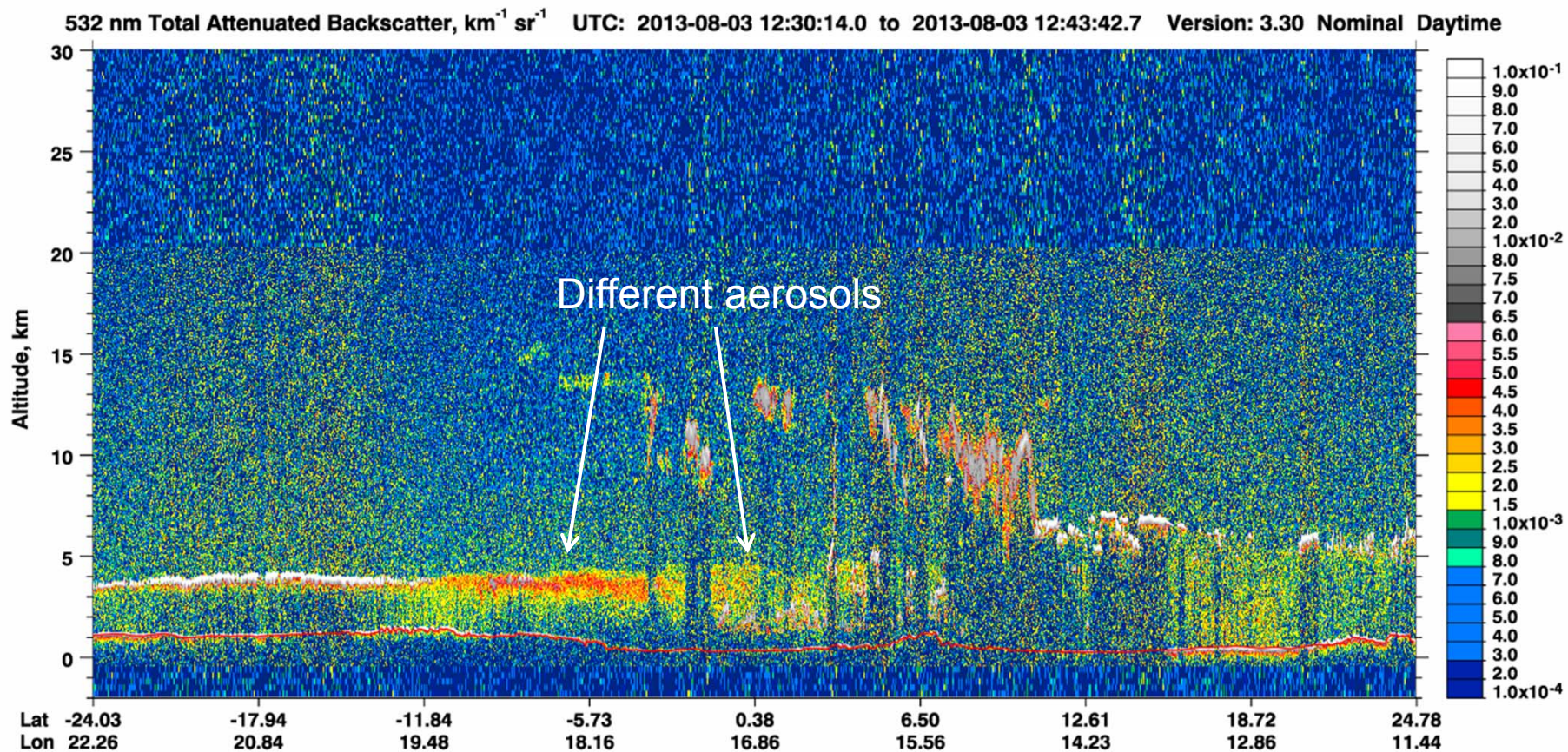


Biomass burning. Africa,
August, 3, 2013

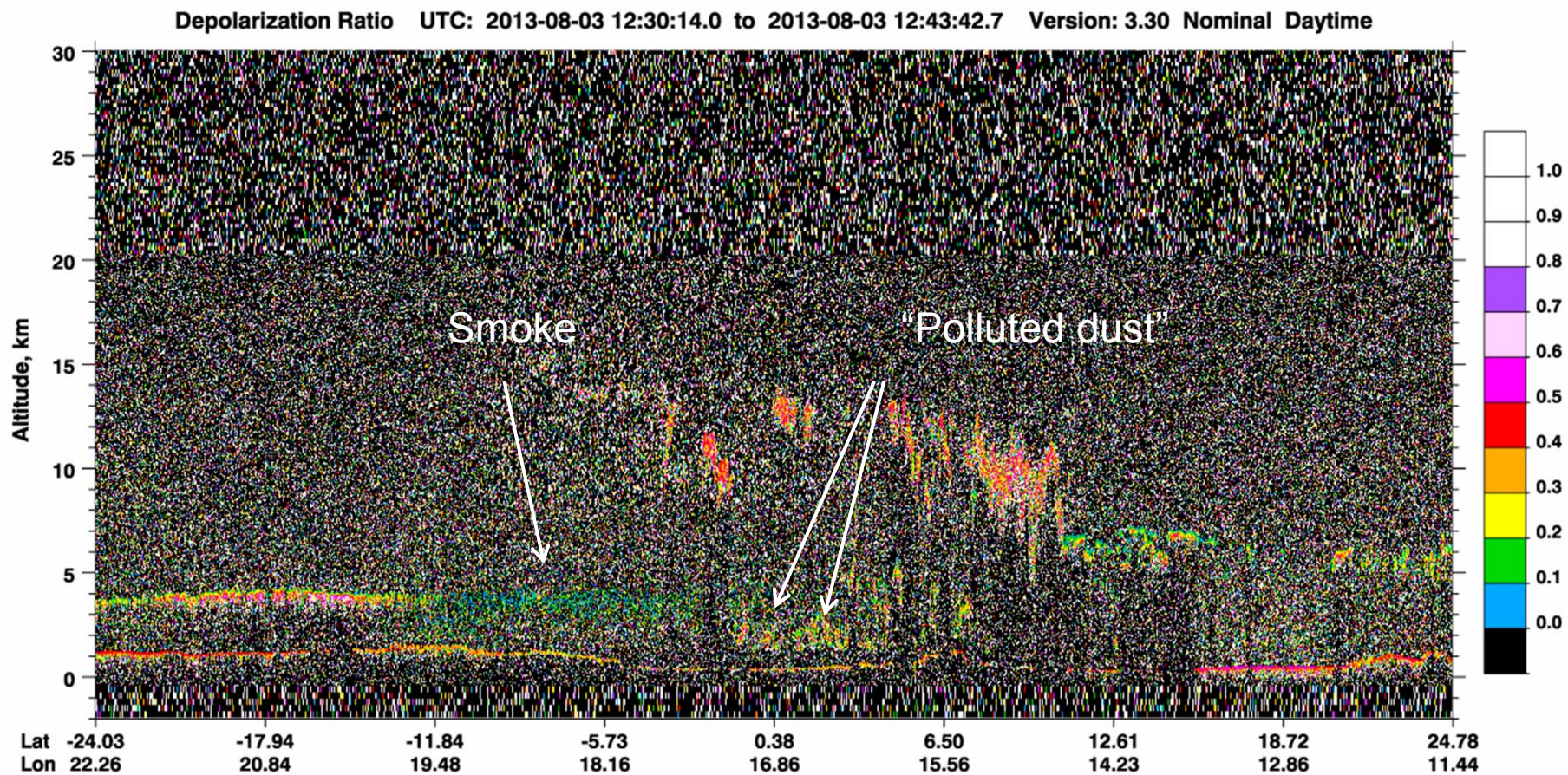
Aged soot-containing
Particles (less
absorbing, bigger
particles)



CALIPSO backscattering



CALIPSO depolarization



1st International Workshop on

Advancement of POLarimetric Observations Calibration and improved aerosol retrieval

APOLO 2017



October 24-27, 2017 Hefei · China

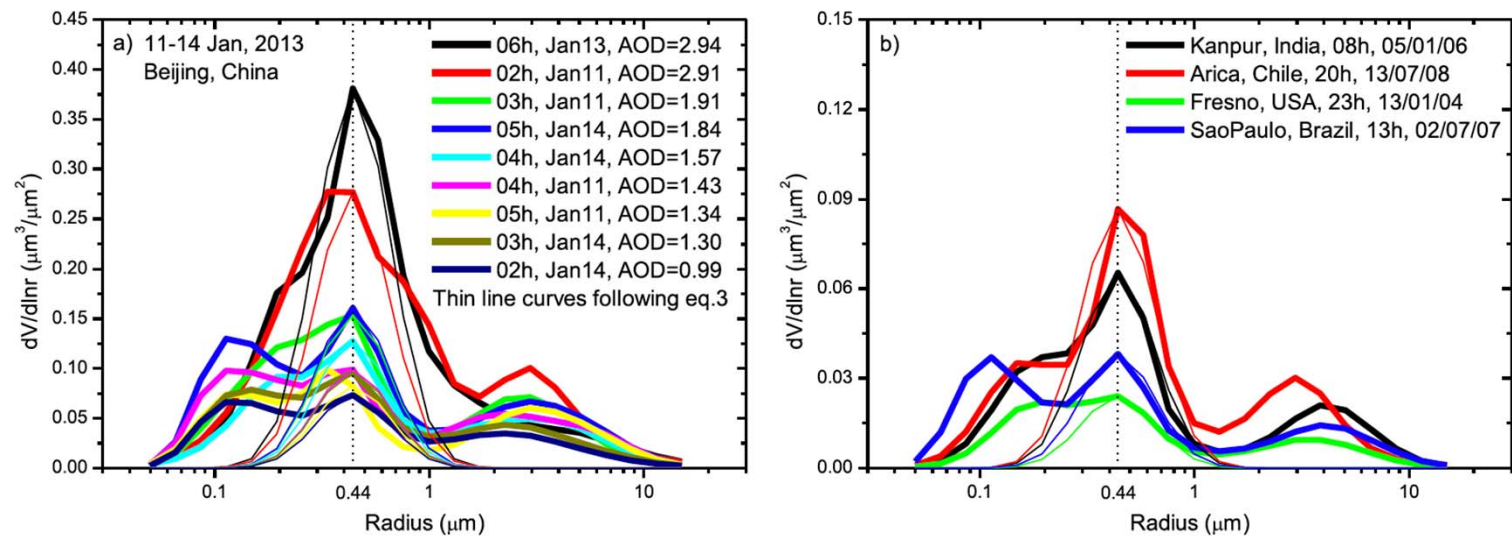
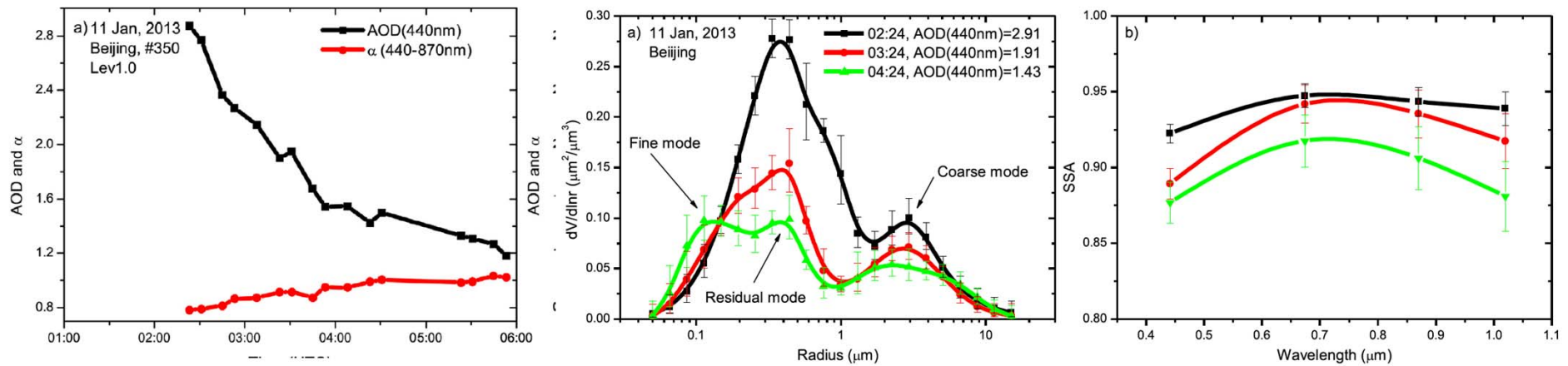
- [Welcome Letter](#)
- [Important Dates](#)
- [Organizing Committee](#)
- [Agenda](#)
- [Invited Speakers](#)
- [Registration](#)
- [Abstract Submission](#)
- [Venue](#)
- [Booking Hotel](#)
- [Sponsorship](#)
- [Tours Information](#)
- [Useful Information](#)
- [Contact Us](#)

Welcome Letter

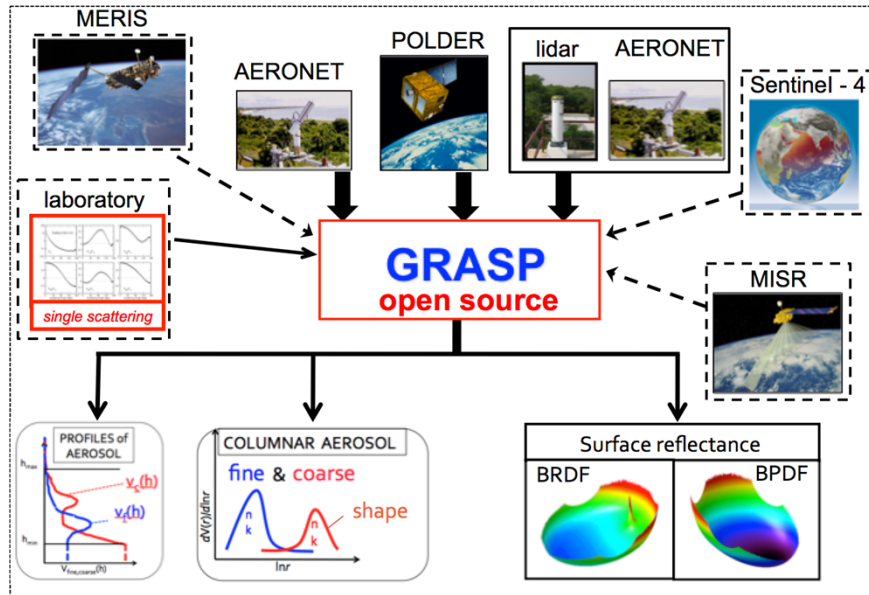
Dear colleagues,

We are glad to announce that the 1st International Workshop on “Advancement of polarimetric observations: calibration and improved aerosol retrievals” (APOLO2017) will be held in Hefei, China from October 24 to 27, 2017. This is the first workshop of a series of polarimetry workshops (<http://www-loa.univ-lille1.fr/workshops/APOLO-2017>).

Several polarimetric missions are scheduled for launch in the coming years by international and national space agencies. Satellite polarimetry is one of the most promising and, at the same time, largely underexploited fields of aerosol remote sensing. This is the 1st meeting of the planned series of workshops on satellite polarimetry. These scientific workshops aim to promote international collaboration as well as in-depth exchange of ideas and experiences on diverse aspects of polarimetric remote sensing, in particular: advances in the theory of polarimetric remote sensing, optimisation of strategies of polarimetric Earth observations, improvement of polarimetric observation quality and information content, advancement of retrieval algorithms and data processing, and long-term Cal/Val.



GRASP: Generalized Retrieval of Aerosol and Surface Properties



Strength of GRASP algorithm concept:

- ✓ Based on accurate rigorous physics and math;
- ✓ **Versatile** (applicable to different sensors and retrieval of different parameters);
- ✓ **Designed for multi-sensor retrieval** (satellite, ground-based, airborne; polar and geostationary,);
- ✓ **Not-stagnant** (different concept can be tested and compared within algorithm);
- ✓ **Flexible:**
 - generalizable (to IR, hypo spectral, to retrieval of gases and clouds, etc.);
 - or degradable (to less accurate but fast solution, LUT,...);
- ✓ **Practical** (rather fast and easy to use for given level fundamental complexity);

Current and potential applications:

Satellite instruments:

polar: POLDER/PARASOL, 3MI/MetOp-SG, MERIS/Envisat, Sentinel-3 (OLCI, SLSTR), etc.

geostationary: Sentinel-4, FCI, GOCO, Himawari-8, etc.

Ground-based, airborne and laboratory instruments:

passive: AERONET radiometers, sun/luna/star-photometers, etc.

active: multi-wavelength elastic and non-elastic lidars; *airborne and laboratory:* polar nephelometers,

Multi-instrument synergy:

ground-based: lidar + radiometers + photometers, sun/luna/star-photometers, etc.

satellite: OLCI + SLSTR, polarimeter + lidar (e.g. PARASOL + CALIPSO)

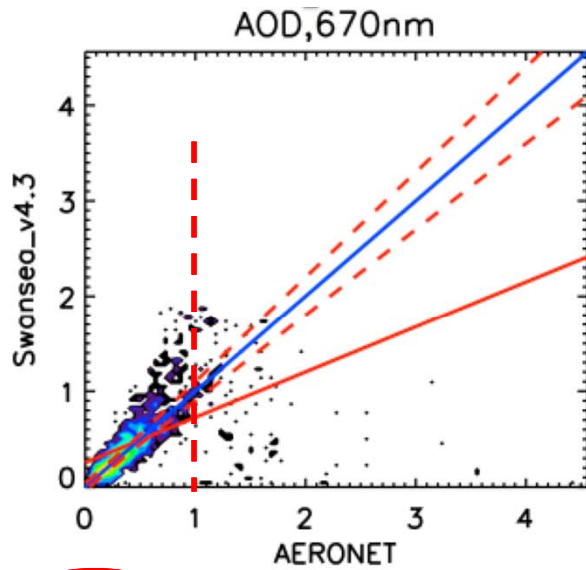
Support: CNES (TOSCA, RD), ANR (CaPPA), ESA (S-4, MERIS/S-3, GPGPU, CCI, CCI-2,CC+); EUMETSAT (3MI NRT), FP6-7 (ACTRIS 1-2), Catalysts GmbH, etc.

Collaborations: NASA/JPL, NASA/GSFC, NASA/GISS, NASA/Langley KNMI, JAXA, Catalysts GmbH (Austria), Chinese Academy of Science and Space Agency, Belarus, Ukraine, etc.

Banizoumbou 1200x 1200 zone

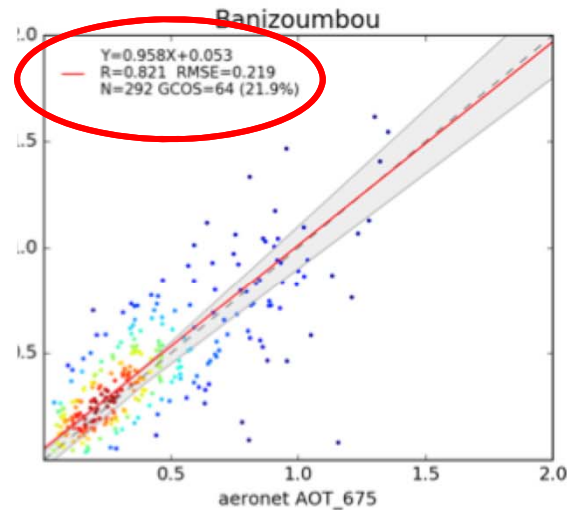
2002-2012

AATSR / SU, R=0.54



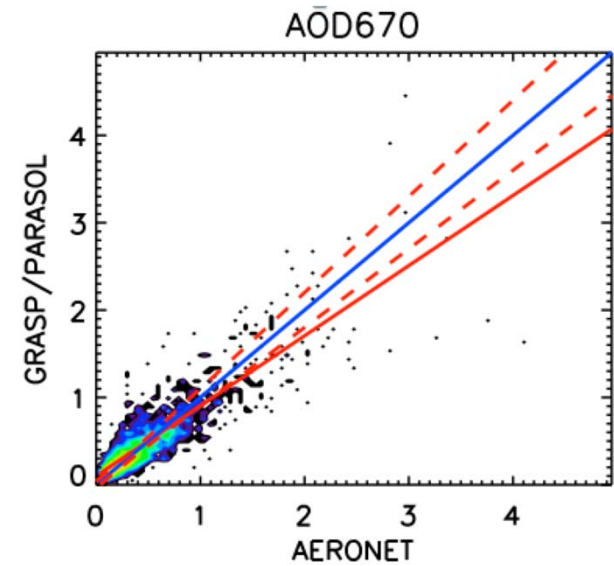
K=0.540 $a = 0.47$ $b = 0.25$ RMSE= 0.392

MERIS / GRASP, R=0.82



2004-2013

PARASOL / GRASP, R=0.87



K=0.867 $a = 0.80$ $b = 0.10$ RMSE= 0.227

AATSR- fails for AOD > 1.0 ???

PARASOL fails with the slope ???

MERIS is surprisingly good ???

Aged soot-containing aerosol. LIDER depolarization measurements and theoretical modeling (Mischenko et al., Applied Optics, 2016)

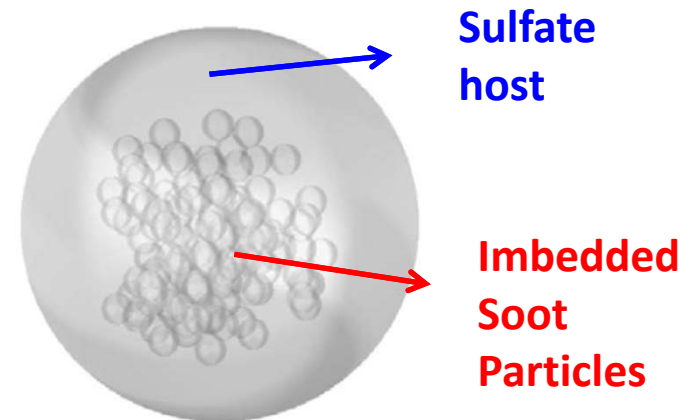
Burton et al., Atmos. Chem. Phys. 2015:

Table 1. Measured Spectral Values of the Linear Depolarization Ratio and Their Ranges [20]

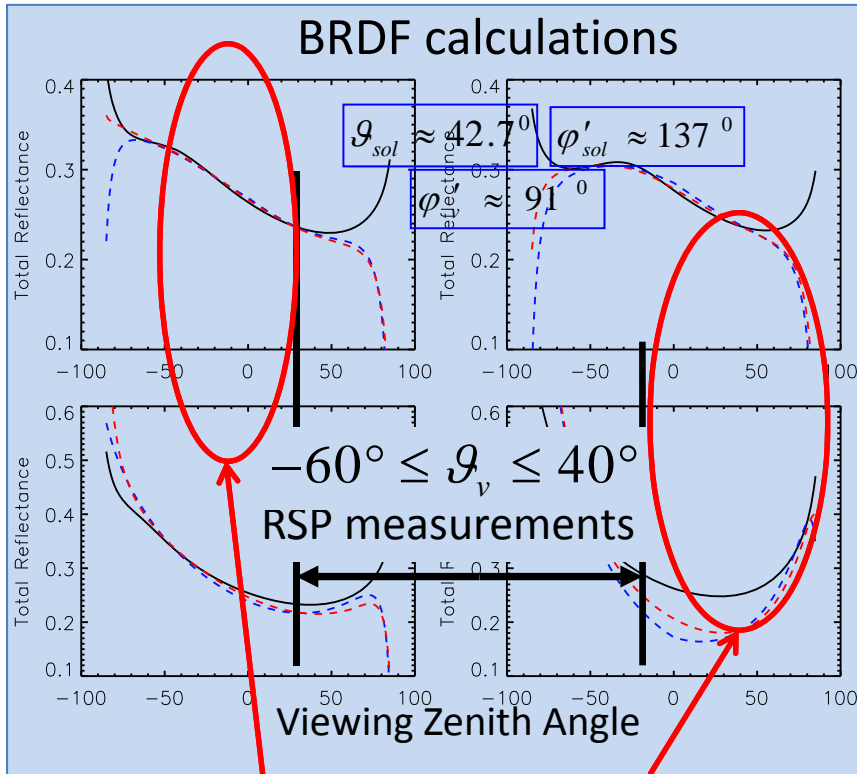
	δ (355 nm)	δ (532 nm)	δ (1064 nm)
Measured	0.203 ± 0.036 (0.017)	0.093 ± 0.015 (0.011)	0.018 ± 0.002 (0.007)
Range	[0.150, 0.256]	[0.067, 0.119]	[0.009, 0.027]

Mischenko et al., Applied Optics, 2016:

Complex morphologies of aged soot-containing aerosols can reproduce the spectral dependence of linear depolarization observed for an aged smoke plume by Burton et al.



BRDF models uncertainties.

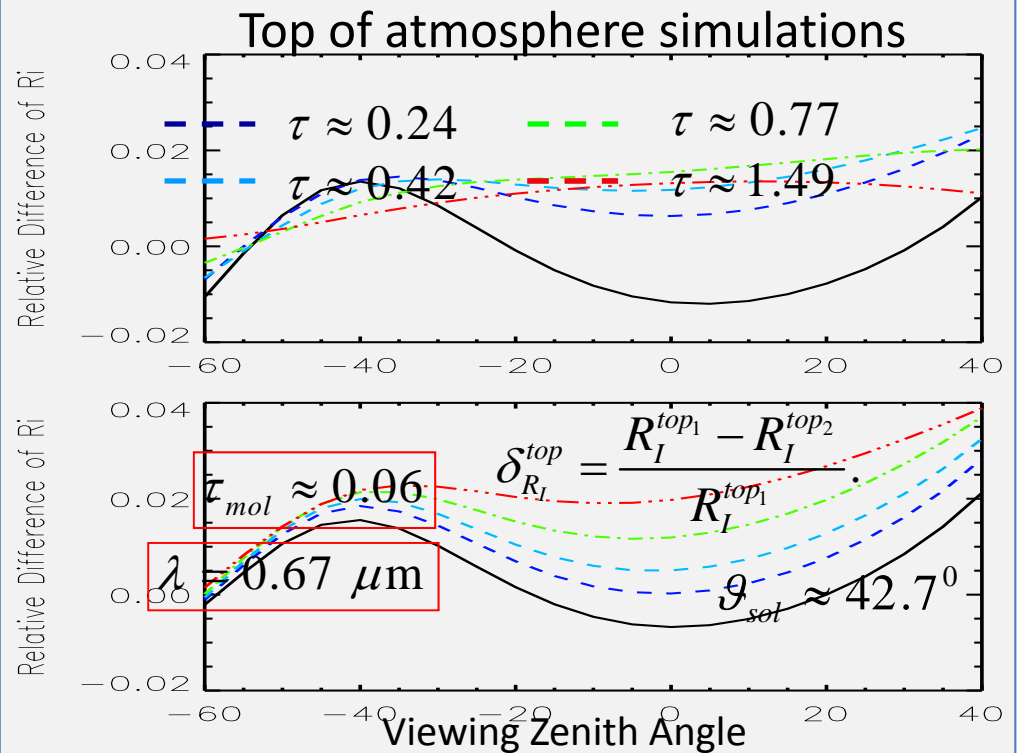


BRDF models uncertainties!

Black curves: RPV model

Blue curves: Ross-Roujean model

Red curves: Ross-Li model

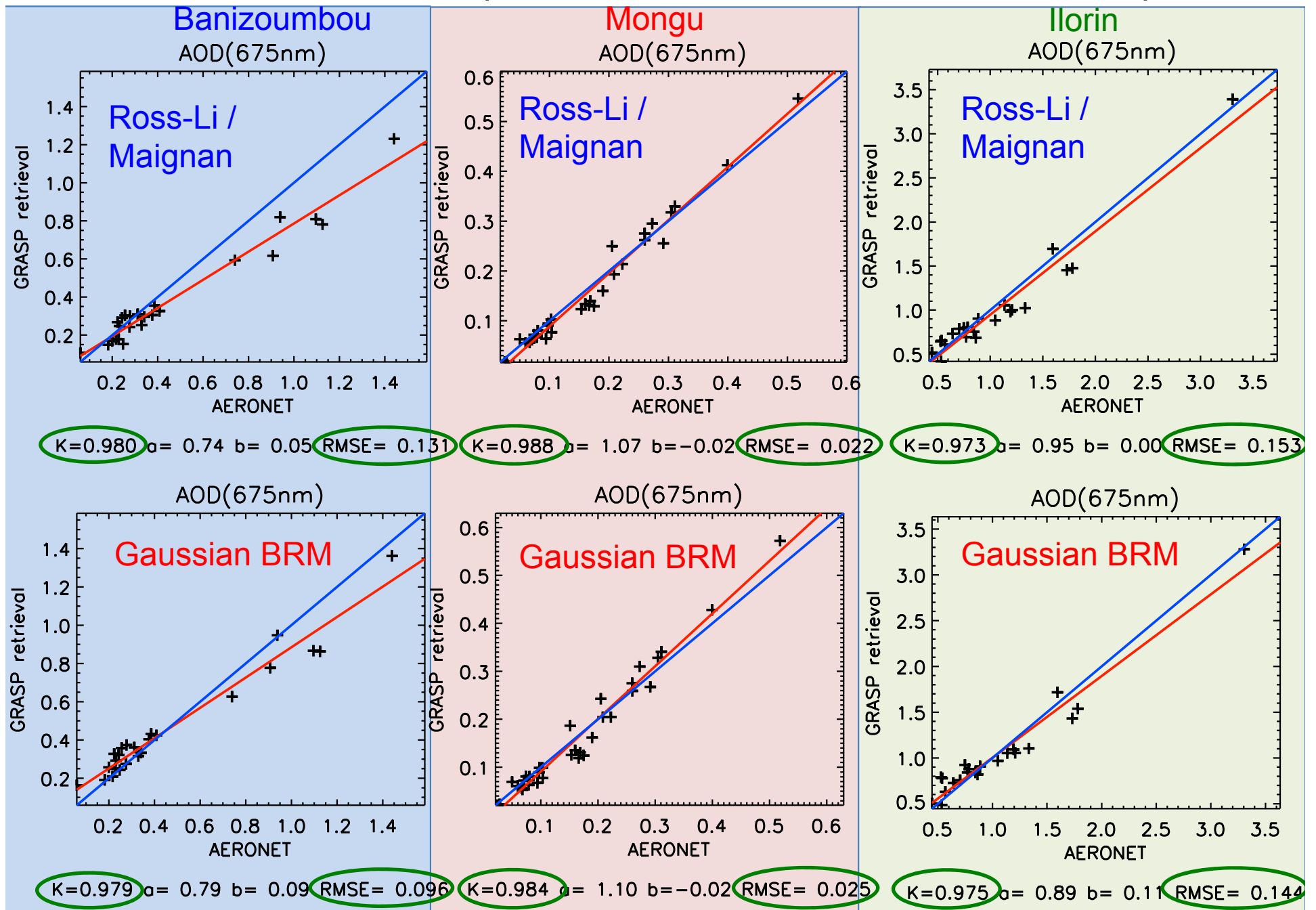


Black curves: the relative differences of the BRDF models (RPV and Ross-Li models)

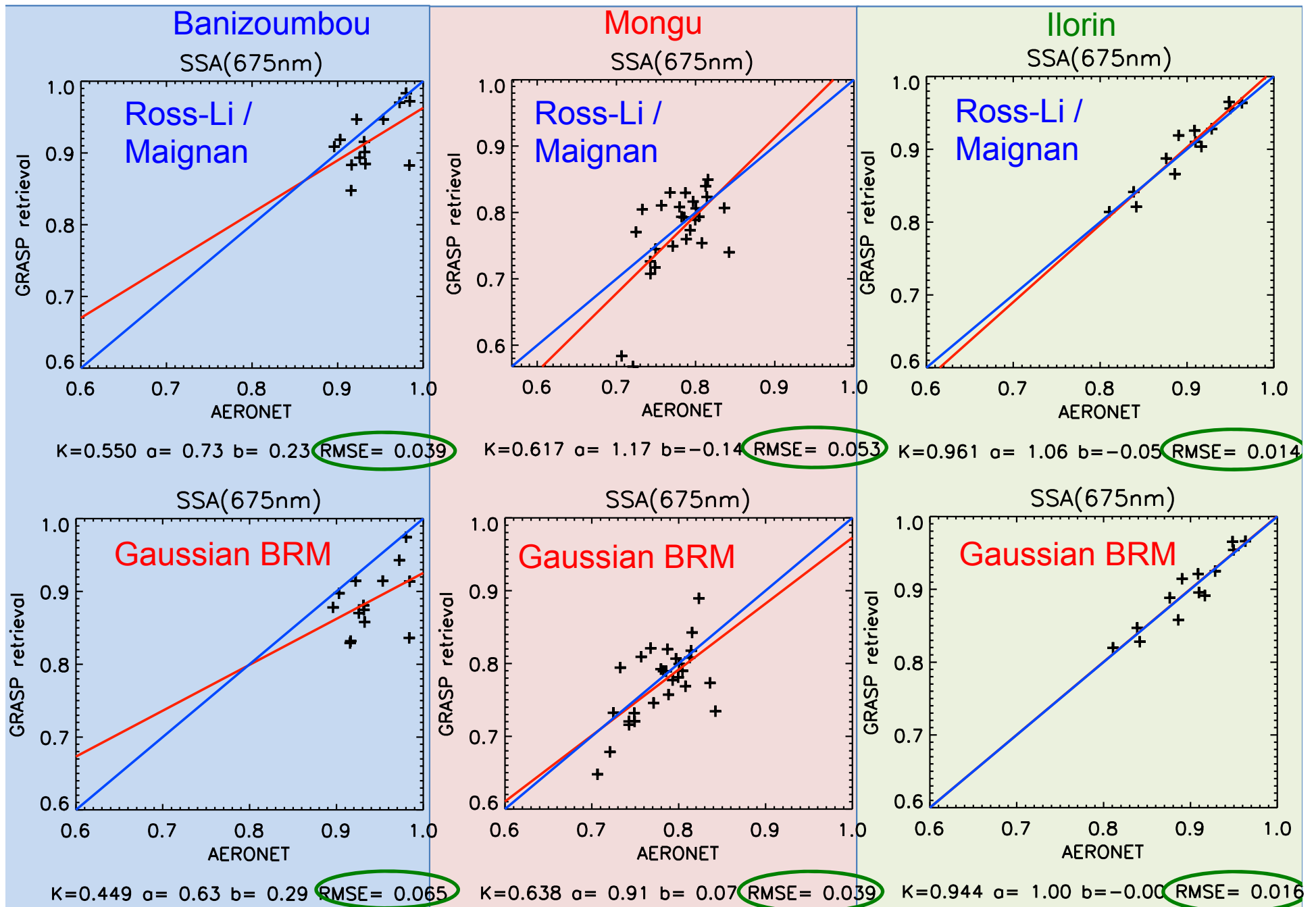
Color curves: the relative differences of the top of atmosphere total reflectances (RPV and Ross-Li model, the same aerosol model)

BRDF models uncertainties can provide up to 2-5% systematic error in top of atmosphere signal! (Litvinov et al., RSE, 2011)

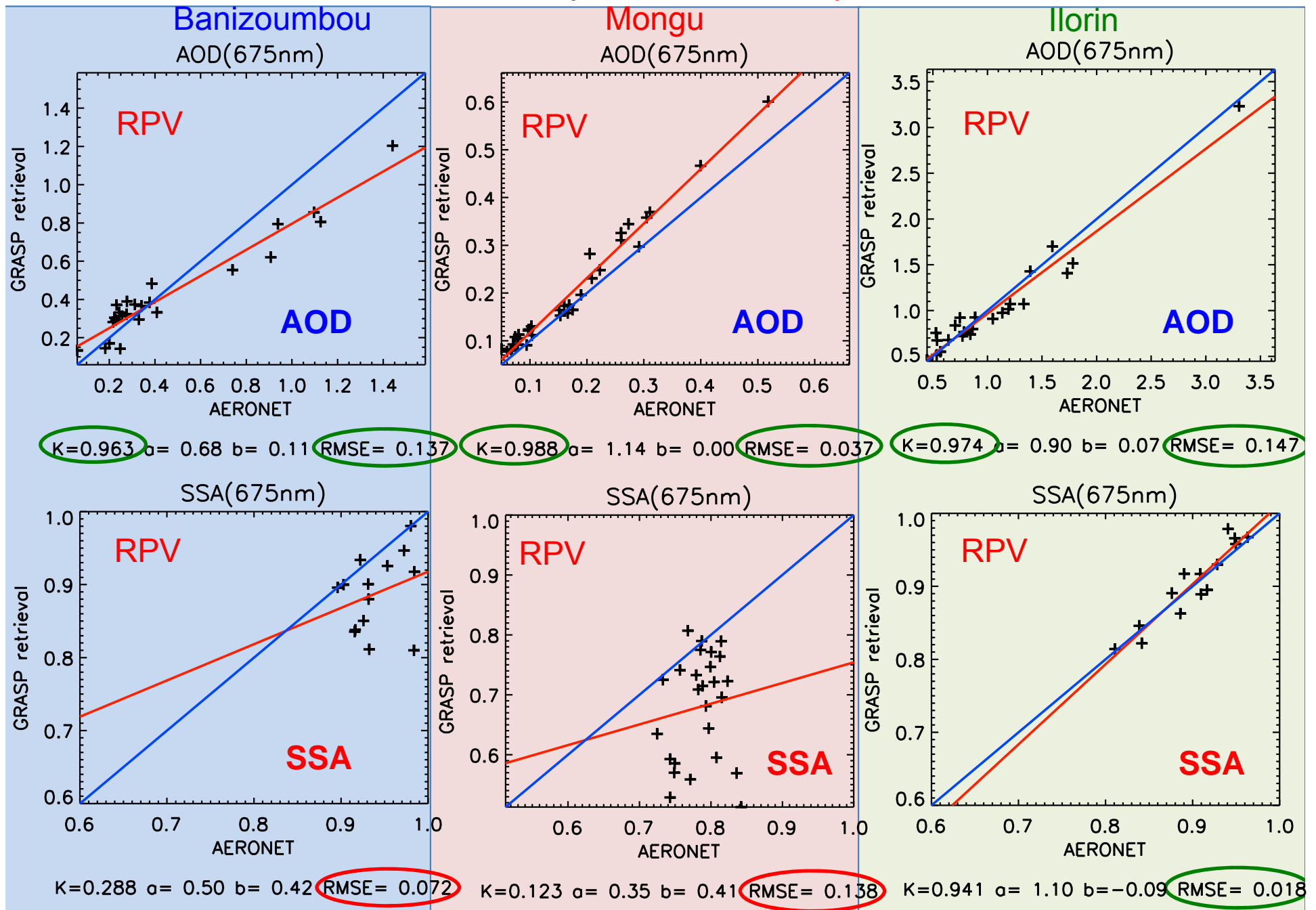
Surface BRM effect (Ross-Li and Gaussian BRDF). AOD.



Surface BRM effect (Ross-Li and Gaussian BRDF). SSA.



Surface BRM effect (RPV BRDF). AOD and SSA.

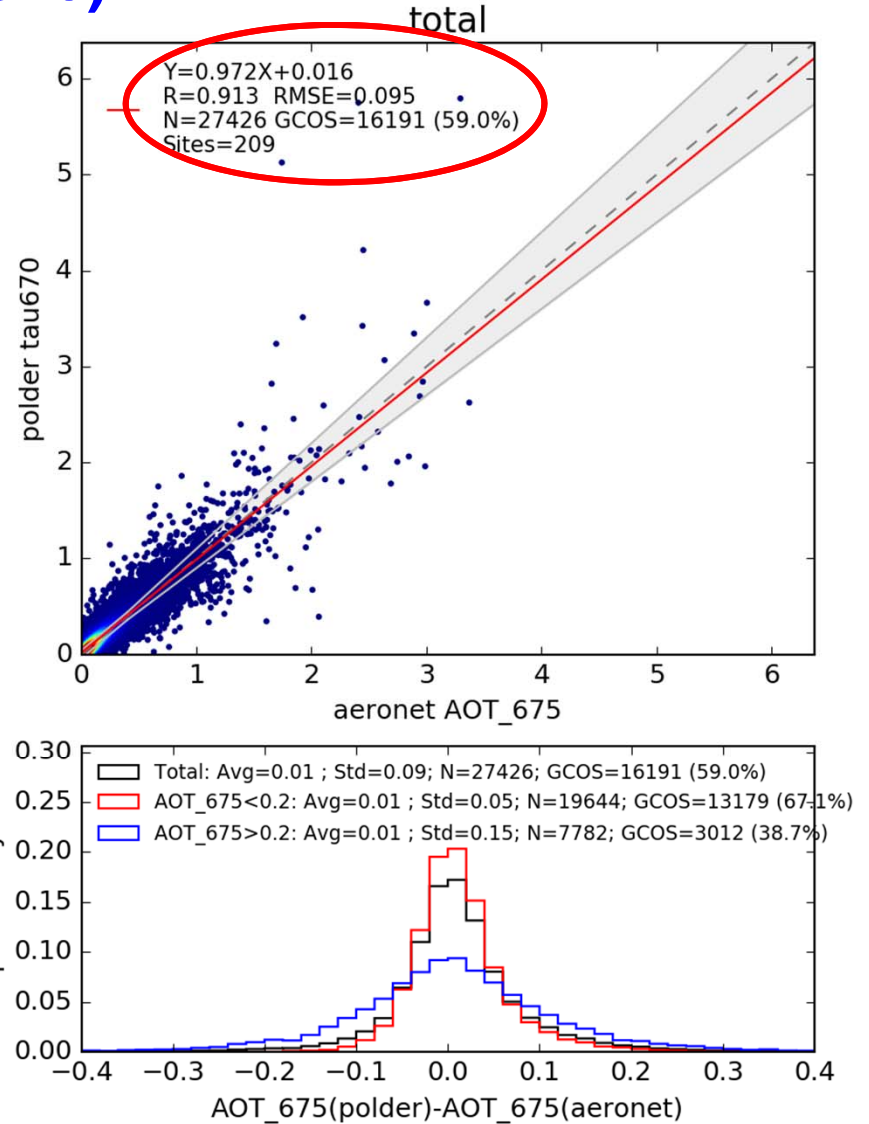
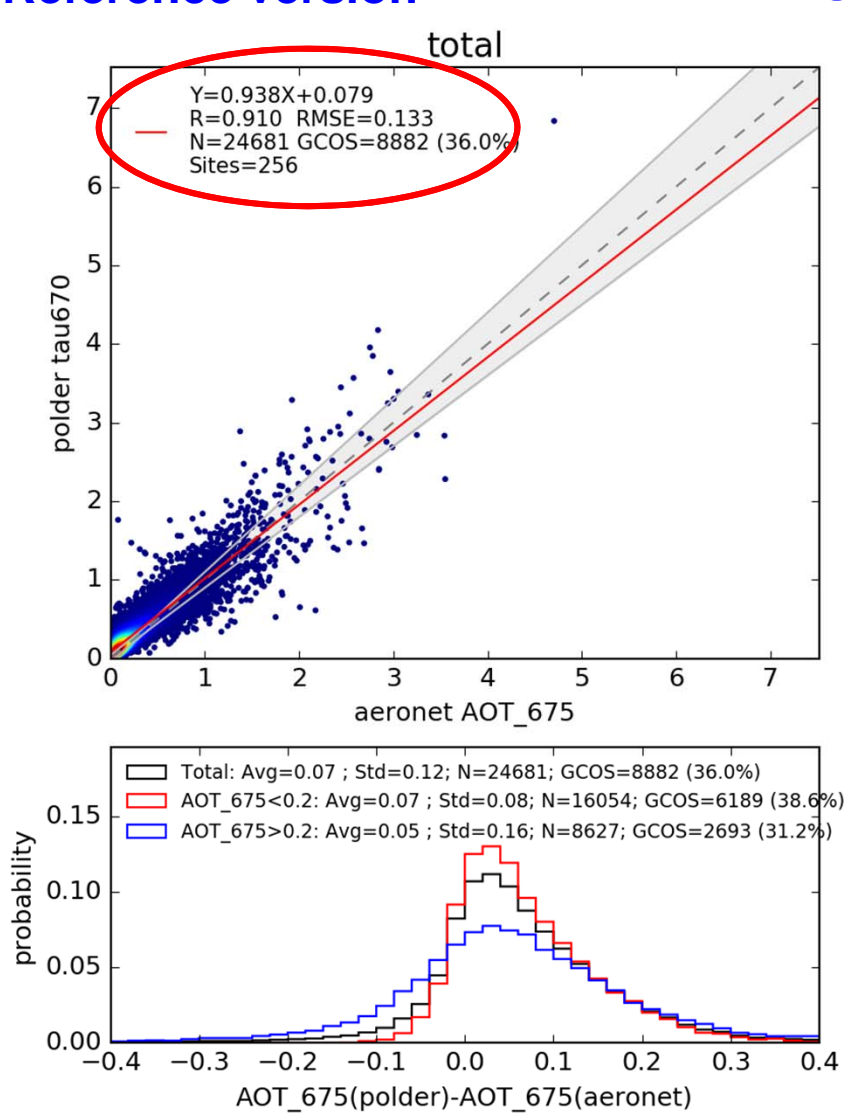


Validation vs AERONET 2004 - 2013

Reference version

AOD(670)

Component mixture

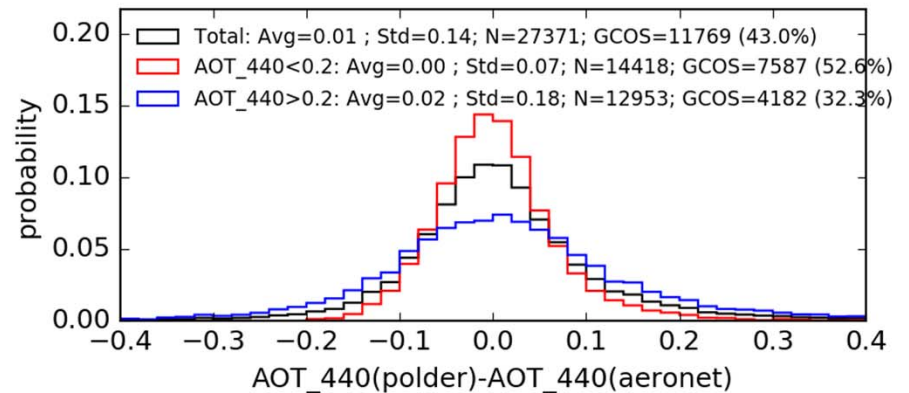
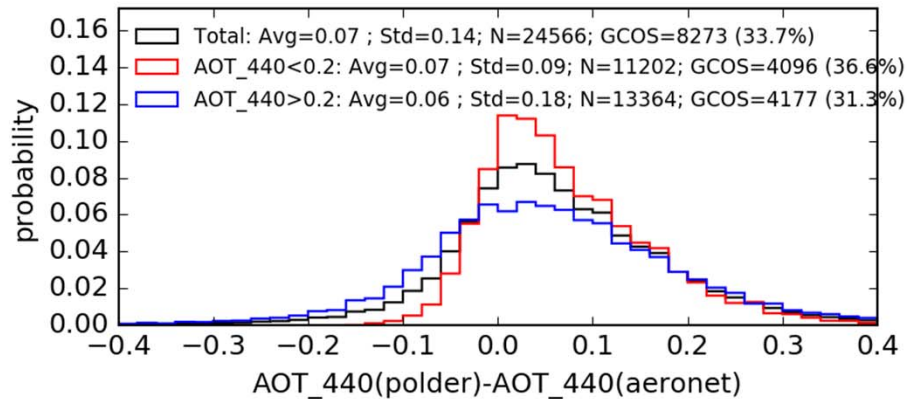
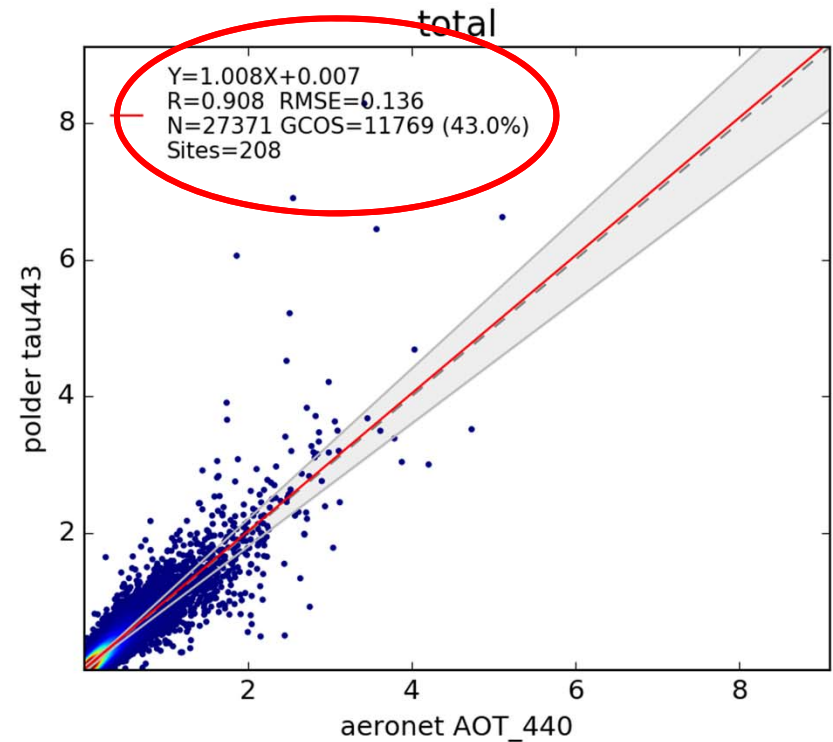
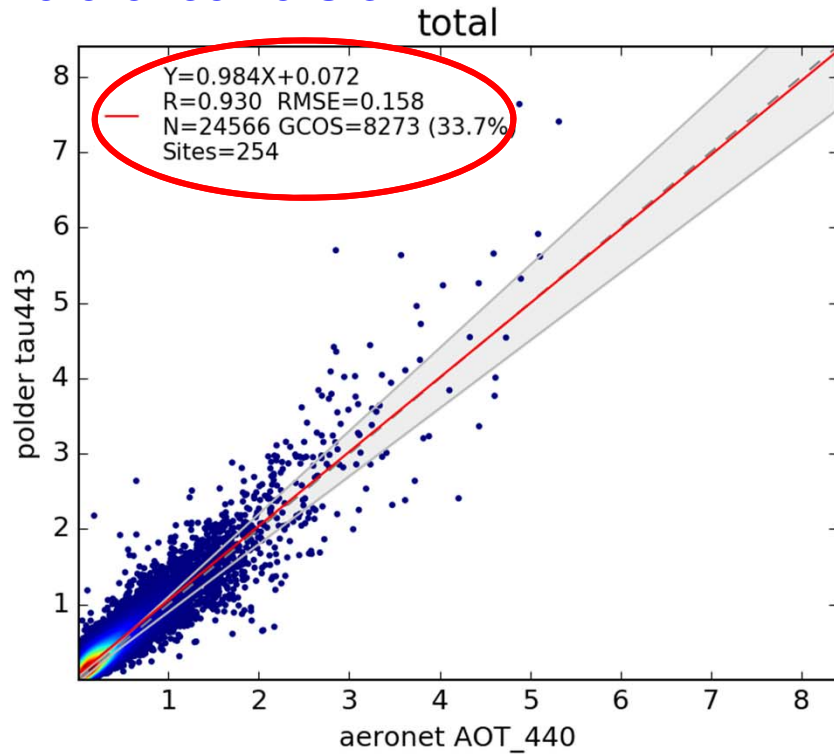


Validation vs AERONET 2004 - 2013

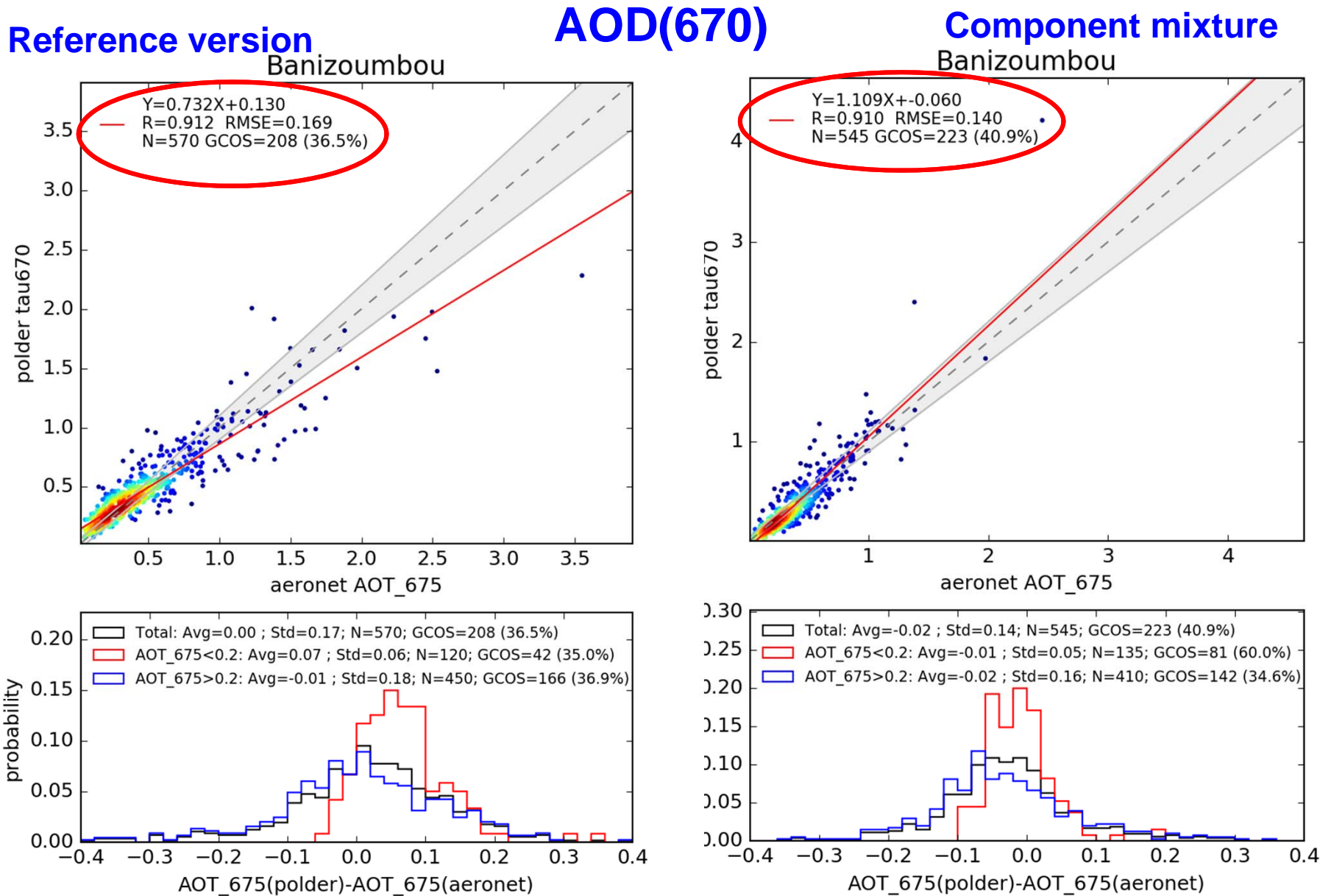
Reference version

AOD(440)

Component mixture



Validation vs AERONET 2004 - 2013

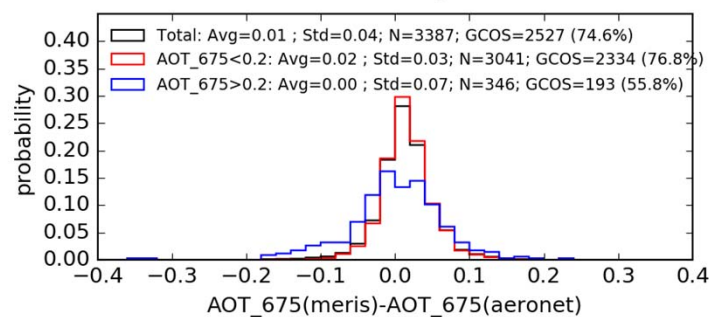
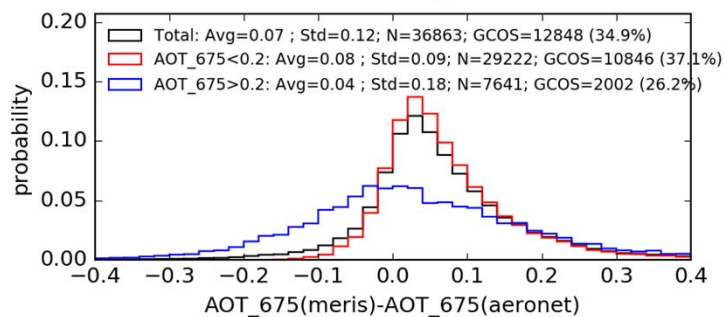
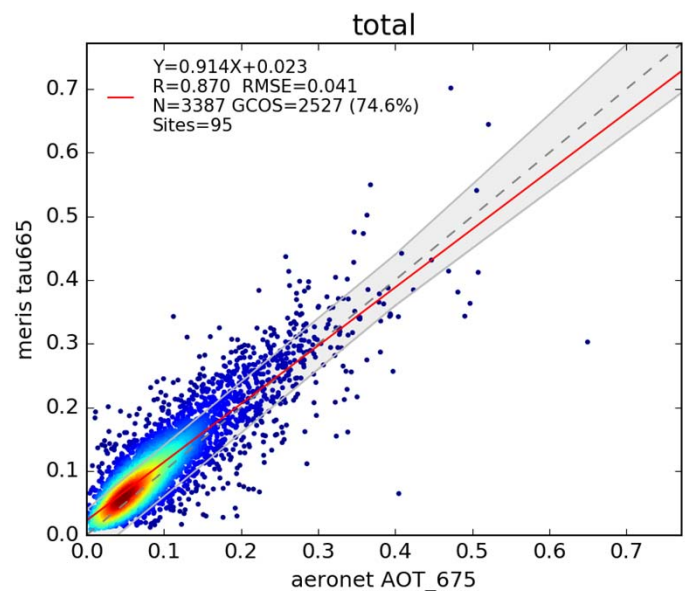
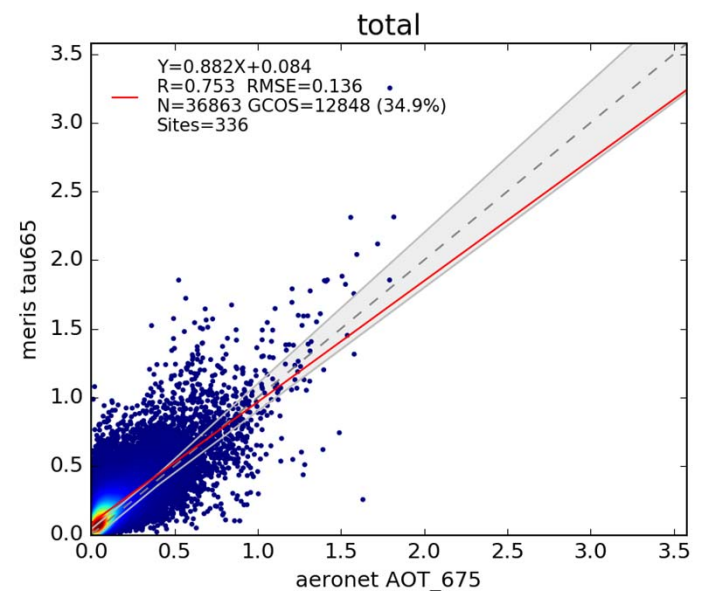


Validation vs AERONET 2002 - 2012

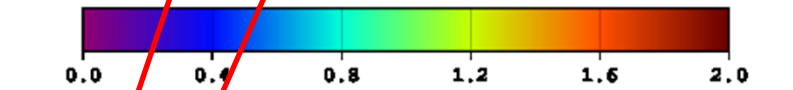
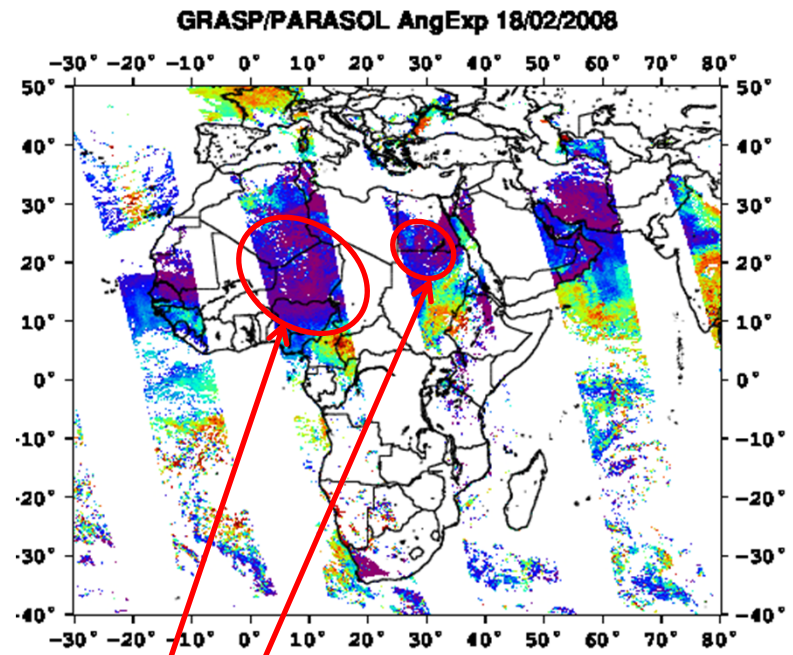
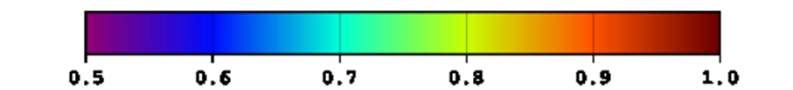
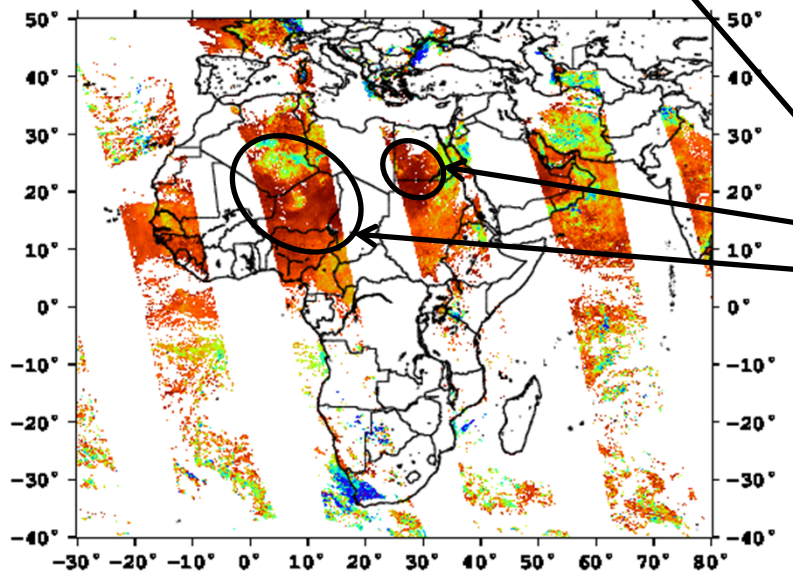
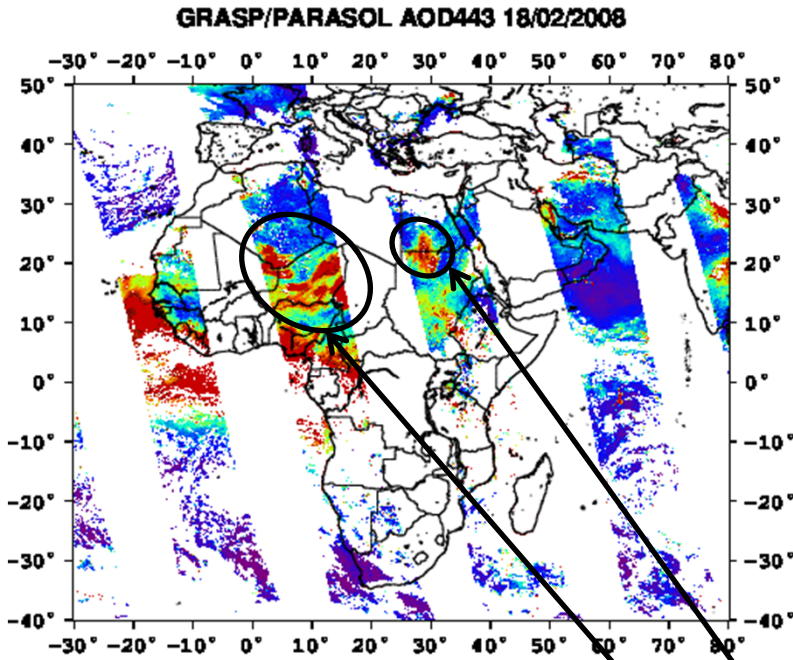
MERIS/GRASP - AOD

Land

Ocean



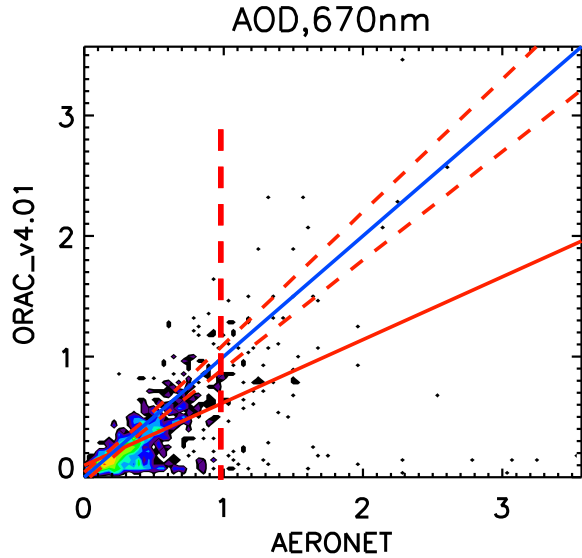
Dust detection with GRASP



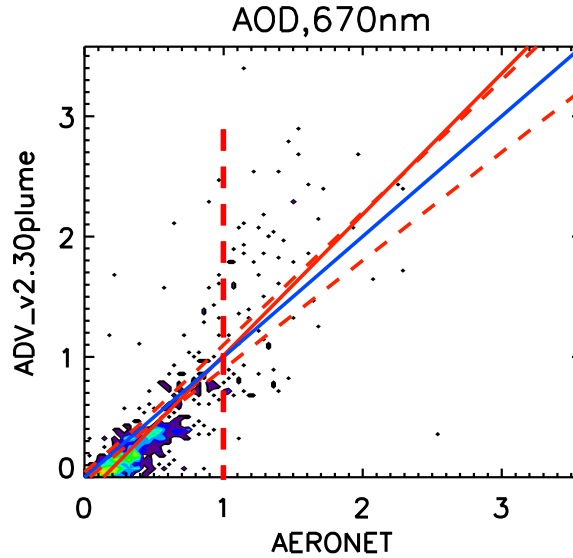
Dust events:

- ✓ High AOD
- ✓ Angstrom Exponent < 0.5
- ✓ SSA (440 - 1020) > 0.9

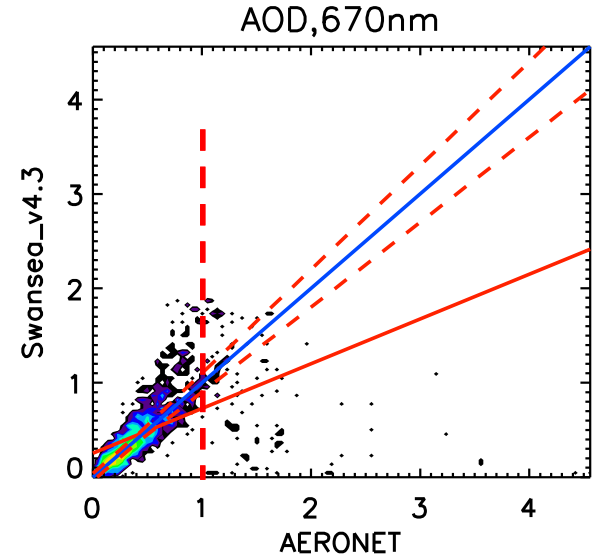
Banizoumbou 1200x 1200 zone. 2002-2012. AATSR.



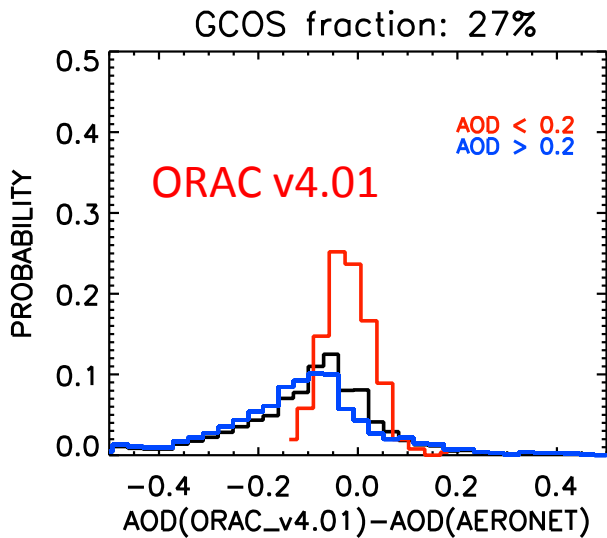
K=0.620 a= 0.52 b= 0.10 RMSE= 0.333



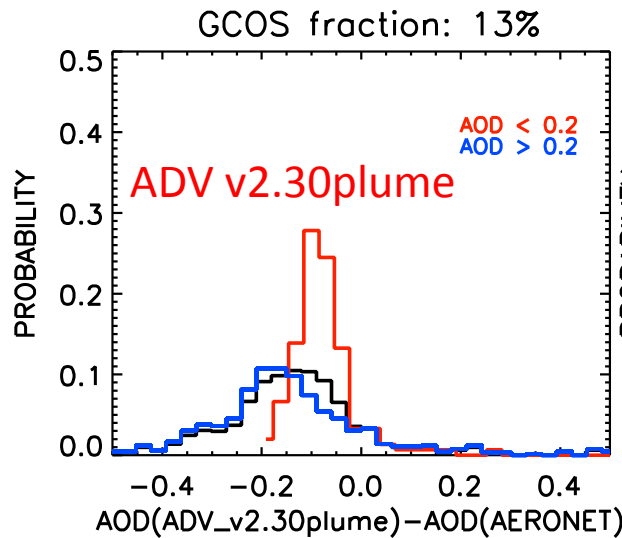
K=0.837 a= 1.17 b=-0.16 RMSE= 0.302



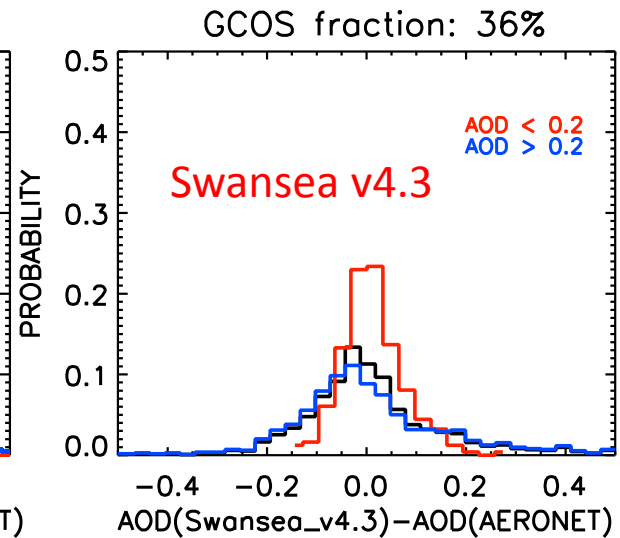
K=0.540 a= 0.47 b= 0.25 RMSE= 0.392



Aver. Value=-0.126 St.D.= 0.309 N=1310
 Aver. Value=-0.006 St.D.= 0.051 N=258
 Aver. Value=-0.156 St.D.= 0.337 N=1052

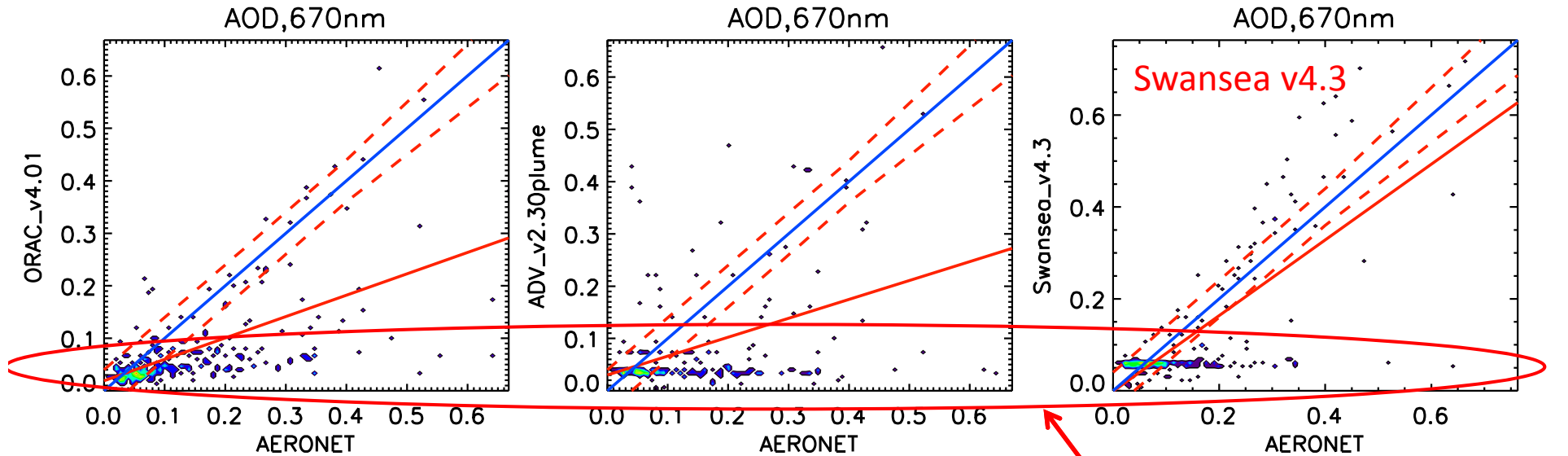


Aver. Value=-0.077 St.D.= 0.292 N=812
 Aver. Value=-0.055 St.D.= 0.108 N=151
 Aver. Value=-0.082 St.D.= 0.319 N=661

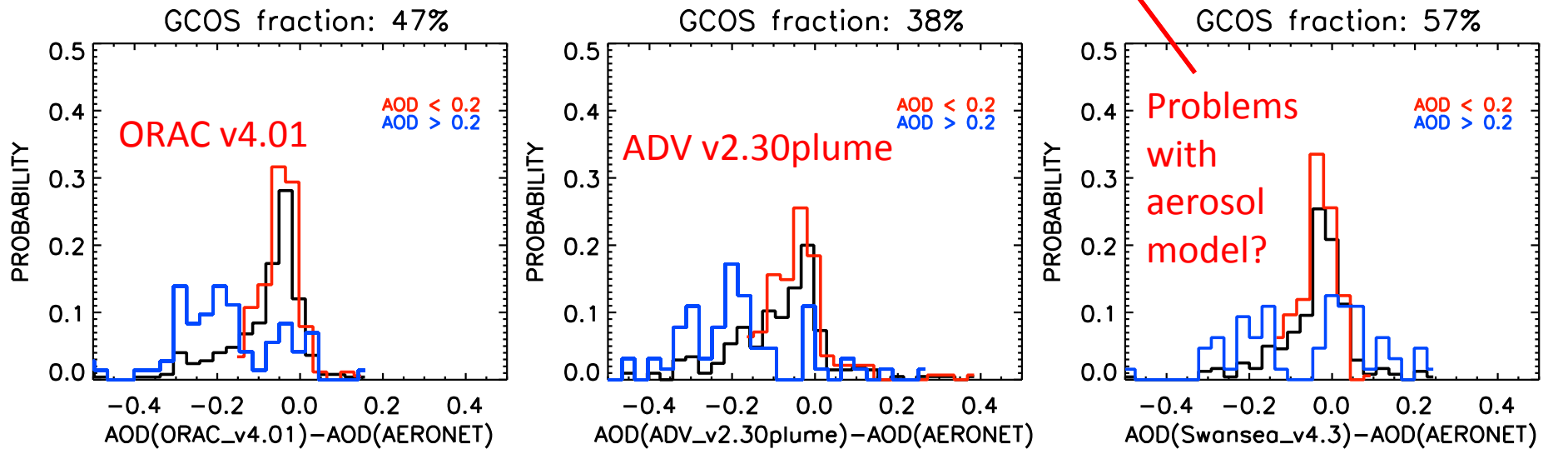


Aver. Value=-0.011 St.D.= 0.392 N=1345
 Aver. Value= 0.028 St.D.= 0.063 N=248
 Aver. Value=-0.020 St.D.= 0.432 N=1097

Mongu 1200x 1200 zone. 2002-2012. AATSR.



$K=0.595$ $a=0.41$ $b=0.02$ $RMSE=0.128$
 $K=0.410$ $a=0.36$ $b=0.03$ $RMSE=0.151$
 $K=0.760$ $a=0.82$ $b=-0.00$ $RMSE=0.101$



<p>Aver. Value=-0.073 St.D.= 0.105 N=249 Aver. Value=-0.033 St.D.= 0.047 N=177 Aver. Value=-0.171 St.D.= 0.139 N= 72</p>	<p>Aver. Value=-0.073 St.D.= 0.133 N=205 Aver. Value=-0.026 St.D.= 0.083 N=141 Aver. Value=-0.177 St.D.= 0.159 N= 64</p>	<p>Aver. Value=-0.028 St.D.= 0.097 N=240 Aver. Value=-0.020 St.D.= 0.045 N=176 Aver. Value=-0.052 St.D.= 0.170 N= 64</p>
--	--	--

Real Part of Ref. Index (565), Summer (PARASOL archive average)

Averaged Summer data of POLDER Ref. Index Real Part 565nm (2005-2013)

